

**Effects of the Wake Turbulence on Aircraft Wing Model:
Experimental Method**

by

Ng Ming Kiat

Dissertation submitted in partial fulfilment of
the requirements for the
Bachelor of Engineering (Hons)
(Mechanical Engineering)

JANUARY 2009

Universiti Teknologi PETRONAS
Bandar Seri Iskandar
31750 Tronoh
Perak Darul Ridzuan

CERTIFICATION OF APPROVAL

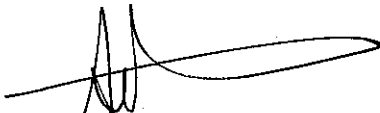
**Effects of the Wake Turbulence on Aircraft Wing Model:
Experimental Method**

by

Ng Ming Kiat

A project dissertation submitted to the
Mechanical Engineering Programme
Universiti Teknologi PETRONAS
in partial fulfilment of the requirement for the
BACHELOR OF ENGINEERING (Hons)
(MECHANICAL ENGINEERING)

Approved by,



(Dr. Ahmed Maher Said Ali)

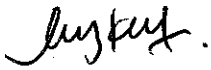
UNIVERSITI TEKNOLOGI PETRONAS

TRONOH, PERAK

January 2009

CERTIFICATION OF ORIGINALITY

This is to certify that I am responsible for the work submitted in this project, that the original work is my own except as specified in the references and acknowledgements, and that the original work contained herein have not been undertaken or done by unspecified sources or persons.



NG MING KIAT

ABSTRACT

A research on studying the effect of the wake generated by an aircraft wing section on a following aircraft wing section is performed. NACA 2412 is chosen as the airfoil model in this project. The airfoil model is fabricated by using CNC machining. Aluminium is chosen as the material for the airfoil model because it provides a good surface finish. Three experiments are conducted by using the open-circuit wind tunnel in Universiti Sains Malaysia (USM). The wind tunnel tests were carried out at the velocity of 5m/s to 30m/s in a test section of the size 0.30m (W), 0.30m (H) and 0.60m (L), at the Reynolds number of 4.10×10^4 to 2.54×10^5 . Experiment 1 is the testing of single airfoil model to define the coefficient of lift, coefficient of drag and Reynolds number at various angles of attack. Experiment 1 is functioning as references for comparison for Experiment 2 and Experiment 3. Experiment 2 and Experiment 3 are the testing of two airfoil models at a separating distance of 1 chord length (13cm) and 2 Chord lengths (26cm) respectively. The main objective of Experiment 2 and Experiment 3 are to study the effects of wake turbulence on the characteristic of coefficient of lift, coefficient of drag and Reynolds number of a following airfoil model when an airfoil model is placed in front of it at a specific distance. The characteristics of the wake generated by an airfoil model on a following airfoil model are observed and studied during the testing in wind tunnel. Further investigations, discussions and conclusions are carried out throughout completing this research project. The results show that the separating distance between the two airfoils affects the coefficient of lift, coefficient of drag and the stall angle of the following airfoil at various angle of attack and free stream velocity.

ACKNOWLEDGEMENTS

First and foremost, I would like to express my utmost gratitude to Dr. Ahmed Maher Said Ali, the project supervisor for my Final Year Project. He has been very supportive during the entire project period. He spent very much time and energy to guide me throughout these two semesters despite his other commitments and packed schedule as a lecturer in Universiti Teknologi Petronas. Under his constant supervision, I managed to complete my project according to the timeframe scheduled.

I would like to express my sincere gratitude to Associate Professor Dr. Mohd Zulklify Abdullah, the senior lecturer from the School of Mechanical Engineering, Universiti Sains Malaysia. He gave me the permission to use the open-circuit wind tunnel for the purpose of testing. He helped me during the modification of airfoil models and perspex wall of the test section. Besides, he shared his ideas in making the testing a success too.

Besides, I would like to thank Mr. Mohd Hafiz, the lab technician of Manufacturing Lab, Universiti Teknologi Petronas, for his help to fabricate the two airfoil models.

Last but not least, thanks to everyone, family and friends who involved directly and indirectly towards the successful of the project.

TABLE OF CONTENTS

ITEMS	PAGE
ABSTRACT.....	i
ACKNOWLEDGEMENTS.....	ii
TABLE OF CONTENTS.....	iii
LIST OF FIGURES.....	vi
LIST OF TABLES.....	ix
CHAPTER 1: INTRODUCTION.....	1
1.1 Background of Study.....	1
1.2 Problem Statement.....	5
1.3 Objectives and Scope of Study.....	6
CHAPTER 2: LITERATURE REVIEW AND/OR THEORY.....	7
2.1 Forces Acting on Aircraft.....	7
2.2 Aircraft Wing and Aerofoil Section.....	8
2.3 Air Flow Around an Aerofoil Section.....	11
2.4 Aerofoil Characteristics.....	17
CHAPTER 3: METHODOLOGY/ PROJECT WORK.....	23
3.1 Procedure Identification.....	23
3.2 Project Activities.....	24
3.2.1 Drawing.....	24
3.2.2 Equipment.....	24
3.2.3 Material.....	25
3.3 Tools Required.....	25
3.4 Gantt Chart.....	26
CHAPTER 4: RESULTS AND DISCUSSION.....	27
4.1 Description of the Open Circuit Wind Tunnel	27
4.2 Selection of Airfoil Wing Type.....	29
4.3 Design of NACA2412 Wing Type Model.....	30

4.4 Fabrication of NACA2412 Wing Type Model.....	32
4.5 Experiments on the Effect of Wake.....	36
4.5.1 Effects of free stream velocity and various angles of attack on the coefficient of lift and coefficient of drag of a single airfoil model (Experiment 1).....	37
4.5.2 Effects of free stream velocity and various angles of attack on the coefficient of lift and coefficient of drag of a two airfoil models with a separating distance of 1 chord length (Experiment 2).....	38
4.5.3 Effects of free stream velocity and various angles of attack on the coefficient of lift and coefficient of drag of a two airfoil models with a separating distance of 2 chord length (Experiment 3).....	39
4.6 Experimental Results and Analysis.....	40
4.6.1 Experimental results for Experiment 1, Experiment 2 and Experiment 3 on the characteristic of coefficient of lift and coefficient of drag.....	40
4.6.2 Analysis of experimental results on the characteristic of coefficient of lift and coefficient of drag.....	52
4.6.3 Analysis of the coefficient of lift with angle of attack...	53
4.6.4 Analysis of the coefficient of drag with angle of attack.	57
4.6.5 Experimental results for Experiment 1, Experiment 2 and Experiment 3 on the characteristic of coefficient of lift, coefficient of drag and Reynolds number.....	59
4.6.6 Analysis of the coefficient of lift with Reynolds number.....	81
4.6.7 Analysis of the coefficient of drag with Reynolds number.....	82
CHAPTER 5: CONCLUSION.....	84
RECOMMENDATION.....	87
REFERENCES.....	88

APPENDIX I.....	90
APPENDIX II.....	91
APPENDIX III.....	92
APPENDIX IV.....	94
APPENDIX V.....	95
APPENDIX VI.....	101
APPENDIX VII.....	107

LIST OF FIGURES

ITEMS	PAGE
Figure 1: Wake vortex generation.....	1
Figure 2: Wake ends and wake begins.....	2
Figure 3: Induced roll.....	2
Figure 4: Vortex Flow Field.....	3
Figure 5: Forces on aircraft in steady level flight.....	7
Figure 6: The direction of the aerodynamic forces.....	8
Figure 7: Wing geometry.....	9
Figure 8: High aspect ratio on the powered glider version of the Europa (lowest aircraft).....	9
Figure 9: Plan view of the Concorde.....	10
Figure 10: Chord line and angle of attack.....	11
Figure 11: Variation of lift with angle of attack and camber.....	12
Figure 12: Flow follows the contour of the section.....	12
Figure 13: Flow separation.....	13
Figure 14: Boundary layer growth on a thin aerofoil.....	14
Figure 15(a): Boundary layer separation at low angle of attack.....	16
Figure 15(b): Boundary layer separation at higher angles of attack.....	16
Figure 15(c): Boundary layer separation as the angles of attack increases.....	17
Figure 16: Airfoil geometric parameters.....	18
Figure 17: Values of C_L for two NACA airfoil sections.....	19
Figure 18: Lift Curve.....	20
Figure 19: Drag Curve.....	21
Figure 20: Lift/Drag Curve.....	21
Figure 21: Centre of pressure and moment coefficient curves.....	22
Figure 22: MAZAK CNC machine.....	24
Figure 23: Gantt Chart.....	26

Figure 24: USM Open-Circuit Wind Tunnel.....	28
Figure 25: Cessna 172 airplane.....	29
Figure 26: Airfoil design.....	30
Figure 27: Aircraft wing model with two hole and dimension is provided.....	31
Figure 28: 3D Aircraft wing model consists of 5 small pieces of aircraft wing models to be connected together.....	31
Figure 29: Aluminium block.....	32
Figure 30: Cutting process by using horizontal saw.....	32
Figure 31: Small pieces of aluminium blocks.....	33
Figure 32: Airfoil with excessive part of aluminium material.....	33
Figure 33: Complete airfoil shape.....	34
Figure 34: Bolt and nuts.....	34
Figure 35: Airfoil wing model to be connected to the perspex wall of the test section during the testing.....	35
Figure 36: Airfoil wing with an aluminium rod to be connected to the three components balance during the testing.....	35
Figure 37: Testing of single airfoil model.....	37
Figure 38: Testing of two airfoils model at a separating distance of 13cm (1 chord length).....	38
Figure 39: Testing of two airfoils model at a separating distance of 26cm (2 chord length).....	39
Figure 40: Graph of coefficient of lift versus angle of attack at 5m/s.....	41
Figure 41: Graph of coefficient of drag versus angle of attack at 5m/s.....	41
Figure 42: Graph of coefficient of lift versus angle of attack at 10m/s.....	43
Figure 43: Graph of coefficient of drag versus angle of attack at 10m/s.....	43
Figure 44: Graph of coefficient of lift versus angle of attack at 15m/s.....	45
Figure 45: Graph of coefficient of drag versus angle of attack at 15m/s.....	45
Figure 46: Graph of coefficient of lift versus angle of attack at 20m/s.....	47
Figure 47: Graph of coefficient of drag versus angle of attack at 20m/s.....	47
Figure 48: Graph of coefficient of lift versus angle of attack at 25m/s.....	49
Figure 49: Graph of coefficient of drag versus angle of attack at 25m/s.....	49

Figure 50: Graph of coefficient of lift versus angle of attack at 30m/s.....	51
Figure 51: Graph of coefficient of drag versus angle of attack at 30m/s.....	51
Figure 52: Graph of coefficient of lift versus Reynolds number at 0°.....	60
Figure 53: Graph of coefficient of drag versus Reynolds number at 0°.....	60
Figure 54: Graph of coefficient of lift versus Reynolds number at 2°.....	62
Figure 55: Graph of coefficient of drag versus Reynolds number at 2°.....	62
Figure 56: Graph of coefficient of lift versus Reynolds number at 4°.....	64
Figure 57: Graph of coefficient of drag versus Reynolds number at 4°.....	64
Figure 58: Graph of coefficient of lift versus Reynolds number at 6°.....	66
Figure 59: Graph of coefficient of drag versus Reynolds number at 6°.....	66
Figure 60: Graph of coefficient of lift versus Reynolds number at 8°.....	68
Figure 61: Graph of coefficient of drag versus Reynolds number at 8°.....	68
Figure 62: Graph of coefficient of lift versus Reynolds number at 10°.....	70
Figure 63: Graph of coefficient of drag versus Reynolds number at 10°.....	70
Figure 64: Graph of coefficient of lift versus Reynolds number at 12°.....	72
Figure 65: Graph of coefficient of drag versus Reynolds number at 12°.....	72
Figure 66: Graph of coefficient of lift versus Reynolds number at 14°.....	74
Figure 67: Graph of coefficient of drag versus Reynolds number at 14°.....	74
Figure 68: Graph of coefficient of lift versus Reynolds number at 16°.....	76
Figure 69: Graph of coefficient of drag versus Reynolds number at 16°.....	76
Figure 70: Graph of coefficient of lift versus Reynolds number at 18°.....	78
Figure 71: Graph of coefficient of drag versus Reynolds number at 18°.....	78
Figure 72: Graph of coefficient of lift versus Reynolds number at 20°.....	80
Figure 73: Graph of coefficient of drag versus Reynolds number at 20°.....	80

LIST OF TABLES

ITEMS	PAGE
Table 1: Radar separation.....	4
Table 2: Non-radar separation.....	5
Table 3: Open Circuit Wind Tunnel Specification.....	27
Table 4: Open Circuit Wind Tunnel Experimental Capabilities.....	28
Table 5: Three experiments conducted on the effect of wake.....	36
Table 6: Experimental results for three experiments at 5m/s.....	40
Table 7: Experimental results for three experiments at 10m/s.....	42
Table 8: Experimental results for three experiments at 15m/s.....	44
Table 9: Experimental results for three experiments at 20m/s.....	46
Table 10: Experimental results for three experiments at 25m/s.....	48
Table 11: Experimental results for three experiments at 30m/s.....	50
Table 12: Stall angle at various free stream velocity.....	52
Table 13: Coefficient of lift at stall angle at various free stream velocity.....	53
Table 14: Experimental results for three experiments when angle of attack is 0°.	59
Table 15: Experimental results for three experiments when angle of attack is 2°.	61
Table 16: Experimental results for three experiments when angle of attack is 4°.	63
Table 17: Experimental results for three experiments when angle of attack is 6°.	65
Table 18: Experimental results for three experiments when angle of attack is 8°.	67
Table 19: Experimental results for three experiments when angle of attack is 10°.....	69
Table 20: Experimental results for three experiments when angle of attack is 12°.....	71
Table 21: Experimental results for three experiments when angle of attack is 14°.....	73
Table 22: Experimental results for three experiments when angle of attack is	75

16°
Table 23: Experimental results for three experiments when angle of attack is 77
18°
Table 24: Experimental results for three experiments when angle of attack is 79
20°

CHAPTER 1

INTRODUCTION

1.1 BACKGROUND OF STUDY

Wake turbulence is generated by aircraft when it flies. The heavier the aircraft, the more severe the turbulence. This disturbance is caused by a pair of tornado-like counter-rotating vortices that trail from the tips of the wings. A vortex circulation is outward, upward and around the wing tips when viewed from either ahead of or behind the aircraft. The wake vortices generated from the aircraft pose problems to encountering aircraft. If an airplane flies directly into the trailing vortex shed by a preceding airplane, the circulatory flow will cause a drop in lift on one side of the wing and an increase on the other. The result is a rolling moment that can place the aircraft in a dangerous attitude. This is particularly true if the following aircraft is much smaller. Two counter rotating cylindrical vortices like those shown in figure 1 are created, which are hazardous to the following aircraft, especially during take off, initial climb, final approach and landing.

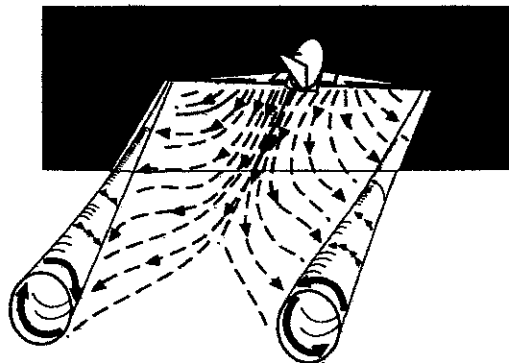


Figure 1: Wake vortex generation [1].

Since wake turbulence is only present when an airplane is generating lift, it is not present when an airplane is in contact with the ground. The turbulence begins when an airplane takes off, and ceases when an airplane touches down on landing. The wake turbulence is normally greatest near the tips of the wing because the lift per unit span decrease most rapidly there. Close to ground, the wake vortices tend to drift down and move sideways from the track of the generating aircraft but may rebound upwards as well as shown in Figure 2.

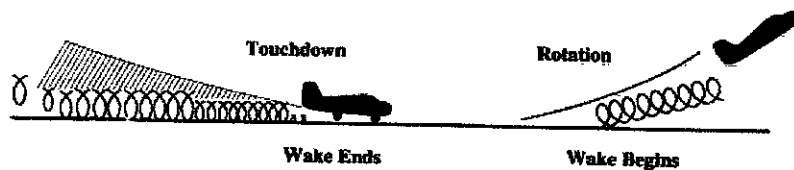


Figure 2: Wake ends and wake begins [1].

The effects of wake turbulence on an aircraft can be three types such as induced roll, loss of height and structural stress. Out of these three, induced roll is considered to have most dangerous effect on aircraft. Figure 3 shows a typical induced roll.

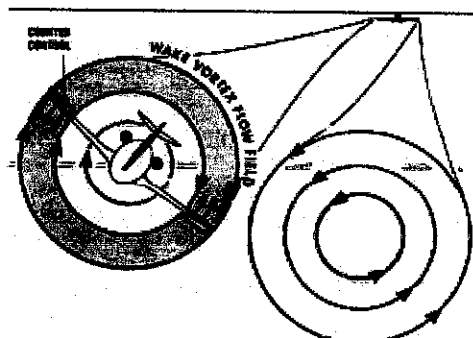


Figure 3: Induced roll [1].

Induced roll is especially dangerous during take-off and landing when there is little altitude or speed for recovery. The tests conducted by NASA have shown that the capability of an aircraft to counteract induced roll primarily depends on wingspan and counter control responsiveness. Even high performance aircraft, if they have a short wing span, may feel greatest induced roll effect and it is more difficult for such aircraft to counter the imposed roll induced by the vortex.

According to the reported roll angle, wake turbulence may be classified into the following three categories such as severe, moderate and slight. Severe means reported roll angle in excess of 30 degrees. Moderate represents reported roll angle of 10 to 30 degrees. Meanwhile, slight represents reported roll angle of less than 10 degrees [1].

The safety issue about the wake generated by an aircraft on a following aircraft is mainly concerned. Many accidents happened due to the aircraft entering the wake field of a preceding aircraft. Trailing vortices have certain behavioral characteristics which can help a pilot visualize the wake location and thereby take avoidance precautions. Vortices are generated from the moment aircraft leave the ground, since trailing vortices are a by-product of wing lift. Prior to takeoff or touchdown pilots should note the rotation or touchdown point of the preceding aircraft.

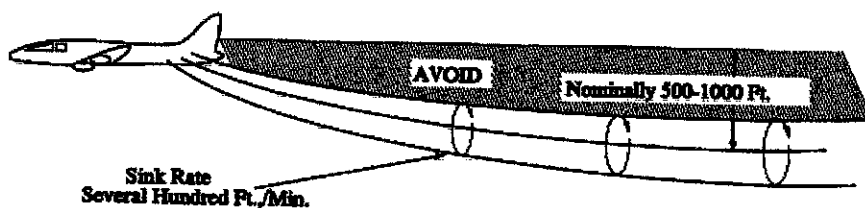


Figure 4: Vortex Flow Field [2].

The vortex circulation is outward, upward and around the wing tips when viewed from either ahead or behind the aircraft. Tests with large aircraft have shown that the vortices

remain spaced a bit less than a wingspan apart, drifting with the wind, at altitudes greater than a wingspan from the ground. In view of this, if persistent vortex turbulence is encountered, a slight change of altitude and lateral position (preferably upwind) will provide a flight path clear of the turbulence.

Flight tests have shown that the vortices from larger (transport category) aircraft sink at a rate of several hundred feet per minute, slowing their descent and diminishing in strength with time and distance behind the generating aircraft. Atmospheric turbulence hastens breakup. Pilots should fly at or above the preceding aircraft's flight path, altering course as necessary to avoid the area behind and below the generating aircraft. However, vertical separation of 1,000 feet may be considered safe [2].

For the purpose of assessing wake turbulence separation, aircraft are divided into three categories based on Maximum Certified Takeoff Weight (MCTOW) as heavy, medium and light. Meanwhile, wake turbulence separation is provided by Air Traffic Control (ATC) to all Aircraft which maybe affected by wake turbulence. ATC applies differing separations depending on the wake turbulence category of the leading aircraft and the equipment available to them to provide separation such as by using radar separation or by using non-radar separations [3].

Table 1: Radar separation [3].

Leading aircraft	Following aircraft	Separation (NM)
Heavy *	Heavy	4 NM
Heavy	Medium	5 NM
Heavy	Light	6 NM
Medium	Light	5 NM

Table 2: Non-radar separation [3].

Leading aircraft	Following aircraft	Separation time arriving	Separation time departing
Heavy	Medium	2 mins	2*mins
Heavy	Light	3 mins	2*mins
Medium	Light	3 mins	2*mins

1.2 PROBLEM STATEMENT

1.2.1 Problem Identification

The wake is a big threat on the safety of an aircraft. Many accidents happened due to the aircraft entering the wake field of a preceding aircraft. Investigation on the effects wing of an aircraft on a following similar wing is the matter of this project.

1.2.2 Significance of the Project

Wake turbulent generated by the aircraft will affect the following aircraft which encountering the wake field. In order to avoid accidents among aircraft due to wake turbulence, there are some rules and regulations which must be followed by the pilots such as separation distance. If a pilot accepts a clearance to visually follow a preceding aircraft, the pilot accepts responsibility for separation and wake turbulent avoidance. Communication with the airport traffic control tower is significant too to get additional information.

1.3 OBJECTIVES AND SCOPE OF STUDY

1.3.1 The Relevancy of the Project

The objectives of this project are stated clearly as follows:

- (a) To study the aerodynamics effects of the wake field on wing section.
- (b) To study the changes in aerodynamics on the wing section when another wing section is preceding it.
- (c) Varying the separating distance with respect to the wing span to study the changes in aerodynamics.

The scope of this project is to undergo a literature research to study and collect information relevant to the wake turbulent on an aircraft, further discussion and analysis of the results of experiment at the wind tunnel. I hope the improvement on the wing section compare to the previous project can lead to better results from the experiment on the wind tunnel. A good and accurate data gathered from this research can be used in the future to prevent the accident due to wake turbulence.

1.3.2 Feasibility of the Project within the Scope and Time Frame

A numbers of studies and simulations on the effects of the wake of an aircraft on a following aircraft have been carried out. So, there are a lot of information regarding this topic can be found from journals, articles, internet, reference book and previous final year thesis. Thus, this project is a feasible project within the scope and time frame.

CHAPTER 2

LITERATURE REVIEW AND THEORY

2.1 FORCES ACTING ON AIRCRAFT

There are four types of forces acting on an aircraft. To sustain an aircraft in the air in steady and level of flight, it is necessary to generate an upward lift force which must exactly balance the weight, as illustrated in Figure 5. The lift exactly balances the weight, and the engine thrust is equal to the drag.

Aircraft do not always fly steady and level, however, and it is often necessary to generate a force that is not equal to the weight, and not acting vertically upwards, as for example, when pulling out of a dive. Therefore, as illustrated in Figure 6, we define lift more generally, as a force at the right angles to the direction of flight. Only in steady level flight is the lift force exactly equal in magnitude to the weight, and directed vertically upwards. It should also be remembered that, as shown in Figure 6, an aircraft does not always point in the direction that it is traveling [4].

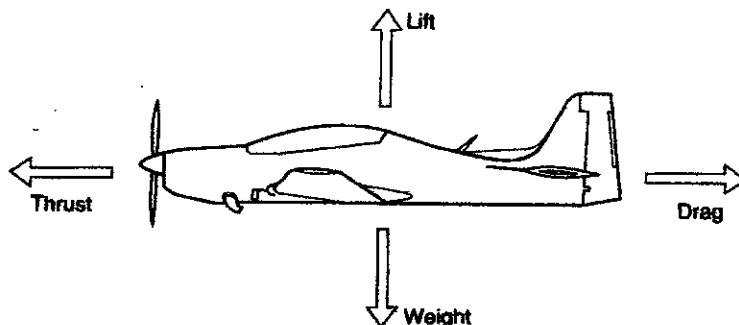


Figure 5: Forces on aircraft in steady level flight [4].

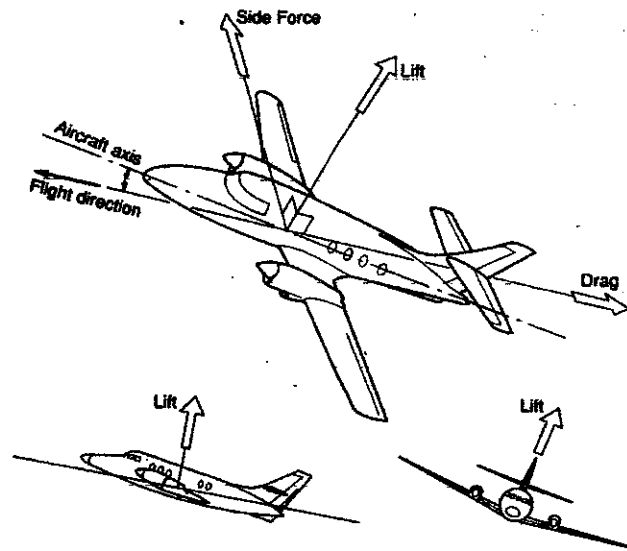
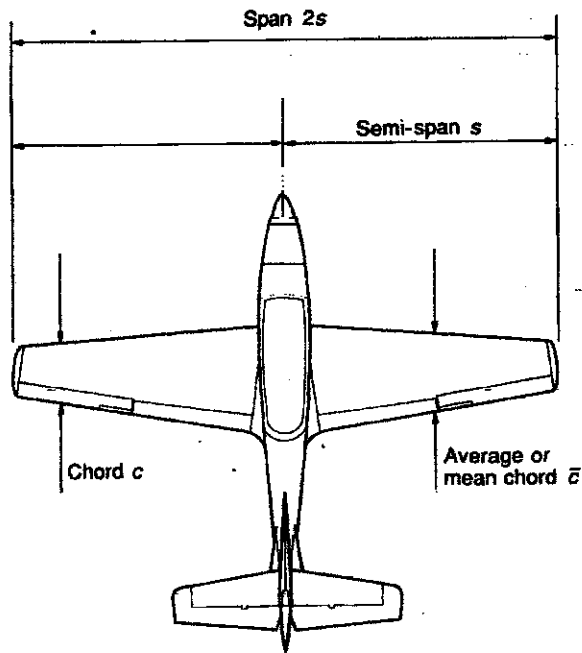


Figure 6: The direction of the aerodynamic forces [4].

Drag is really made up from only two basic constituents, a component of the force due to the pressure distribution, and a force due to viscous shearing. The contribution such as trailing vortex drag act by modifying the pressure distribution or shear forces, and so the contributions are not entirely independent of each other, as is often conveniently supposed.

2.2 AIRCRAFT WING AND AEROFOIL SECTION

The ratio of the overall wing span (length) to the average chord (width) is known as its aspect ratio. The terms span and chord are defined in Figure 7. A wing such as that shown in Figure 8, has a high aspect ratio, while Concorde, shown in plan view in Figure 9, is rare example of an aircraft with a wing aspect ratio of less than 1. The early pioneers noted that the wing of birds always have a much greater span than the chord. Simple experiments confirmed that high aspect ratio wings produced a better ratio of lift to drag than short stubby ones for flight at subsonic speeds [5].



$$\text{Aspect ratio} = \frac{\text{Span}}{\text{Mean chord}} = \frac{\text{Span}^2}{\text{Area}}$$

Figure 7: Wing geometry [5].

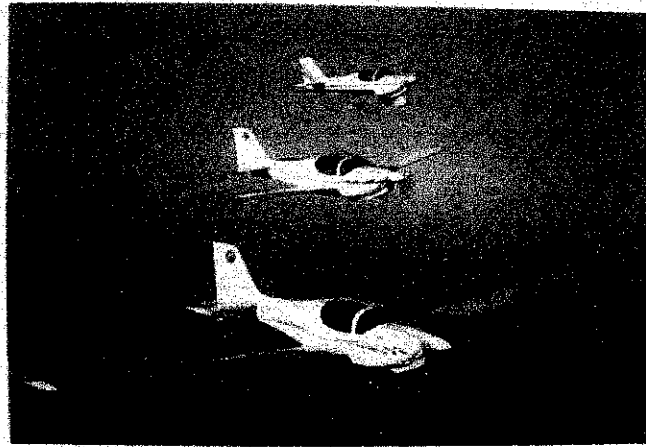


Figure 8: High aspect ratio on the powered glider version of the Europa (lowest aircraft) [5].

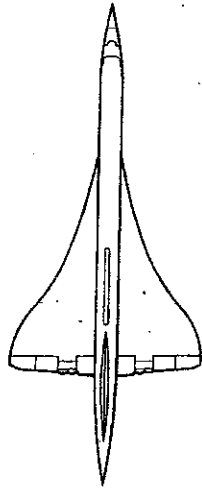


Figure 9: Plan view of Concorde [5].

On a curved aerofoil it is not particularly easy to define this angle, since we must first decide on some straight line in the aerofoil section from which we can ensure the angle to the direction of the airflow. Unfortunately, owing to the large variety of shapes used as aerofoil sections it is not easy to define this chord line to suit all aerofoils. Nearly all modern aerofoils have a convex under-surface; and the chord must be specially defined, although it is usually taken as the line joining the leading edge to the trailing edge. This is the centre in the particular case of symmetrical aerofoils.

We call the angle between the chord of the aerofoil and the direction of the airflow the angle of attack as shown in Figure 10 [6].

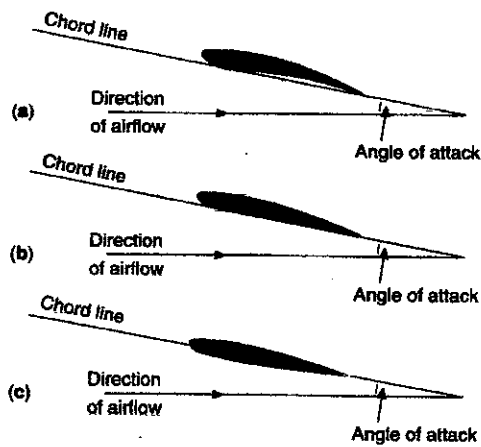


Figure 10: Chord line and angle of attack [6].

(a) Aerofoil with concave undersurface.

(b) Aerofoil with flat undersurface.

(c) Aerofoil with convex undersurface.

2.3 AIR FLOW AROUND AN AEROFOIL SECTION

For most wing sections, the amount of lift generated is directly proportional to the angle of attack, for small, angles; the graph of C_L against angle of attack is a straight line, as shown in Figure 11. The increase in lift due to camber is almost independent of the angle of attack. However, as illustrated, a point is reached where the lift starts to fall off. This effect is known as stalling. The fall-off may occur quite sharply, as in Figure 11 which shows the variation of lift coefficient with angle of attack for a wing with a moderately thick aerofoil section (15 percent thickness to chord ratio) [7].

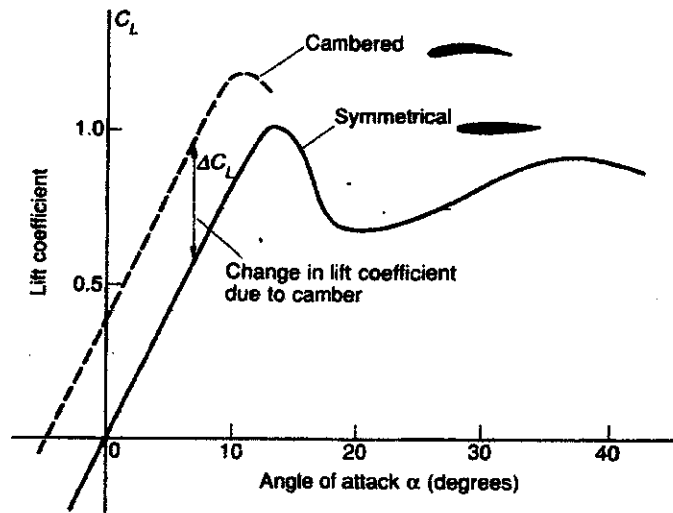


Figure 11: Variation of lift with angle of attack and camber [7].

A sudden loss in lift can obviously have disastrous consequences, particularly if it happens without warning. Stalling occurs when the air flow fails to follow the contours of the aerofoil and becomes separated, as illustrated in Figure 12 and 13.

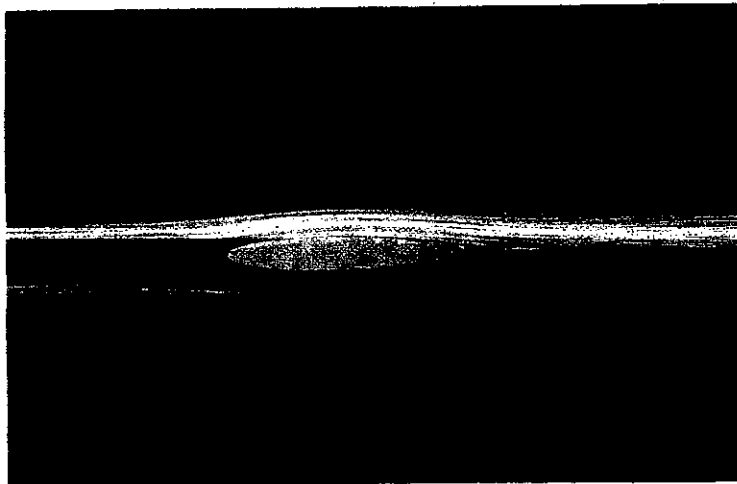


Figure 12: Flow follows the contour of the section [7].

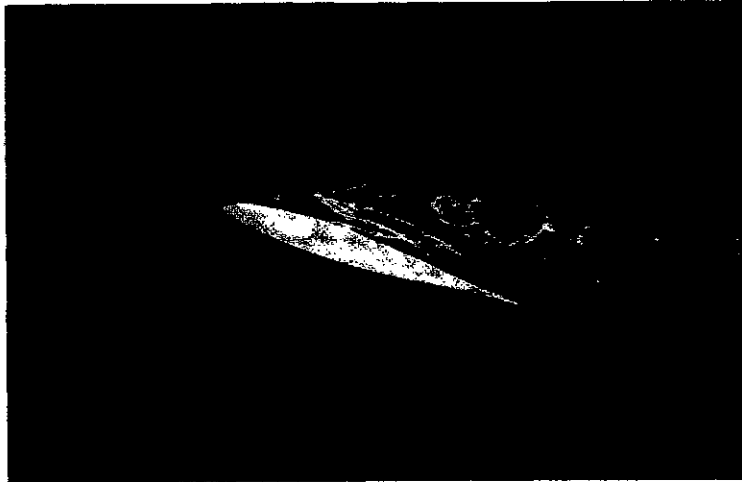


Figure 13: Flow separation [7].

At large angles of attack, the flow fails to follow the contours of the section and separates leaving a highly turbulent wake. Once the flow separates, the leading edge suction and associated tangential force component are almost completely lost. Therefore, the resultant force due to pressure does act more or less at right angles to the surface, so there is a significant rearward drag component. The onset of stall is thus accompanied by an increase in drag. Unless the thrust is increased to compensate, the aircraft will slow down, further reducing the lifting ability of the wing. After the stall has occurred, it may be necessary to reduce the angle of attack to well below the original stalling angle, before the lift is fully restored.

From an aeronautical point of view, it is the wing boundary layer that is of greatest importance, as in Figure 14 we show a typical example of how the boundary layer develops on an aerofoil. It will be seen that the thickness of this layer grows with distance from the front or leading edge.

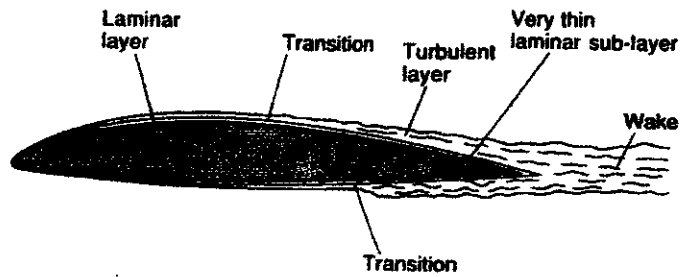


Figure 14: Boundary layer growth on a thin aerofoil [5].

There are two distinct types of boundary layer flow. Near the leading edge, the air flows smoothly in a streamlined manner, and appears to behave rather like a stack of flat sheets or laminar sliding over each other with friction. This type of flow is, therefore, called laminar flow. Further along, as indicated in Figure 14, there is a change or transition to a turbulent type in which a random motion is superimposed on the average flow velocity.

In a laminar boundary layer, molecules from the slow-moving air near the surface mix and collide with those further out, tending to slow more the flow. The slowing effect produced by the surface thus spreads outwards, and the region affected, the boundary layer, becomes progressively thicker along the direction of the flow.

At the position called transition, instability develops, and the flow in the layer becomes turbulent. In the turbulent boundary layer, eddies form that are relatively large compared to molecules, and the slowing down process involves a rapid mixing of fast and slow-moving masses of air. The turbulent eddies extend the influence outwards from the surface, so the boundary layer effectively become thicker. Very close to the surface, there is a thin sub-layer of laminar flow.

Just as the surface slows the relative motion of the air, the air will try to drag along the surface along with the flow. The whole process appears rather similar to the friction

between solid surfaces and is known as viscous friction. It is the process by which surface friction drag is produced.

The surface friction drag force depends on the rate at which the air adjacent to the surface is trying to slide relative to it. In the case of the laminar boundary layer, the relative air speed decreases steadily through the layer. In the turbulent layer, however, air from the outer edge of the layer is continually being mixed with the slower-moving air, so that the average air speed close to the surface is relatively high. Thus, the turbulent layer produces the greater amount of drag for a given thickness of layer.

Pressure varies around a wing section. The top portion of an aircraft wing has a curved surface, while the lower portion is almost flat. Since the top of the wing is curved, the distance from the leading edge of the wing to the trailing edge is further along the upper surface than it is along the lower surface. This means that molecules of air must travel farther and thus faster, along the top of the wing than the bottom. According to Bernoulli's theorem, the faster air results in a lower pressure on the top of the wing, thus lifting the wing by a form of suction. As the moving air departs the wing from the trailing edge and wing tips, the upper low pressure air meets the lower high-pressure air and the result is turbulence. In this research project, the wake turbulence generated by an aircraft wing on a following aircraft wing is mainly concerned [8].

Figure 15(a) shows a typical low speed wing section under normal flight conditions. The pressure reaches its minimum value at a point A, somewhere around the position of maximum thickness on the upper surface. After this, the pressure gradually rises again, until it returns to a value close to the original free-stream pressure, at the trailing edge at B. This means, that over the rear part of the upper surface, the air has to travel from low to high pressure. The air can do this by slowing down and giving up some of the extra kinetic energy that is possessed at A, according to the Bernoulli relationship $p + \rho V^2$ is constant. Close to the surface, in the boundary layer, however, some of the available energy is dissipated in friction, and the air can no longer return to its original free-stream conditions at B. If the increase in pressure is gradual, then the process of turbulent

mixing or molecular impacts allows the outer layers to effectively pull the inner ones along. The boundary layer merely thickens, leaving a slow-moving wake at the trailing edge, as in Figure 15(a).

If the rate of increase in pressure is rapid, the mixing process is too slow to keep the lower part of the layer moving, and a dead-water region starts to form. The boundary layer flow stops following the direction of the surface, and separates, as shown in Figure 15(b). Air particles in the dead-water region tend to move forwards the lower pressure, in the reverse direction to the main flow. This mechanism is the primary cause of stalling. As the aerofoil angle of attack is increased, the pressure difference between A and B increases, and the separation position moves forward, as in Figure 15(c).

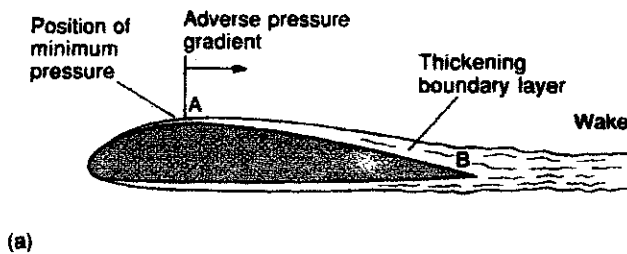


Figure 15(a): Boundary layer separation at low angle of attack [5].

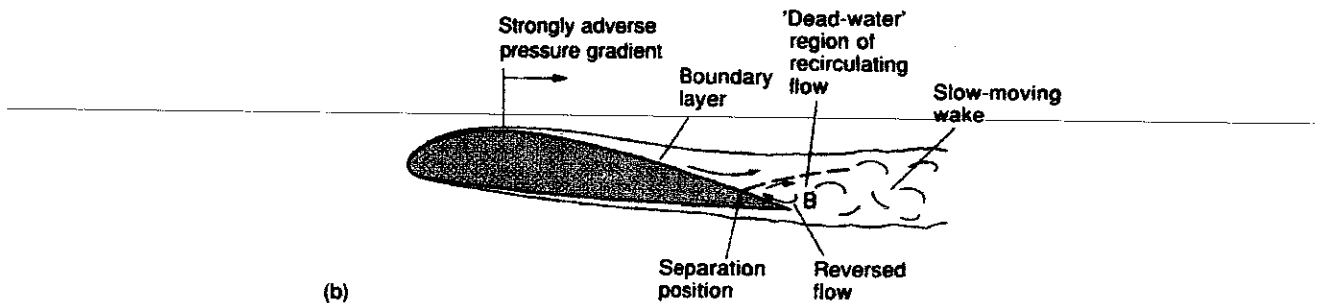


Figure 15(b): Boundary layer separation at higher angles of attack [5].

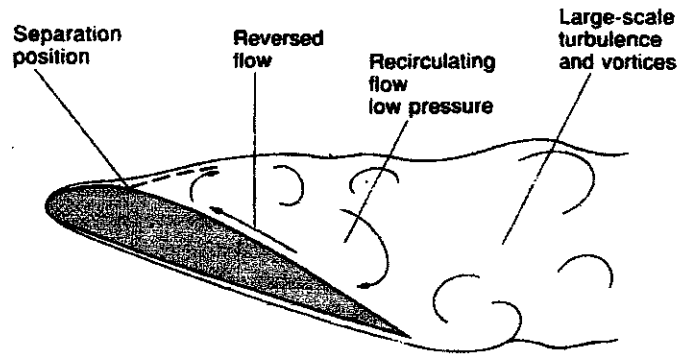


Figure 15(c): Boundary layer separation as the angles of attack increases [5].

2.4 AEROFOIL CHARACTERISTICS

The shape of aircraft wing is determined by the airfoil. Airfoil is the cross-sectional shape of the aircraft wing as defined as by the intersections with planes parallel to the free stream and normal to the plane of the wing. The characteristics of airfoil is significant with the leading edge should be rounded, with the radius of curvature sufficiently high to avoid excessive suction. Then, the trailing edge must be sharp in order to establish the Kutta-Joukowski condition. A substantial radius at the trailing edge of an airfoil at an angle of attack could allow the fluid to flow part of the way from the lower surface to the upper surface without excessive velocities. This would reduce the circulation and lift [9].

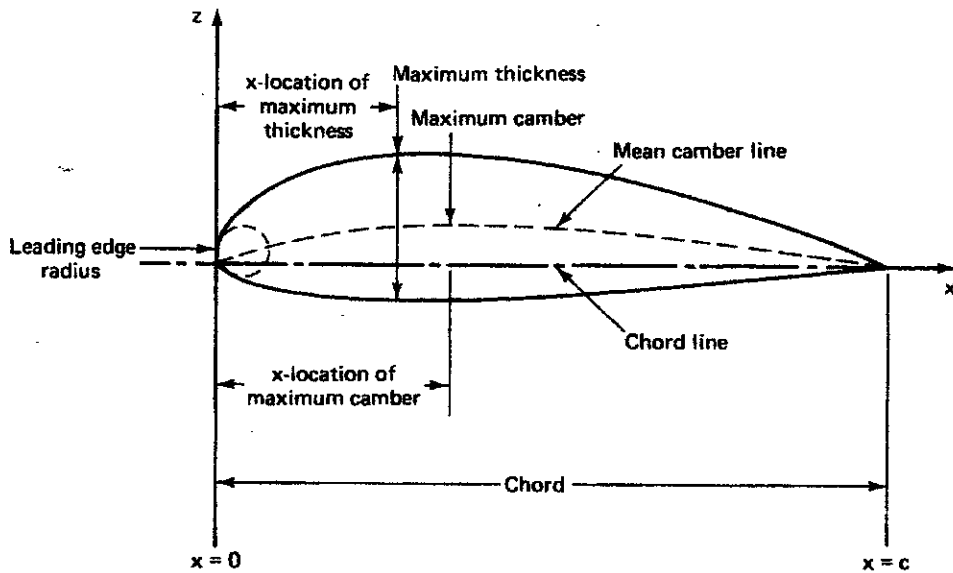


Figure 16: Airfoil geometric parameters [9].

Different mathematical equations described the curvature of the mean line between the upper and lower surfaces. Camber is the amount of curvature. It is usually expressed in terms of the maximum mean line ordinate as a percent of chord. The NACA (National Advisory Committee for Aeronautics) airfoil series are the most widely used. NACA provides a lots of airfoil design for various type of aircraft application.

In this research project, the airfoil model is determined by the shape of NACA 4 digits profiles. The shape of NACA 4 digits profiles is determined by 3 important parameters. The first digit of NACA 4 digits profiles represents the camber and the second digit represents the position of camber. Meanwhile, the last two digits of the NACA 4 digits profiles represent the thickness in percent. The profiles without a camber are symmetrical in shape.

The flow separation near the leading edge of the airfoil produces deviations (high drag and low lift) from the ideal flow predictions at the high angles of attack. Hence, experiment in wind tunnel tests are always made to evaluate the performance of a given

type of airfoil section. For example, the experimentally determined values of lift coefficient versus angles of attack for two airfoils are shown in Figure 17.

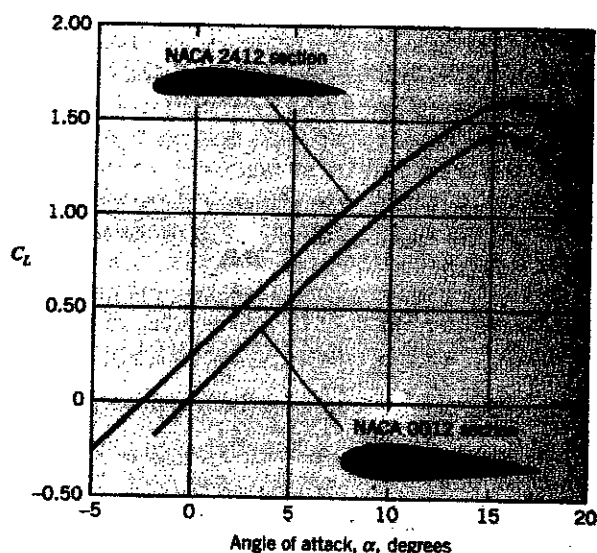


Figure 17: Values of C_L for two NACA airfoil sections [9].

Note that coefficient of lift increase with the angle of attack to a maximum value and decrease with further increase of angle of attack. This condition where lift coefficient start to decrease with a further increase in angle of attack is called stall. Stall occurs because of the onset of separation over the top of the airfoil, which changes the pressure distribution in such a way not to decrease lift but also to increase drag [10].

The easiest way of setting out the results of experiments on aerofoil sections is to draw curves showing how the lift coefficient, the drag coefficient, the ratio of lift to drag and the position of the centre of pressure, or the pitching moment coefficient alters as the angle of attack is increased over the ordinary angles of flight. It is much satisfactory to plot the coefficients of the lift, drag and pitching moment rather than the total lift, drag and pitching moment, because the coefficients are practically independent of the air density, the scale of the aerofoil and the velocity used in the experiment, whereas the

total lift, drag and moment depend on the actual conditions at the time of the experiment. In other words, suppose we take a particular aerofoil section and test it on different scales and different velocities in various wind tunnels throughout the world, and also full scaled in actual flight, we should in each case obtain the same curves showing how the coefficients changes with the angle of attack [11].

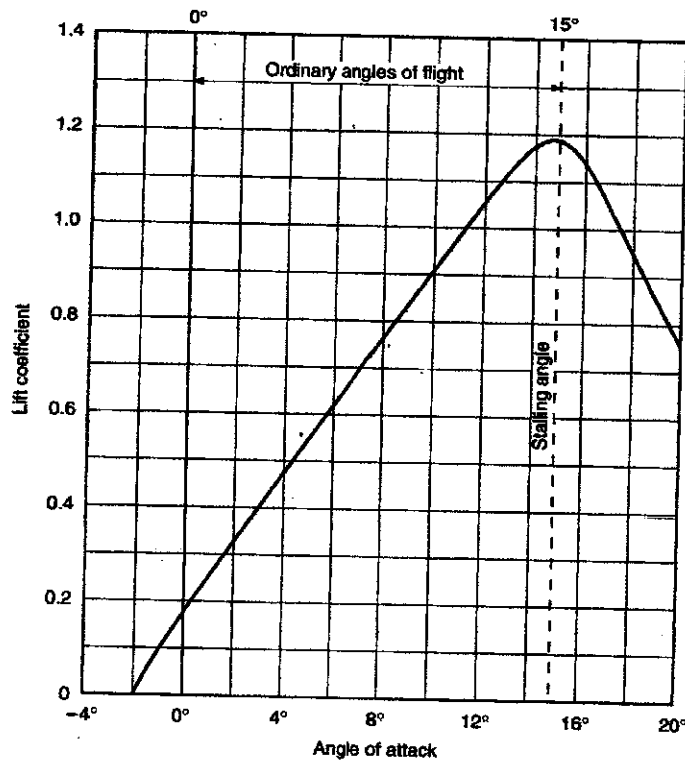


Figure 18: Lift Curve [11].

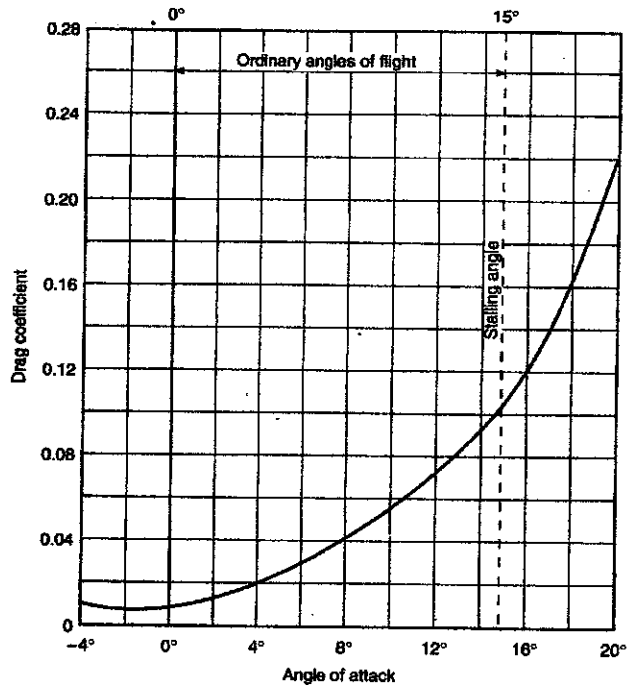


Figure 19: Drag Curve [11].

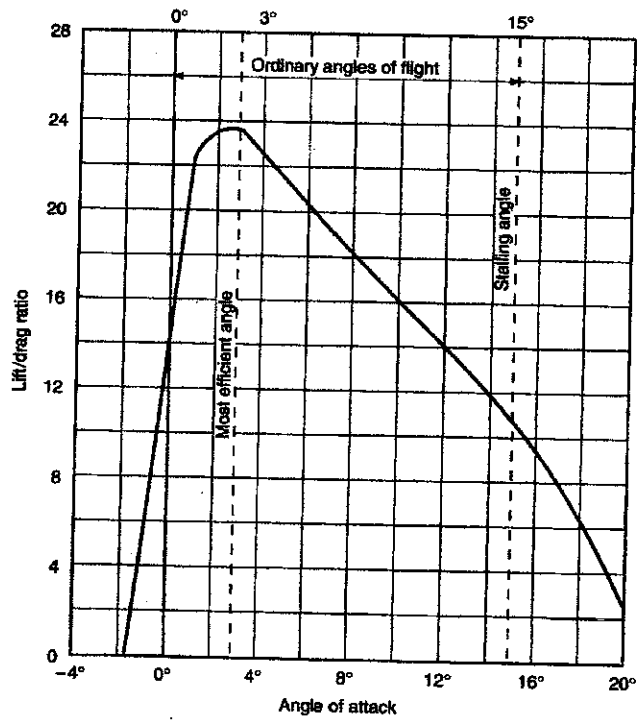


Figure 20: Lift/Drag Curve [11].

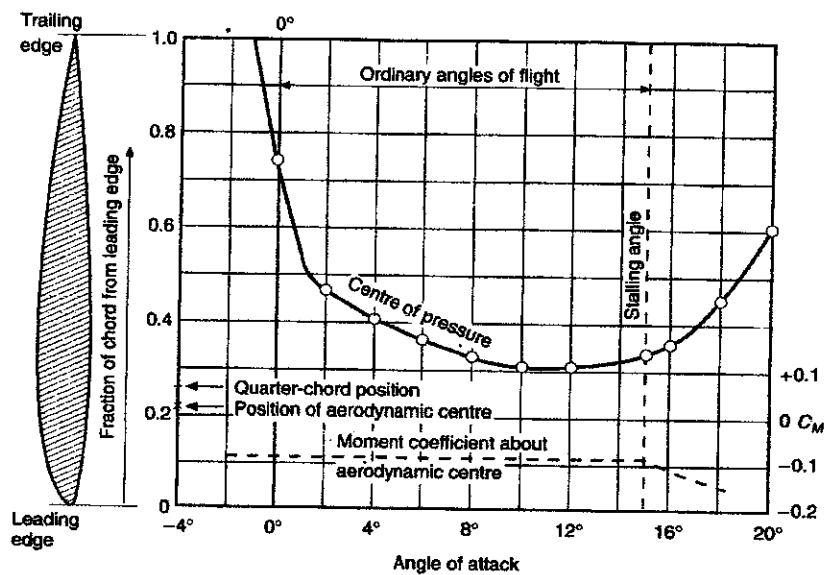


Figure 21: Centre of pressure and moment coefficient curve [11].

CHAPTER 3

METHODOLOGY/PROJECT WORK

3.1 PROCEDURE IDENTIFICATION

There are few procedures used to gather the information and study about the effects of wake turbulence of an aircraft on the following aircraft such as:

- (a) Own research on previous available case studies such as case studies from journals, internet and final year thesis.
- (b) Selection of airfoil model.
- (c) Drawing of the airfoil by using AutoCAD program.
- (d) Fabrication of the airfoil by using the CNC machine available at the lab.
- (e) Testing models in wind tunnel
 - (i) The experiment to observe the drag and lift forces around the airfoil models at variable air stream.
 - (ii) The experiment to observe the relation between Reynold's Number with drag and lift coefficient at variable air stream velocity.
- (f) Discussion and analysis will be based on the results obtained from the experiment in wind tunnel. The measurement will be recorded and graph to be plotted.

3.2 PROJECT ACTIVITIES

3.2.1 Drawing

The airfoil model is drawn by using AutoCAD program in order to get the accurate shape and dimension.

3.2.2 Equipment

After the drawing process, the aircraft wing models are fabricated by using the CNC machining. The MAZAK CNC machine as shown in Figure 22 is available at the block 16 of Mechanical Engineering Department in UTP for the fabrication of aircraft wing.

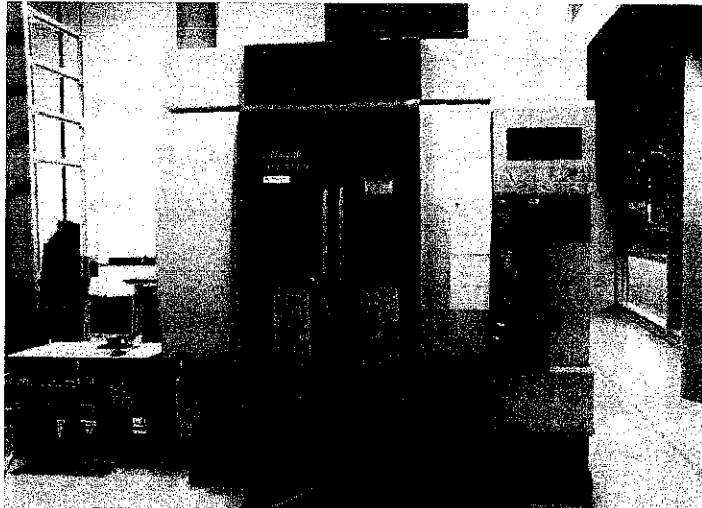


Figure 22: MAZAK CNC machine.

3.2.3 Material

Besides, aluminium is chosen as the material for the aircraft wing. Aluminium is suitable for CNC machining and it is available at the lab. It can provide a good surface finish to the aircraft wing too. A good surface finish of the aircraft wing is important in this project because it may affect air passes through the surface of aircraft wing during the experiment in the wind tunnel. Any unnecessary disturbance must be avoided in order to obtain better results throughout the experiment.

3.3 TOOLS REQUIRED

The tools required are a wind tunnel calibrated equipment and at least two aerofoil wings for the experimental purposes.

3.4 GANTT CHART

ID	Task Name	Start	Finish	Duration	Jan 2009		Feb 2009					Mar 2009				Apr 2009				
					1/18	1/25	2/1	2/8	2/15	2/22	3/1	3/8	3/15	3/22	3/29	4/5	4/12	4/19	4/26	
					Gantt Chart Visualization															
1	Fabrication of Aircraft Wing by CNC Machining	1/19/2009	1/30/2009	1.71w	[Task Bar]															
2	Process of Completion of Aircraft Wing	2/2/2009	2/7/2009	.86w	[Task Bar]															
3	Drilling of Holes at Aircraft Wing	2/9/2009	2/13/2009	.71w	[Task Bar]															
4	Submission of Progress Report 1	2/16/2009	2/20/2009	.71w	[Task Bar]															
5	Discussion about Fixing Aircraft Wing in Wind Tunnel	2/23/2009	2/27/2009	.71w	[Task Bar]															
6	Literature Review Based on Previous Works	3/2/2009	3/6/2009	.71w	[Task Bar]															
7	Submission of Progress Report 2	3/9/2009	3/13/2009	.71w	[Task Bar]															
8	Seminar	3/16/2009	3/20/2009	.71w	[Task Bar]															
9	Testing of Aircraft Wing in Wind Tunnel	3/23/2009	3/27/2009	.71w	[Task Bar]															
10	Testing of Aircraft Wing in Wind Tunnel + Submission of Poster	3/30/2009	4/3/2009	.71w	[Task Bar]															
11	Testing of Aircraft Wing in Wind Tunnel	4/6/2009	4/10/2009	.71w	[Task Bar]															
12	Discussion of Testing Results	4/17/2009	4/17/2009	.14w	[Task Bar]															
13	Submission of Soft Bound Dissertation	4/20/2009	4/26/2009	1w	[Task Bar]															
14	Oral Presentation	4/20/2009	4/24/2009	.71w	[Task Bar]															
15	Submission of Hard Bound Dissertation	4/27/2009	5/1/2009	.71w	[Task Bar]															

Legend

1. Task Bar [Task Bar Icon]

Figure 23: Gantt Chart.

CHAPTER 4

RESULTS AND DISCUSSION

4.1 DESCRIPTION OF THE OPEN CIRCUIT WIND TUNNEL

The main characteristics and capabilities of the wind tunnel are shown in Table 3 and Table 4:

Table 3: Open Circuit Wind Tunnel Specification.

No	Item	Specification
1.	Type of Tunnel	Open circuit, low speed, suction
2.	Mach Number	0.1
3.	Test Section	300H x 300W x 600L mm
4.	Overall Dimension	1900H x 1400W x 5500L mm
5.	Max Speed in the Test Section	36m/s equal to 130km/h
6.	Drive	Two-stage fan, 1500rpm DC motor
7.	Motor	Two 3 phase, 3kW, cage type, 380V, 50Hz, 1440rpm motors
8.	Power Requirement	AC, 3ph 415 volts, 30 Amps Electrical supply with neutral and earth connection
9.	Material of Construction	Each section is made of painted steel, lengthwise welded. The whole duct is supported by a basement in rectangular steel sections.

Table 4: Open Circuit Wind Tunnel Experimental Capabilities.

No	Testing Capabilities
1.	Drag and lift measuring of models or of aerofoil with adjustable inclination in respect of the wind.
2.	Pressure distribution measurement on the aerofoil or on other models.
3.	Visualization of streamlines inside the test section by using the smoke generator.

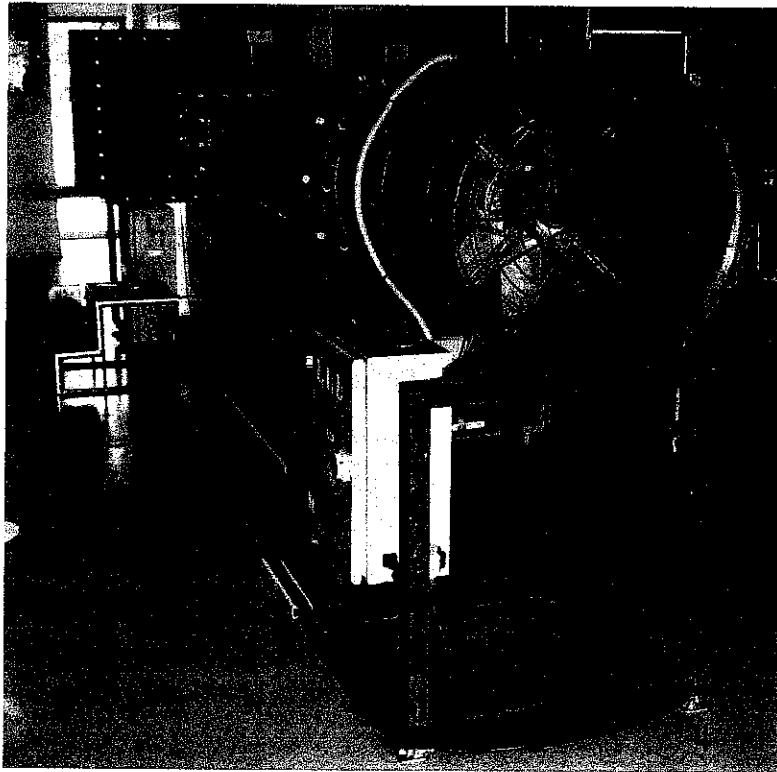


Figure 24: USM Open-Circuit Wind Tunnel.

Besides, the components of the USM Open-Circuit Wind Tunnel are shown in Appendix III too.

4.2 SELECTION OF AIRFOIL WING TYPE

The Cessna 172 as shown in Figure 25 is a general aviation airplane used primarily for flight, touring and personal flying. NACA2412 airfoil wing type is used in Cessna 172 airplane. NACA2412 airfoil wing type is selected to be tested through out completing this project.

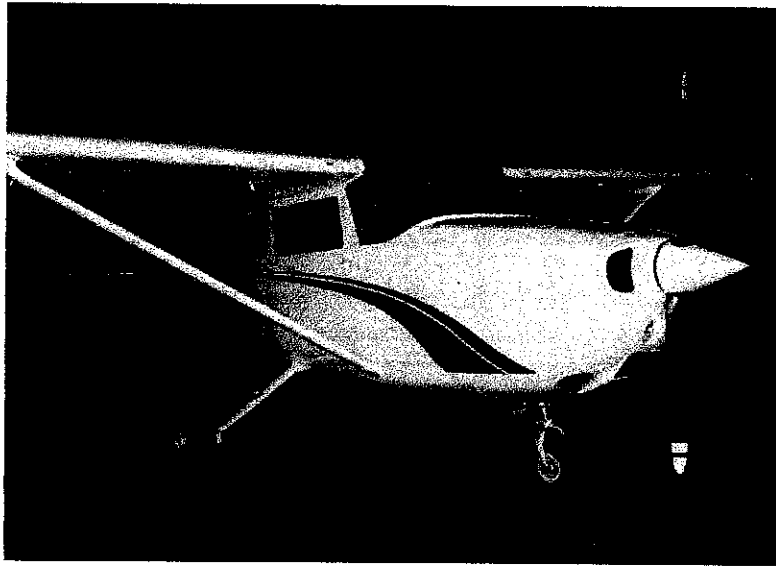


Figure 25: Cessna 172 airplane [12].

4.3 DESIGN OF NACA2412 WING TYPE MODEL

NACA 2412 is chosen as the design of the aircraft wing in this project. The design of the airfoil is taken from NACA (National Advisory Committee for Aeronautics). The design of airfoil NACA 2412 represents the profiles is not symmetrical in shape, 4 is the position of the camber and 12% is the percentage of the thickness.

Before proceeding with the drawing, the design of the airfoil is obtained from the NACA 4 digits series generator. NACA 4 digits series generator provides the x and y coordinates of the design of the airfoil [13]. Then, the x and y coordinates generated from the NACA 4 digits series generator is used to draw the airfoil by using AutoCAD program. After inserting all the coordinates into AutoCAD program, the coordinates are joined to get the shape of the airfoil design as shown in Figure 26.

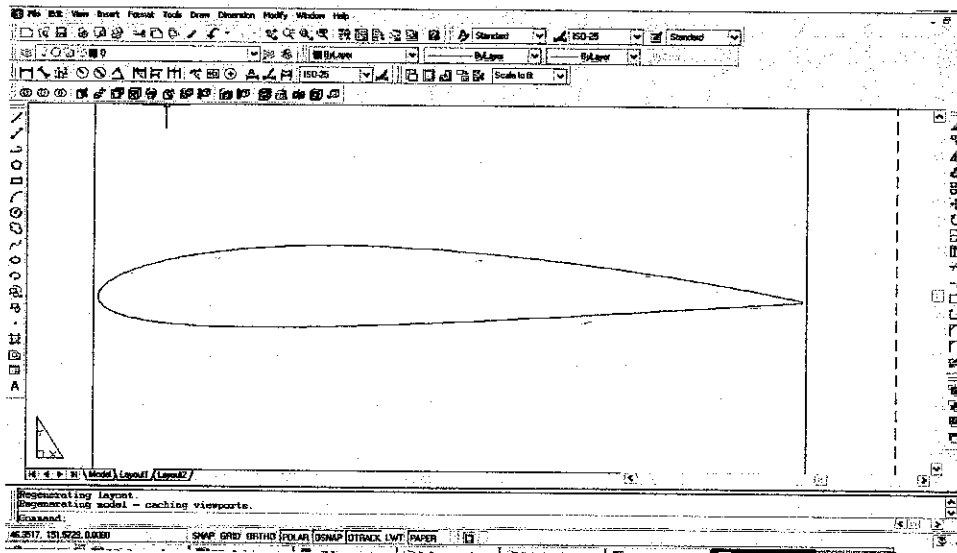


Figure 26: Airfoil design.

The airfoil design of NACA2412 is prepared by using AutoCAD program. Due to the limitation of CNC machining, two holes are drilled at each aircraft wing model in order

to connect all five pieces of aircraft wing as shown in Figure 27. The diameter of the hole is 6.2mm and the chord length is 130mm.

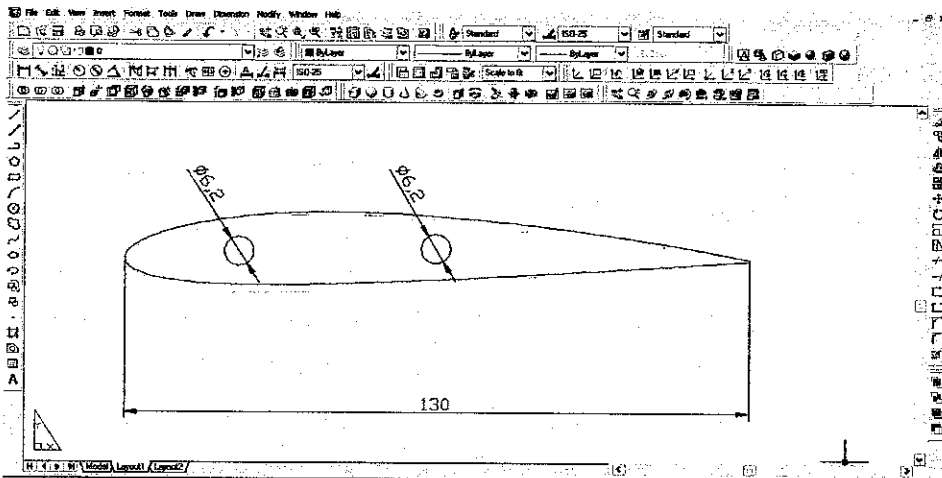


Figure 27: Aircraft wing model with two hole and dimension is provided.

The complete aircraft wing model with a depth of cut of 20cm is made from five small pieces of aircraft wing models. The depth of cut of each small pieces of aircraft wing model is 4cm. All five small pieces of aircraft wing models are to be connected as shown in Figure 28.

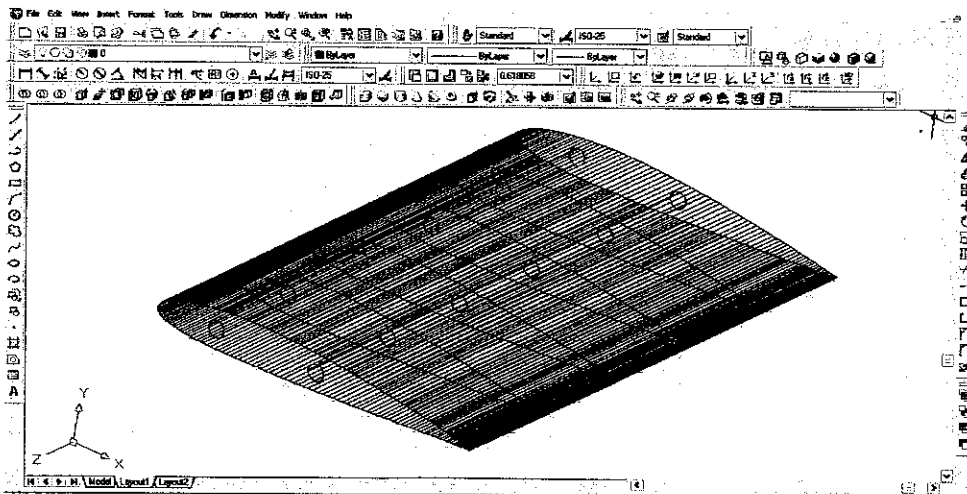


Figure 28: 3D Aircraft wing model consists of 5 small pieces of aircraft wing models to be connected together.

4.4 FABRICATION OF NACA2412 AIRFOIL TYPE MODEL

The material used in fabrication of NACA2412 airfoil wing is aluminium. The aluminium material is available in UTP Manufacturing Lab as shown in Figure 29.

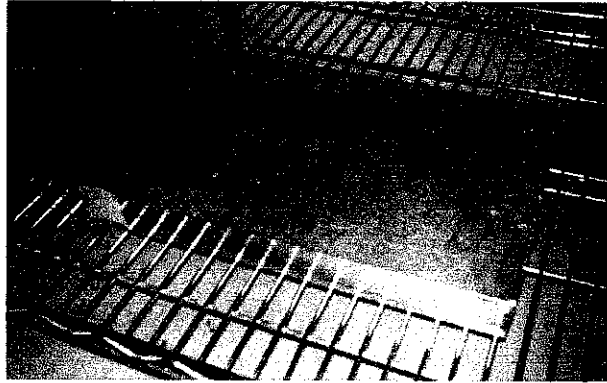


Figure 29: Aluminium block.

The size of the aluminum block is too big and not suitable for the CNC machining process. So, the aluminium block is cut into the required size which is 15cm x 7cm x 2cm by using the horizontal band saw as shown in Figure 30. The aluminium block is cut into a total of 10 small pieces. The small aluminum blocks are shown in Figure 31.

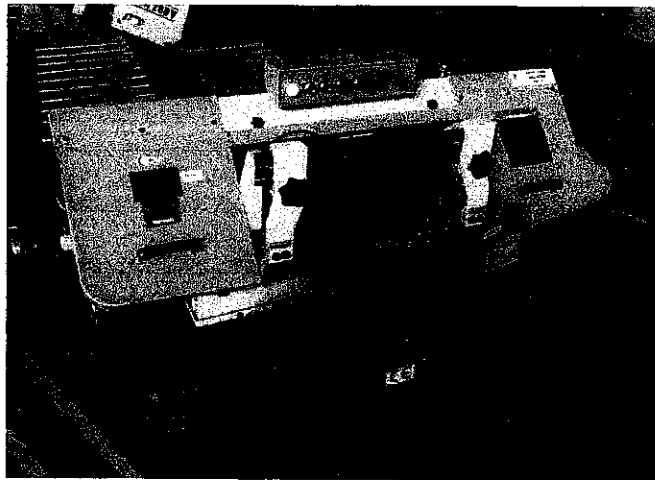


Figure 30: Cutting process by using horizontal saw.

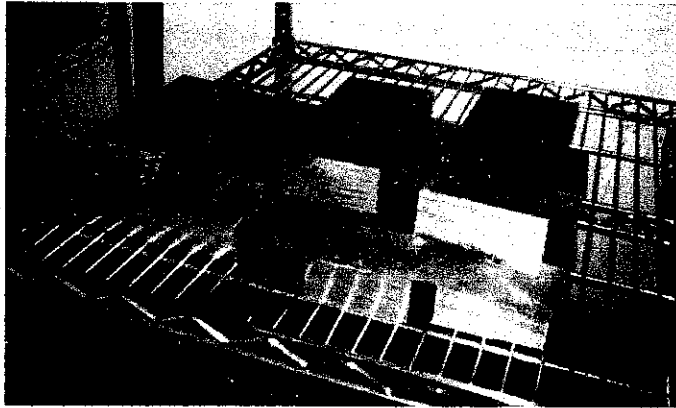


Figure 31: Small pieces of aluminium blocks.

Then, the small pieces of aluminium blocks are ready for the MAZAK CNC machining. Each small piece of aluminium block is cut into the required airfoil shape as shown in Figure 32. The excessive aluminium material at the bottom of the airfoil is cut again in order to get the complete airfoil shape as shown in Figure 33.

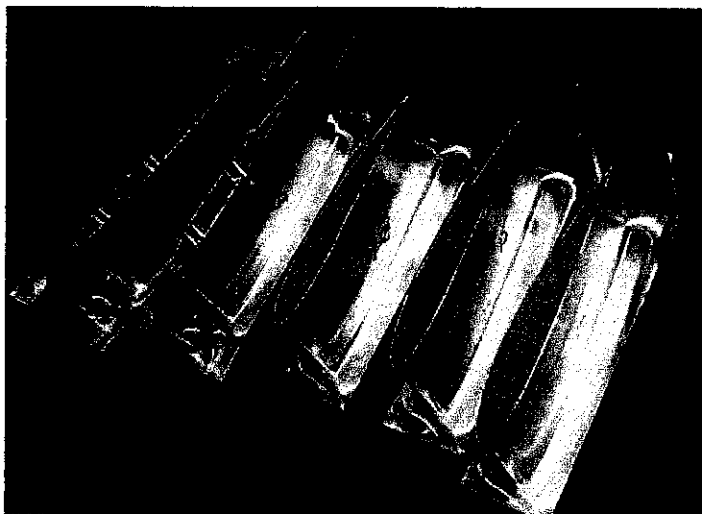


Figure 32: Airfoil with excessive part of aluminium material.

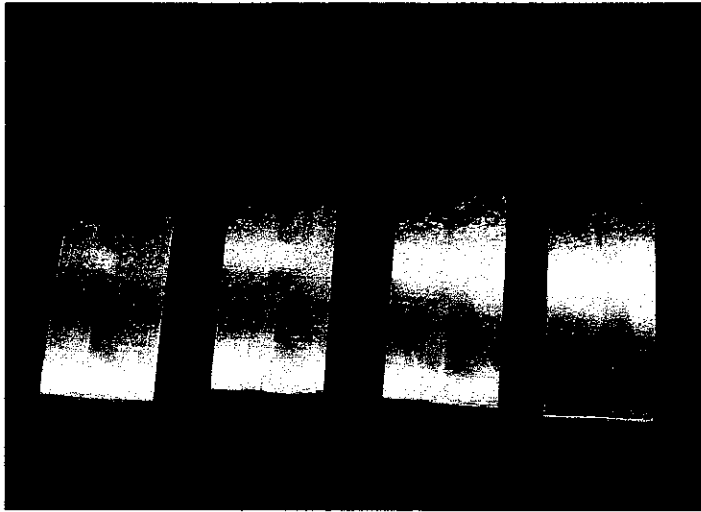


Figure 33: Complete airfoil shape.

Then, the bolt and nut are used to assemble the small pieces of airfoil into a complete airfoil wing. The bolt and nuts are shown in Figure 34.

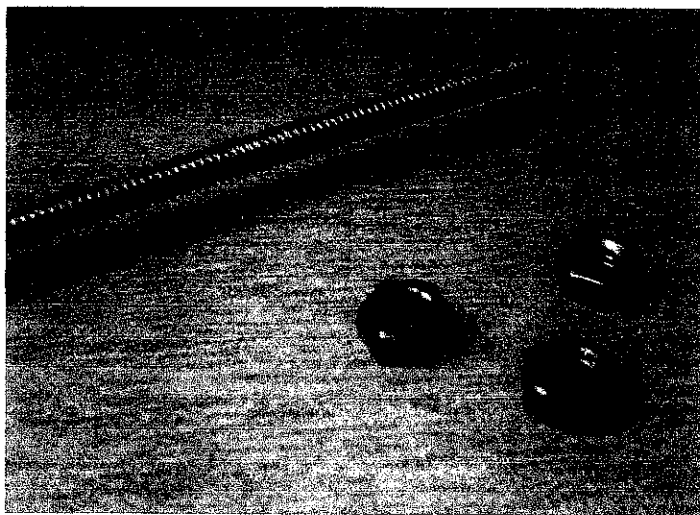


Figure 34: Bolt and nuts.

Lastly, the complete airfoil wings are shown in Figure 35 and Figure 36. The airfoil wing model shown in Figure 35 is fixed at the perspex wall of the wind tunnel test section during the testing. Meanwhile, the airfoil wing model shown in Figure 36 is welded with an aluminium rod to be connected to the three components balance to measure the lift and drag forces exerted on this airfoil wing during the testing. Appendix VI shows the details of the perspex wall of the test section.

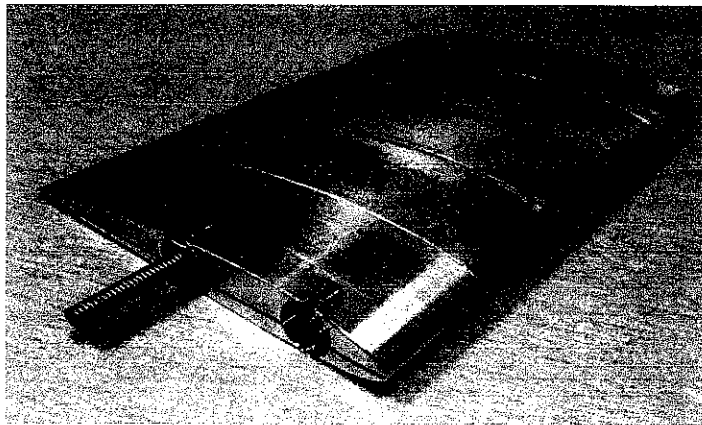


Figure 35: Airfoil wing model to be connected to the perspex wall of the test section during the testing.

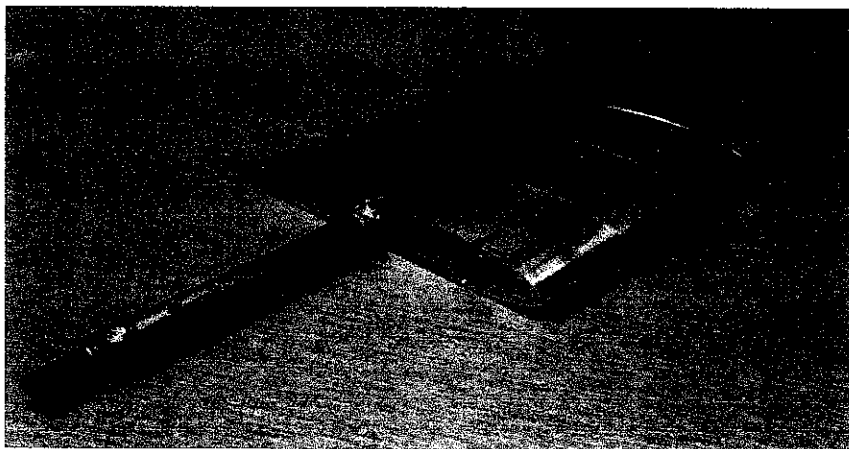


Figure 36: Airfoil wing with an aluminium rod to be connected to the three components balance during the testing.

4.5 EXPERIMENTS ON THE EFFECT OF WAKE

The experiments are conducted using the fabricated airfoil models and tested using the wind tunnel. Three experiments conducted are shown in Table 5 below:

Table 5: Three experiments conducted on the effect of wake.

Experiment	Purpose
1	Testing of a single airfoil model.
2	Testing of two airfoils model with a separating distance of 1 chord length (13cm).
3	Testing of two airfoils model with a separating distance of 2 chord length (26cm).

In Experiment 1, a single airfoil model is tested to define the coefficient of lift and coefficient of drag and it is functioning as references for comparison for Experiment 2 and Experiment 3. The main objective of Experiment 2 and Experiment 3 are to study the characteristic of coefficient of lift and coefficient of drag of a following airfoil model when an airfoil model is placed in front of the following airfoil model at a specific distance. Besides, the sensitivity of Reynolds number on the coefficient of lift and coefficient drag of the airfoil model is studied too.

4.5.1 Effects of free stream velocity and various angles of attack on the coefficient of lift and coefficient of drag of a single airfoil model (Experiment 1).

In Experiment 1, an airfoil model is tested at various free stream velocity (5m/s, 10m/s, 15m/s, 20m/s, 25m/s and 30m/s) and different angle of attack (0° , 2° , 4° , 6° , 8° , 10° , 12° , 14° , 16° , 18° , 20°) as shown in Figure 37. The objective is to define the characteristic of coefficient of lift, coefficient of drag and Reynolds number at all the conditions as stated above.

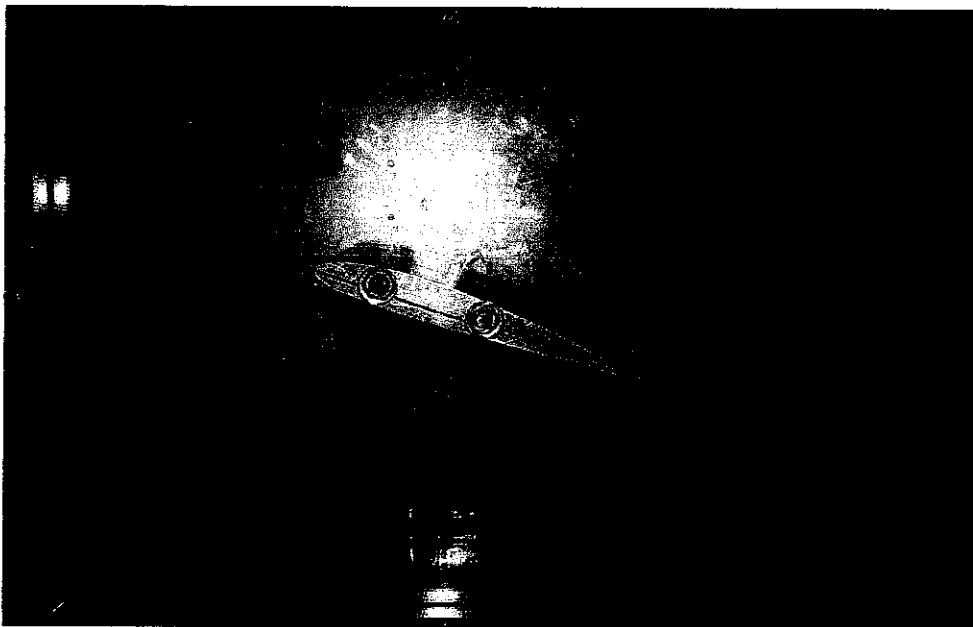


Figure 37: Testing of single airfoil model.

4.5.2 Effects of free stream velocity and various angles of attack on the coefficient of lift and coefficient of drag of two airfoil models with a separating distance of 1 chord length (Experiment 2).

In Experiment 2, two airfoils model are separated with a separating distance of 1 chord length (13cm) as shown in Figure 38. Two airfoils model are tested at various free stream velocity (5m/s, 10m/s, 15m/s, 20m/s, 25m/s and 30m/s) and different angle of attack (0° , 2° , 4° , 6° , 8° , 10° , 12° , 14° , 16° , 18° , 20°). The objective is to define the characteristic of coefficient of lift, coefficient of drag and Reynolds number at all the conditions as stated above.



Figure 38: Testing of two airfoils model at a separating distance of 13cm (1 chord length).

4.5.3 Effects of free stream velocity and various angles of attack on the coefficient of lift and coefficient of drag of two airfoil models with a separating distance of 2 chord length (Experiment 3).

In Experiment 3, two airfoils model are separated with a separating distance of 2 chord length (26cm) as shown in Figure 39. Two airfoils model are tested at various free stream velocity (5m/s, 10m/s, 15m/s, 20m/s, 25m/s and 30m/s) and different angle of attack (0° , 2° , 4° , 6° , 8° , 10° , 12° , 14° , 16° , 18° , 20°). The objective is to define the characteristic of coefficient of lift, coefficient of drag and Reynolds number at all the conditions as stated above.



Figure 39: Testing of two airfoils model at a separating distance of 26cm (2 chord length).

4.6 EXPERIMENTAL RESULTS AND ANALYSIS

4.6.1 Experimental results for Experiment 1, Experiment 2 and Experiment 3 on the characteristic of coefficient of lift and coefficient of drag.

The lift and drag forces are measured by using the 3-components balance shown in Appendix III. The lift and drag forces are recorded and shown in Appendix V. Meanwhile, the coefficient of lift and coefficient of drag are calculated and shown in Table 6 to Table 11.

Table 6: Experimental results for three experiments at 5m/s.

Angle of Attack (Degree)	Experiment 1: Single airfoil		Experiment 2: Two airfoils with separating distance of 1 chord length (13cm)		Experiment 3: Two airfoils with separating distance of 2 chord length (26cm)	
	C_L	C_D	C_L	C_D	C_L	C_D
0	0.10	0.08	0.15	0.08	0.02	0.02
2	0.28	0.10	0.18	0.08	0.13	0.05
4	0.33	0.08	0.23	0.05	0.33	0.05
6	0.51	0.12	0.41	0.05	0.39	0.05
8	0.52	0.15	0.46	0.10	0.41	0.10
10	0.59	0.15	0.57	0.10	0.54	0.15
12	0.72	0.14	0.77	0.13	0.67	0.15
14	0.82	0.19	0.80	0.17	0.77	0.21
16	0.84	0.29	0.85	0.18	0.90	0.21
18	0.79	0.30	1.00	0.23	0.80	0.23
20	0.77	0.46	0.87	0.29	0.95	0.31

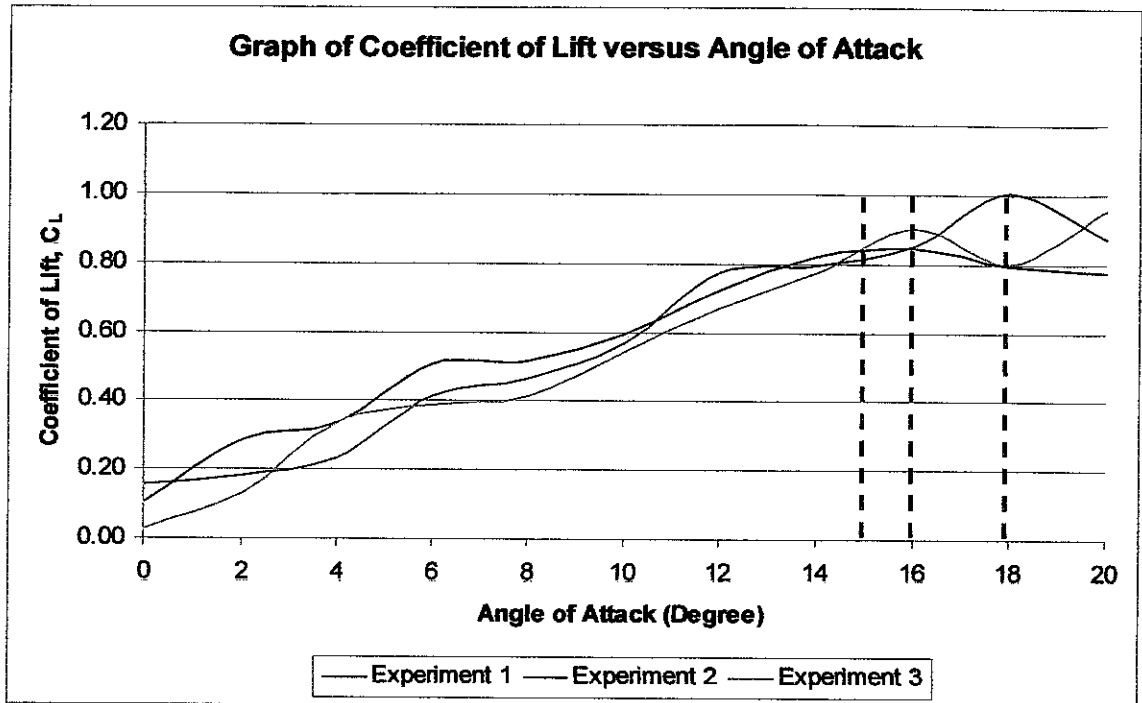


Figure 40: Graph of coefficient of lift versus angle of attack at 5m/s.

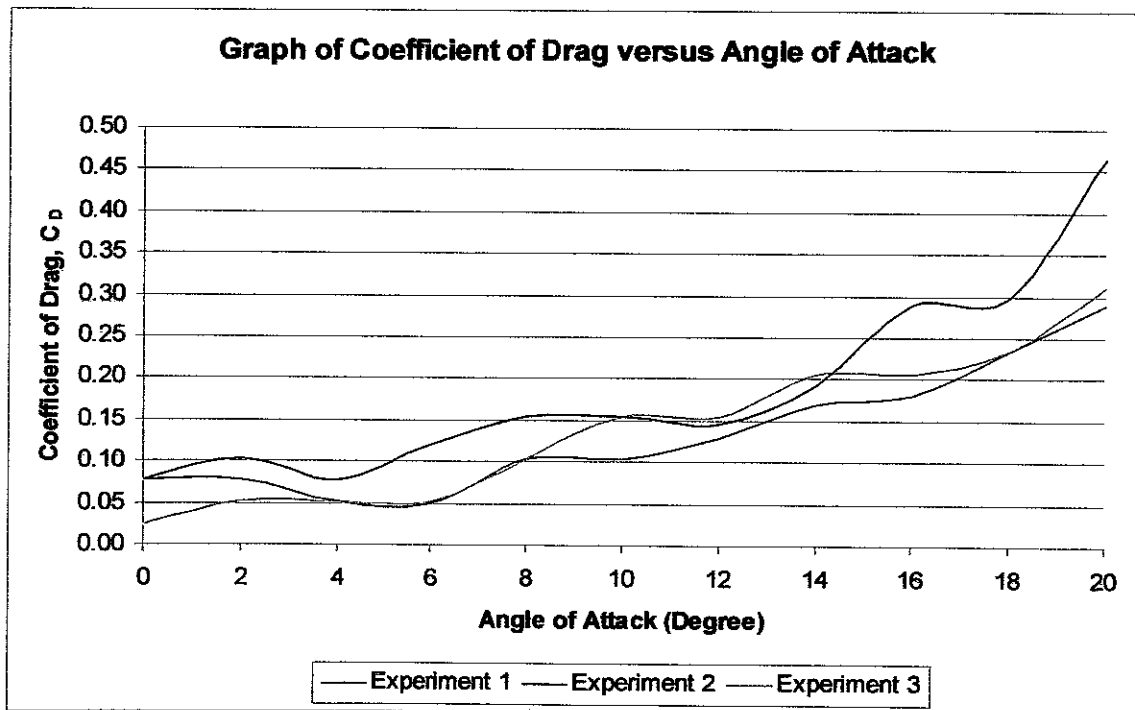


Figure 41: Graph of coefficient of drag versus angle of attack at 5m/s.

Table 7: Experimental results for three experiments at 10m/s.

Angle of Attack (Degree)	Experiment 1: Single airfoil		Experiment 2: Two airfoils with separating distance of 1 chord length (13cm)		Experiment 3: Two airfoils with separating distance of 2 chord length (26cm)	
	C_L	C_D	C_L	C_D	C_L	C_D
0	0.21	0.07	0.04	0.08	0.09	0.03
2	0.32	0.05	0.19	0.04	0.19	0.03
4	0.37	0.05	0.27	0.04	0.32	0.05
6	0.50	0.08	0.41	0.06	0.42	0.04
8	0.59	0.08	0.50	0.08	0.50	0.08
10	0.66	0.11	0.61	0.11	0.61	0.08
12	0.75	0.13	0.73	0.14	0.73	0.12
14	0.84	0.16	0.86	0.16	0.86	0.14
16	0.90	0.21	0.93	0.19	0.93	0.17
18	0.89	0.32	1.04	0.23	0.85	0.21
20	0.82	0.40	1.02	0.27	1.01	0.39

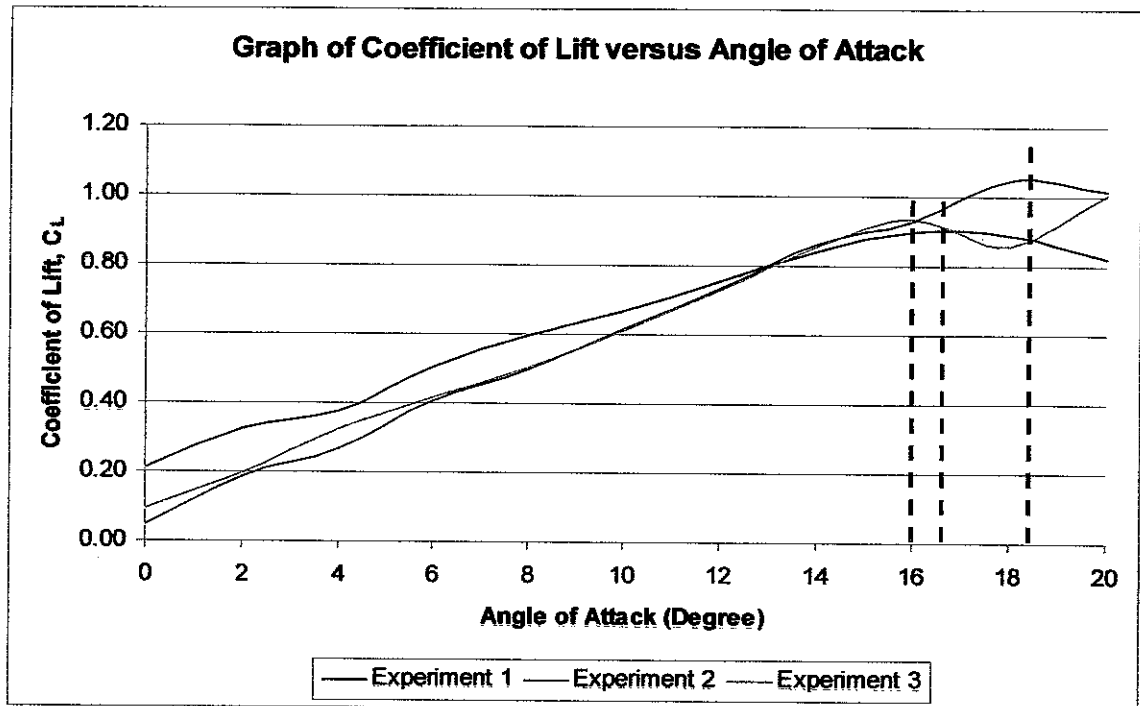


Figure 42: Graph of coefficient of lift versus angle of attack at 10m/s.

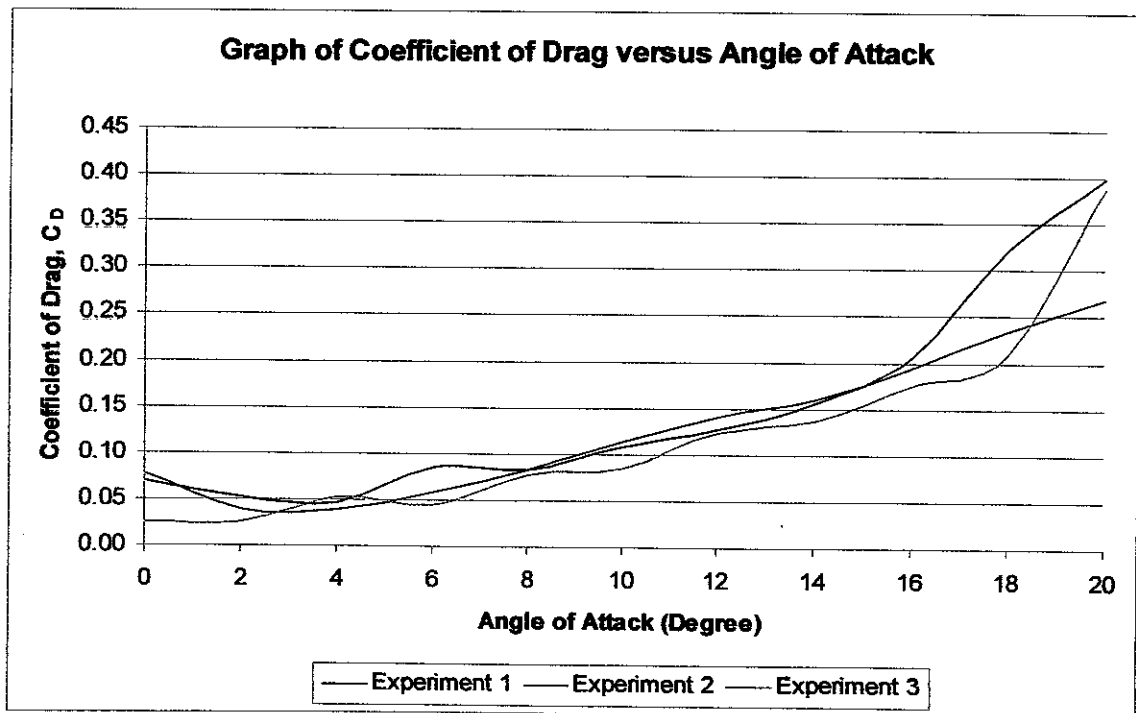


Figure 43: Graph of coefficient of drag versus angle of attack at 10m/s.

Table 8: Experimental results for three experiments at 15m/s.

Angle of Attack (Degree)	Experiment 1: Single airfoil		Experiment 2: Two airfoils with separating distance of 1 chord length (13cm)		Experiment 3: Two airfoils with separating distance of 2 chord length (26cm)	
	C_L	C_D	C_L	C_D	C_L	C_D
0	0.24	0.04	0.05	0.06	0.10	0.03
2	0.34	0.04	0.18	0.04	0.21	0.03
4	0.41	0.05	0.28	0.04	0.33	0.05
6	0.51	0.07	0.42	0.06	0.44	0.05
8	0.58	0.07	0.53	0.09	0.53	0.07
10	0.69	0.10	0.66	0.11	0.65	0.11
12	0.79	0.13	0.78	0.14	0.79	0.14
14	0.88	0.17	0.90	0.18	0.89	0.16
16	0.94	0.18	0.98	0.23	1.01	0.21
18	0.95	0.32	1.10	0.25	0.99	0.23
20	0.87	0.40	1.07	0.33	1.04	0.36

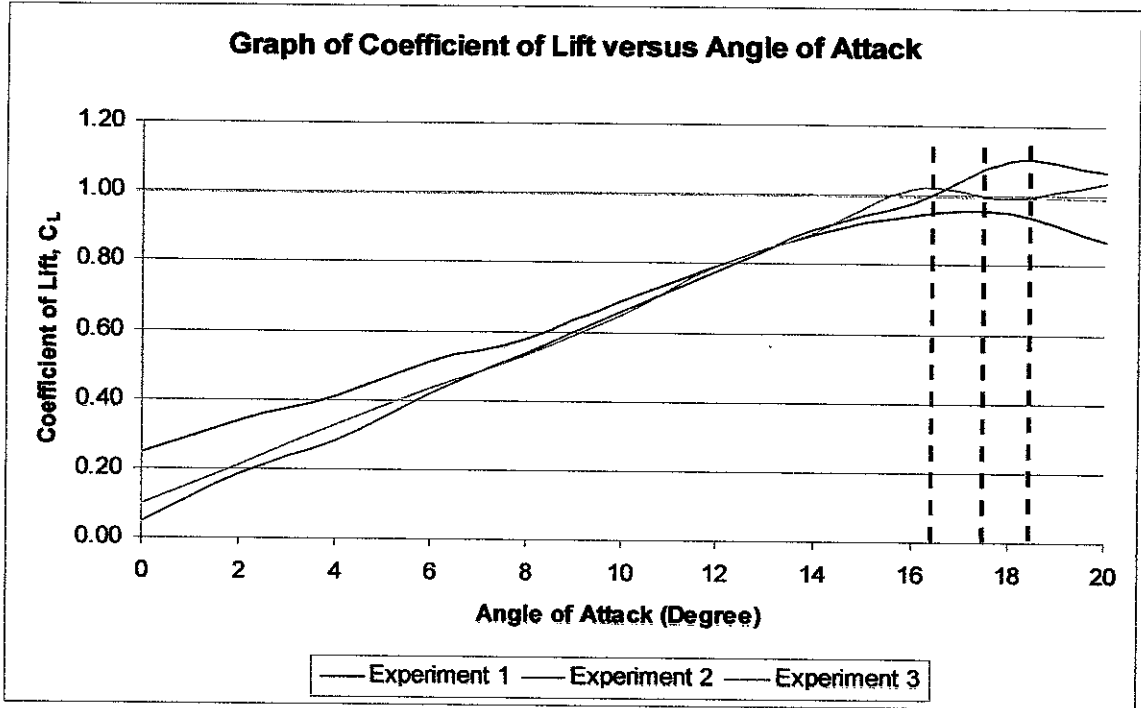


Figure 44: Graph of coefficient of lift versus angle of attack at 15m/s.

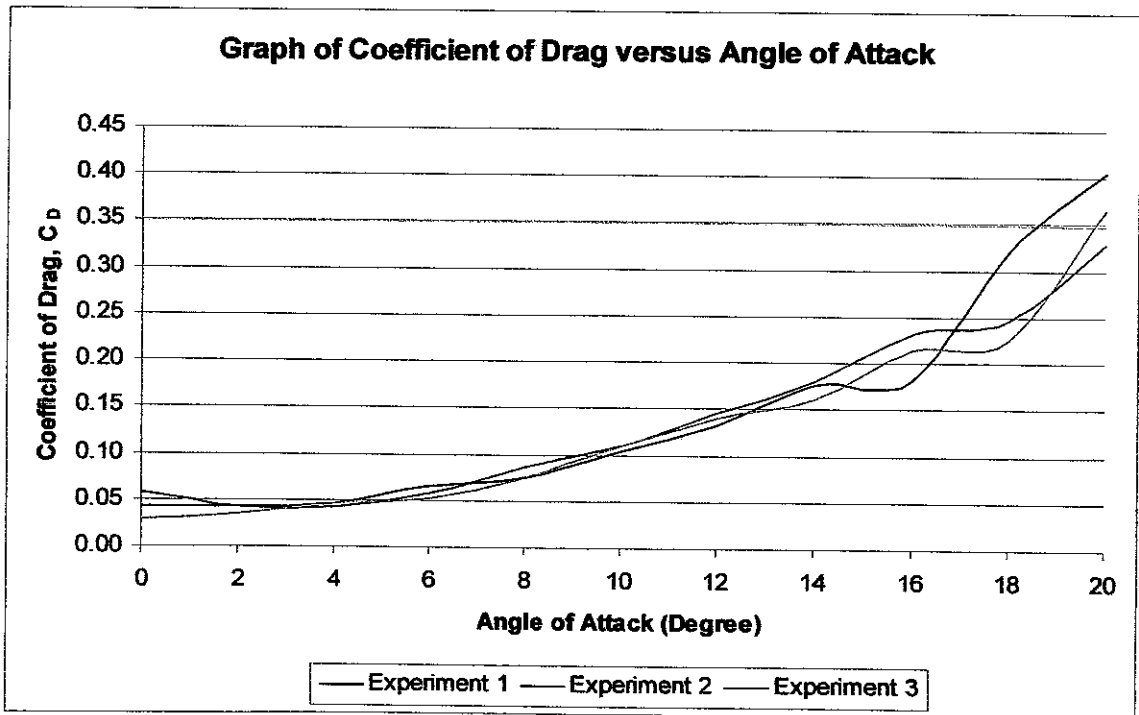


Figure 45: Graph of coefficient of drag versus angle of attack at 15m/s.

Table 9: Experimental results for three experiments at 20m/s.

Angle of Attack (Degree)	Experiment 1: Single airfoil		Experiment 2: Two airfoils with separating distance of 1 chord length (13cm)		Experiment 3: Two airfoils with separating distance of 2 chord length (26cm)	
	C_L	C_D	C_L	C_D	C_L	C_D
0	0.25	0.05	0.06	0.04	0.12	0.03
2	0.33	0.04	0.19	0.04	0.22	0.03
4	0.41	0.05	0.30	0.05	0.34	0.05
6	0.52	0.07	0.43	0.07	0.44	0.06
8	0.60	0.08	0.56	0.09	0.56	0.08
10	0.71	0.11	0.66	0.11	0.68	0.10
12	0.82	0.13	0.79	0.14	0.81	0.13
14	0.91	0.16	0.91	0.18	0.88	0.16
16	0.96	0.18	1.03	0.22	1.02	0.20
18	0.95	0.22	1.08	0.23	1.01	0.22
20	0.91	0.40	0.95	0.37	0.97	0.36

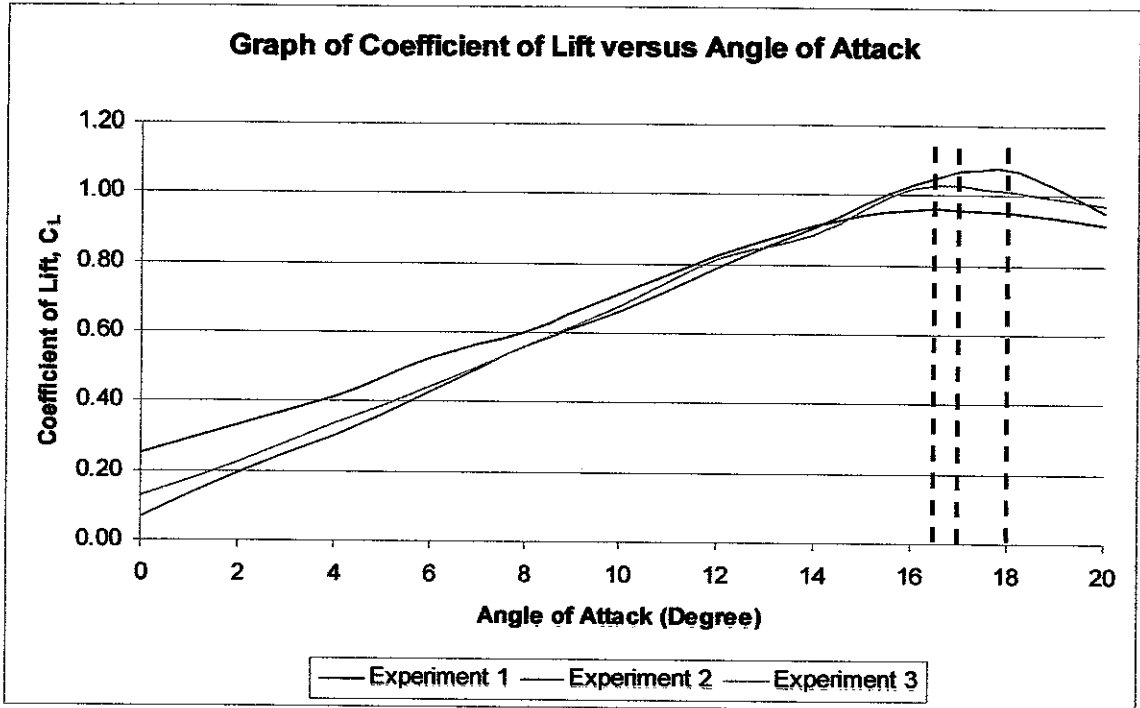


Figure 46: Graph of coefficient of lift versus angle of attack at 20m/s.

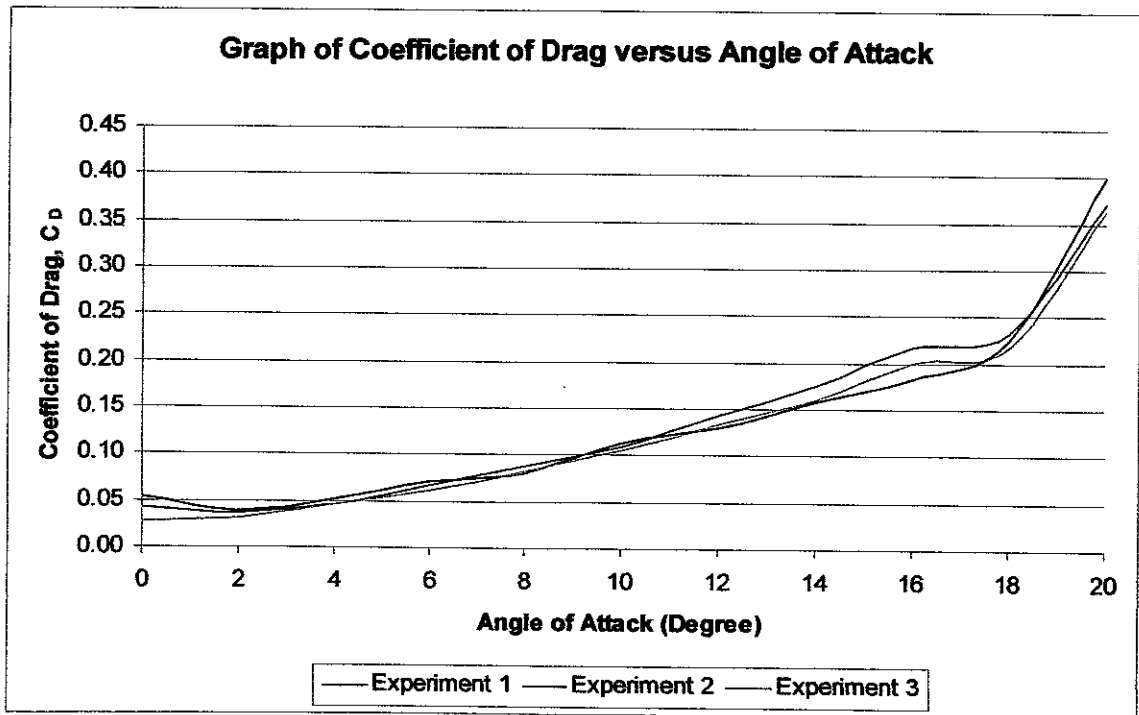


Figure 47: Graph of coefficient of drag versus angle of attack at 20m/s.

Table 10: Experimental results for three experiments at 25m/s.

Angle of Attack (Degree)	Experiment 1: Single airfoil		Experiment 2: Two airfoils with separating distance of 1 chord length (13cm)		Experiment 3: Two airfoils with separating distance of 2 chord length (26cm)	
	C_L	C_D	C_L	C_D	C_L	C_D
0	0.25	0.04	0.07	0.04	0.13	0.03
2	0.32	0.04	0.19	0.03	0.23	0.03
4	0.42	0.05	0.30	0.05	0.36	0.05
6	0.53	0.07	0.44	0.07	0.46	0.06
8	0.62	0.08	0.57	0.09	0.58	0.08
10	0.73	0.10	0.68	0.10	0.71	0.10
12	0.82	0.12	0.80	0.14	0.85	0.13
14	0.92	0.15	0.93	0.17	0.96	0.16
16	0.98	0.18	1.06	0.21	1.07	0.19
18	0.99	0.21	1.09	0.23	1.06	0.21
20	0.97	0.36	0.96	0.37	1.04	0.35

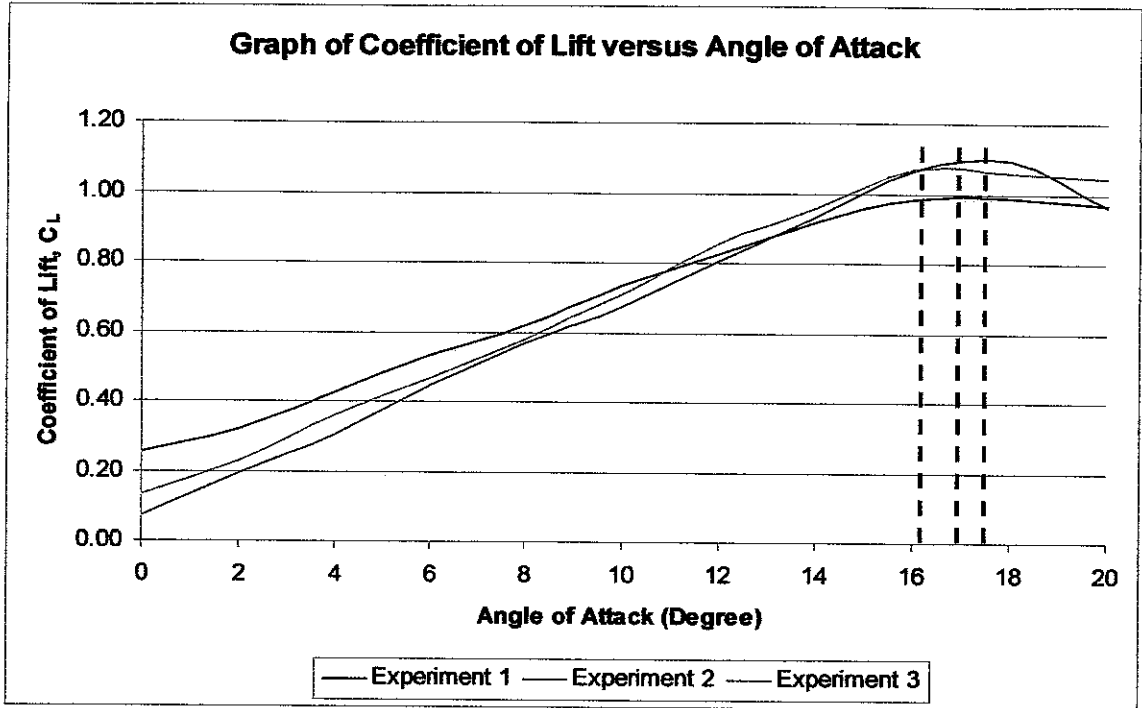


Figure 48: Graph of coefficient of lift versus angle of attack at 25m/s.

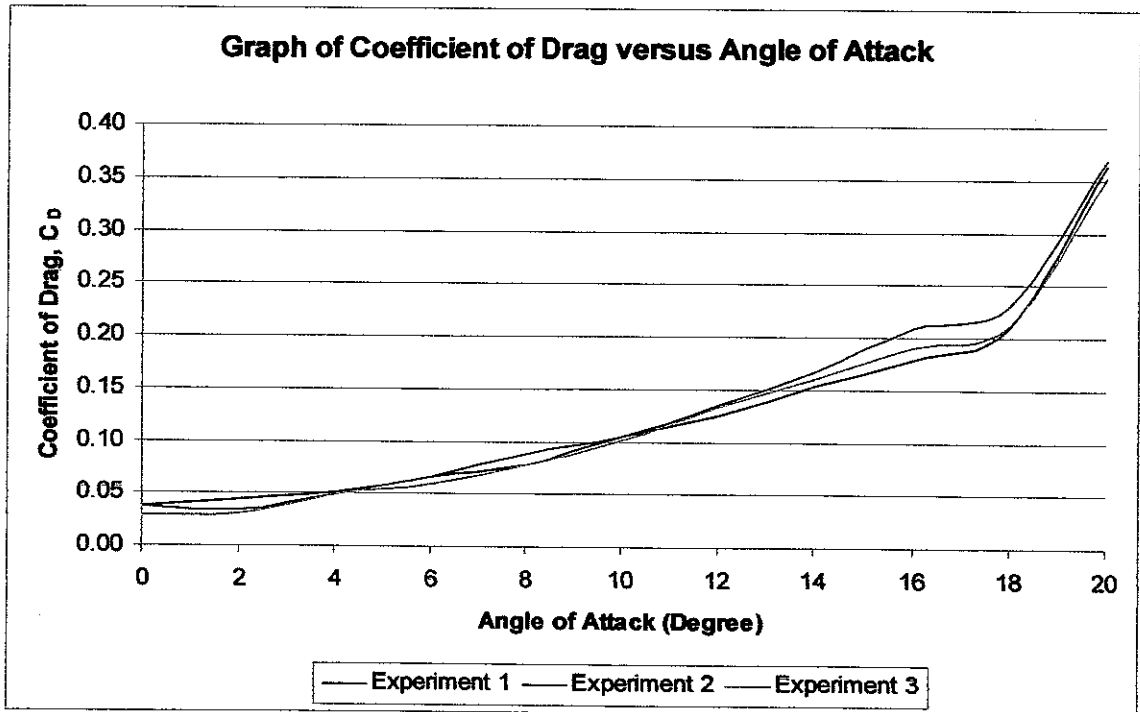


Figure 49: Graph of coefficient of drag versus angle of attack at 25m/s.

Table 11: Experimental results for three experiments at 30m/s.

Angle of Attack (Degree)	Experiment 1: Single airfoil		Experiment 2: Two airfoils with separating distance of 1 chord length (13cm)		Experiment 3: Two airfoils with separating distance of 2 chord length (26cm)	
	C_L	C_D	C_L	C_D	C_L	C_D
0	0.25	0.04	0.08	0.03	0.15	0.03
2	0.34	0.04	0.20	0.04	0.23	0.03
4	0.44	0.05	0.31	0.05	0.37	0.05
6	0.53	0.06	0.45	0.06	0.46	0.06
8	0.62	0.08	0.57	0.08	0.59	0.07
10	0.73	0.10	0.68	0.10	0.71	0.10
12	0.83	0.12	0.80	0.13	0.87	0.13
14	0.93	0.15	0.94	0.16	0.94	0.16
16	0.98	0.18	1.08	0.20	0.97	0.19
18	0.98	0.25	1.11	0.22	0.81	0.21
20	0.92	0.39	0.96	0.36	0.80	0.31

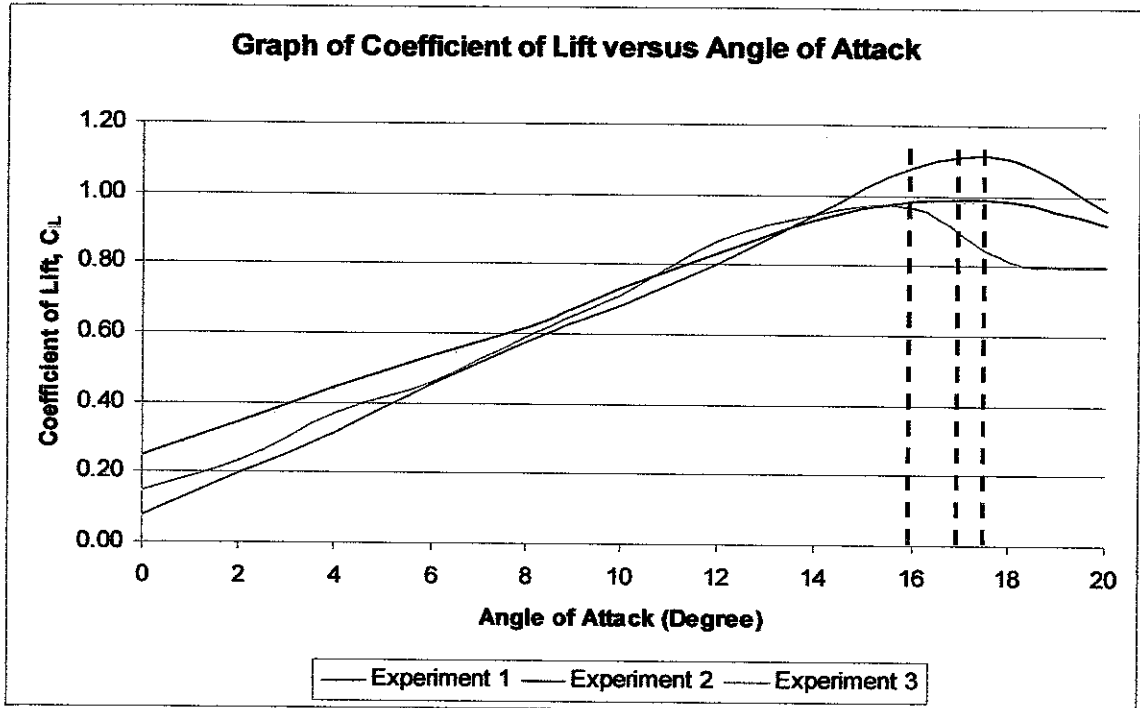


Figure 50: Graph of coefficient of lift versus angle of attack at 30m/s.

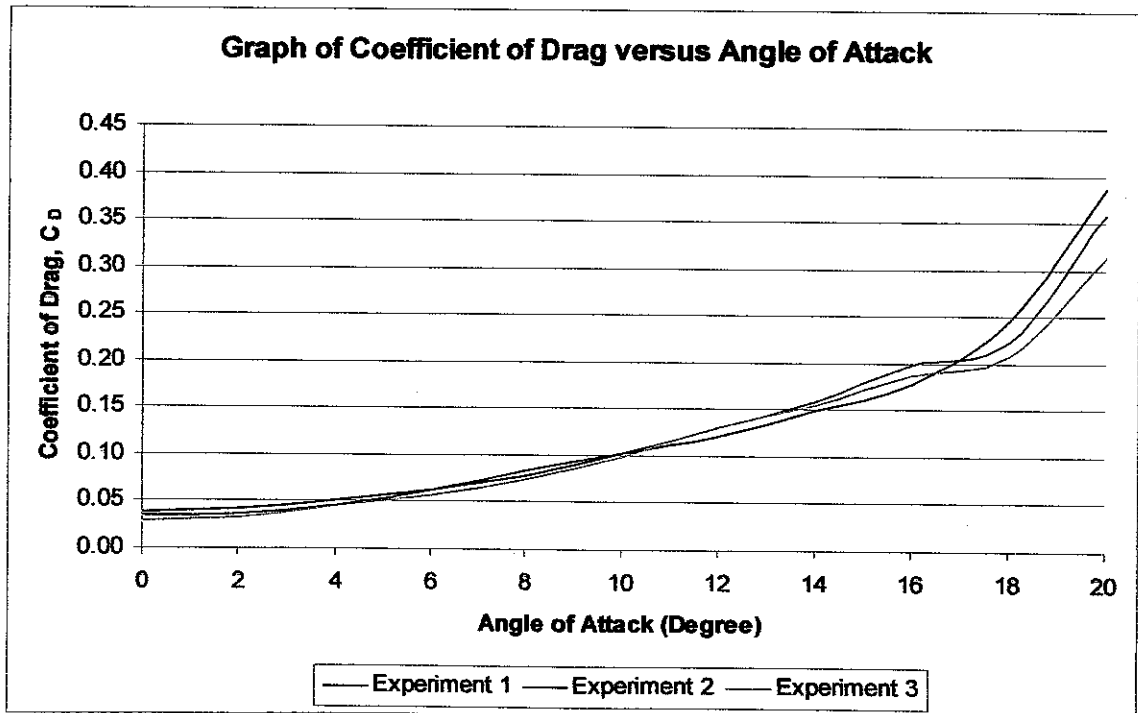


Figure 51: Graph of coefficient of drag versus angle of attack at 30m/s.

4.6.2 Analysis of experimental results on the characteristic of coefficient of lift and coefficient of drag.

Table 12: Stall angle at various free stream velocity.

Free Stream Velocity (m/s)	Stall Angle (Degree)		
	Experiment 1: Single airfoil	Experiment 2: Two airfoils with separating distance of 1 chord length (13cm)	Experiment 3: Two airfoils with separating distance of 2 chord length (26cm)
5	15	18	16
10	16.5	18.5	16
15	17.5	18.5	16.5
20	17	18	16.5
25	17	17.5	16.3
30	17	17.5	16

Table 13: Coefficient of lift at stall angle at various free stream velocity.

Free Stream Velocity (m/s)	Coefficient of Lift, C_L at Stall Angle		
	Experiment 1: Single airfoil	Experiment 2: Two airfoils with separating distance of 1 chord length (13cm)	Experiment 3: Two airfoils with separating distance of 2 chord length (26cm)
5	0.86	1.00	0.90
10	0.92	1.05	0.93
15	0.97	1.12	1.03
20	0.98	1.08	1.04
25	0.99	1.10	1.08
30	0.98	1.12	0.97

4.6.3 Analysis of the coefficient of lift with angle of attack.

Experiment 1

In Figure 40, the coefficient of lift for Experiment 1 increases when the angle of attack increases from 0° to 15° and decrease from 15° to 20° at the free stream velocity of 5m/s. The coefficient of lift is 0.86 at the stall angle of 15° . At the free stream velocity of 10m/s, the coefficient of lift increases from 0° to 16.5° and decreases from 16.5° to 20° as shown in Figure 42. The coefficient of lift is 0.92 at the stall angle of 16.5° . In Figure 44, when the free stream velocity is 15m/s, the coefficient of lift increases from 0° to 17.5° and decreases from 17.5° to 20° . The coefficient of lift is 0.97 at the stall angle of 17.5° . Meanwhile, the coefficient of lift increases from 0° to 17° and decreases from 17° to 20° at the free stream velocity of 20m/s, 25m/s and 30m/s as shown in Figure 46, Figure 48 and Figure 50. The coefficient of lift are 0.98, 0.99 and 0.98 at the stall angle of 17.5° for the free stream velocity of 20m/s, 25m/s and 30m/s respectively. The results show that coefficient of lift increases up to the stall angle and decreases after

the stall angle. The stall angles for Experiment 1 are in the range of 15° to 17.5° and the coefficients of lift are in the range of 0.86 to 0.99.

Comparing the results from Experiment 1 with the airfoil data for NACA 2412 wing section [14] in Appendix I, the stall angles are in the range of 14° to 18° and the coefficients of lift are in the range of 1.2 to 1.7 at different Reynolds number. The stall angles for Experiment 1 are within the range of stall angles for airfoil data for NACA 2412 wing section in Appendix I. But, the coefficients of lift for Experiment 1 are lower than the coefficient of lift for airfoil data for NACA 2412 wing section in Appendix I because Experiment 1 is carried out at lower free stream velocity and lower Reynolds number.

Experiment 2

Figure 40 shows that the coefficient of lift for Experiment 2 increases when the angle of attack increases from 0° to 18° and decrease from 18° to 20° at the free stream velocity of 5m/s. The coefficient of lift is 1.00 at the stall angle of 18° . At the free stream velocity of 10m/s and 15m/s, the coefficient of lift increases from 0° to 18.5° and decreases from 18.5° to 20° as shown in Figure 42 and Figure 44. The coefficients of lift are 1.05 and 1.12 at the stall angles of 18.5° for the free stream velocity of 10m/s and 15m/s respectively. In Figure 46, when free stream velocity is 20m/s, the coefficient of lift increases from 0° to 18° and decreases from 18° to 20° . The coefficient of lift is 1.08 at the stall angle of 18° . Meanwhile, the coefficient of lift increases from 0° to 17.5° and decreases from 17.5° to 20° at the free stream velocity of 25m/s and 30m/s as shown in Figure 48 and Figure 50. The coefficients of lift are 1.10 and 1.12 at the stall angle of 17.5° for the free stream velocity of 25m/s and 30m/s respectively. The results show that the stall angles are in the range of 17.5° to 18.5° and the coefficients of lift are in the range of 1.00 to 1.12.

Experiment 3

Figure 40 and Figure 42 show the coefficient of lift for Experiment 3 increases when the angle of attack increases from 0° to 16° , decrease from 16° to 18° and increase again

from 18° to 20° at the free stream velocity of 5m/s and 10m/s. The coefficients of lift are 0.90 and 0.93 at the stall angle of 16° for the free stream velocity of 5m/s and 10m/s respectively. At the free stream velocity of 15m/s, the coefficient of lift increases from 0° to 16.5° , decrease from 16.5° to 18° and increases again from 18° to 20° as shown in Figure 44. Figure 46 shows that the coefficient of lift increases from 0° to 16.5° , decrease from 16.5° to 20° at the free stream velocity of 20m/s. The coefficients of lift are 1.03 and 1.04 at the stall angles of 16.5° for the free stream velocity of 15m/s and 20m/s respectively. In Figure 48, when the free stream velocity is 25m/s, the coefficient of lift increases from 0° to 16.3° and decreases from 16.3° to 20° . The coefficient of lift is 1.08 at the stall angle of 16.3° . Meanwhile, the coefficient of lift increases from 0° to 16° and decreases from 16° to 20° at the free stream velocity of 30m/s as shown in Figure 50. The coefficient of lift is 0.97 at the stall angle of 16° for the free stream velocity of 30m/s. The results show that the stall angles are in the range of 16° to 16.5° and the coefficients of lift are in the range of 0.90 to 1.08.

Comparison between Experiment 1, Experiment 2 and Experiment 3

Comparing the results from Experiment 2 with the results from Experiment 1, the stall angle for Experiment 2 is in the range of 17.5 to 18.5 which is higher than the stall angles for Experiment 1 in the range of 15° to 17.5° . At the same time, the coefficient of lift for Experiment 2 is in the range of 1.00 to 1.12 which is higher than the coefficient of lift for Experiment 1 in the range of 0.86 to 0.99. During Experiment 2, the trailing airfoil model is oscillating and vibrating at most of the angle of attack. This may be due to the effects of wake produced by the front airfoil model extending up to the leading edge of the trailing airfoil model and disturbing the flow at the inlet. The velocity at the inlet for the trailing airfoil model is not uniform and may be decreased also. So, the coefficient of lift for the trailing airfoil model is increased. Besides, the wake generated from the front airfoil model may affect the stall angle of the trailing airfoil model. When the velocity is not uniform or decreases, the flow over the trailing airfoil model is affected. The separation over the trailing airfoil model may be delayed and the stall angle is increased in Experiment 2.

Comparing the results from Experiment 3 with the results from Experiment 1, the stall angle for Experiment 3 is in the range of 16° to 16.5° which is almost same as the stall angle for Experiment 1 in the range of 15° to 17.5° . The coefficient of lift for Experiment 3 is in the range of 0.90 to 1.08 which is slightly higher than the coefficient of lift for Experiment 1 in the range of 0.86 to 0.99. During Experiment 3, the trailing airfoil model is oscillating and vibrating slightly from the angle attack of 12° onwards. The effect of wake produced by the front airfoil model is very weak. It may be still extending up to the leading edge of the trailing airfoil model. The weak wake produced may have little effects to the flow at the inlet. The velocity at the inlet for the trailing airfoil model can be assumed to be uniform or it may have little effect to the trailing airfoil model only. When the velocity is affected, it shows the flow over the trailing airfoil model may be affected and the coefficient of lift in Experiment 3 is slightly higher. The flow over the trailing airfoil model may be affected but it is not obvious. So, the stall angle in Experiment 3 is almost same as the stall angle in Experiment 1.

When the separating distance between two airfoil models is increased from 1 chord length (13cm) in Experiment 2 to 2 chord length (26cm) in Experiment 3, the stall angle is decreased from the range of 17.5° to 18.5° in Experiment 2 to the range of 16° to 16.5° in the Experiment 3. The coefficient of lift for Experiment 3 is in the range of 0.90 to 1.04 which is lower than the coefficient of lift for Experiment 2 in the range of 1.00 to 1.12. When the separating distance is increased, the wake produced is very weak and the effect of wake to the trailing airfoil model is not very obvious. The trailing airfoil model is oscillating and vibrating slightly from the angle attack of 12° onwards only. The velocity at the inlet for the trailing airfoil model can be assumed to be uniform or it may have little effect to the trailing airfoil model only. Thus, the results show the coefficient of lift for Experiment 3 is lower than Experiment 2. The separation of flow over the trailing airfoil model is more obvious and the stall angle is higher in Experiment 2.

4.6.4 Analysis of the coefficient of drag with angle of attack.

Experiment 1

The results show that the coefficient of drag for Experiment 1 increases with the angle of angle of attack at the free stream velocity from 5m/s to 30m/s. Figure 41 shows that the coefficient of drag is in the range of 0.08 to 0.46 at the free stream velocity of 5m/s. The coefficients of drag are in the range of 0.04 to 0.40 at the free stream velocity of 10m/s, 15m/s and 20m/s as shown in Figure 43, Figure 45 and Figure 47. When the free stream velocity are 25m/s and 30m/s, the coefficient of drag is in the range of 0.04 to 0.36 and 0.04 to 0.39 respectively as shown in Figure 49 and Figure 51. Coefficient of drag shows steady behavior and increases with the angle of attack at various free stream velocities. The overall coefficient of drag for Experiment 1 is in the range of 0.04 to 0.46. Coefficient of drag does not decrease after the stall angle, but increases rapidly after the stall angle. It is shown that skin friction drag is acting on the trailing airfoil all the times. At the same time, the separated flow over the airfoil may create a large pressure drag at the stall angle. Thus, the coefficient of drag increases rapidly after the stall angle.

Experiment 2

The coefficient of drag for Experiment 2 increases with the angle of angle of attack at the free stream velocity from 5m/s to 30m/s. The coefficient of drag is in the range of 0.08 to 0.29 at the free stream velocity of 5m/s as shown in Figure 41. Figure 43 and Figure 45 show that the coefficients of drag are in the range of 0.08 to 0.27 and 0.06 to 0.33 at the free stream velocity of 10m/s and 15m/s respectively. When the free stream velocities are 20m/s and 25m/s, the coefficients of drag are in the range of 0.04 to 0.37 as shown in Figure 47 and Figure 49. Meanwhile, Figure 51 shows that the coefficient of drag is in the range of 0.03 to 0.36 at the free stream velocity of 30m/s. Coefficient of drag shows steady behavior and increases with the angle of attack at various free stream velocities. The overall coefficient of drag for Experiment 2 is in the range of 0.03 to 0.37.

Experiment 3

The coefficient of drag for Experiment 3 increases with the angle of angle of attack at the free stream velocity from 5m/s to 30m/s. Figure 41 shows that the coefficient of drag is in the range of 0.02 to 0.31 at the free stream velocity of 5m/s. The coefficients of drag are in the range of 0.03 to 0.39 at the free stream velocity of 10m/s as shown in Figure 43. In Figure 45, Figure 47 and Figure 49, when the free stream velocity is at 15m/s, 20m/s and 25m/s, the coefficient of drag is in the range of 0.03 to 0.36. Meanwhile, Figure 51 shows that the coefficient of drag is in the range of 0.03 to 0.31 at the free stream velocity of 30m/s. Coefficient of drag shows steady behavior and increases with the angle of attack at various free stream velocities. The overall coefficient of drag for Experiment 3 is in the range of 0.02 to 0.39.

Comparison between Experiment 1, Experiment 2 and Experiment 3

The coefficient of drag from Experiment 2 is compared with the coefficient of drag in Experiment 1. The coefficient of drag for Experiment 2 is in the range of 0.03 to 0.37 which is slightly lowers than the coefficient of drag in Experiment 1 in the range of 0.04 to 0.46. This may be due to the blockage of the front airfoil model to the trailing airfoil model. The front airfoil model blocks the airflow over the leading edge of the trailing airfoil model. Besides, it may disturb the velocity at the inlet of the trailing airfoil wing section and decrease the pressure drag acting on the trailing airfoil model during the separation of flow. Thus, the coefficient of drag for Experiment 2 is decreased.

Comparing the coefficient of drag from Experiment 3 with the coefficient of drag in Experiment 1 and Experiment 2, the coefficient of drag for Experiment 3 is in the range of 0.02 to 0.39 which is slightly lowers than the coefficient of drag in Experiment 1 in the range of 0.04 to 0.46 and almost similar to the coefficient of drag in Experiment 2 in the range of 0.03 to 0.37. It was found that the phenomenon in Experiment 3 is almost similar to Experiment 2. This may be due to the blockage of the front airfoil model to the trailing airfoil model. The front airfoil model blocks the airflow over the leading edge of the trailing airfoil model. Thus, the velocity at the inlet of the trailing airfoil model cannot be considered uniform. During the separation of flow over the trailing

airfoil model, the pressure drag created may be not really obvious compared to Experiment 1. As a result, the coefficient of drag for Experiment 3 and Experiment 2 are lower than the coefficient of drag for the Experiment 1.

4.6.5 Experimental results for Experiment 1, Experiment 2 and Experiment 3 on the characteristic of coefficient of lift, coefficient of drag and Reynolds number.

The lift and drag forces are measured by using the 3-components balance shown in Appendix III. The lift and drag forces are recorded and shown in Appendix VI. Meanwhile, the coefficient of lift, coefficient of drag and Reynolds number are calculated and shown in Table 14 to Table 24.

Table 14: Experimental results for three experiments when angle of attack is 0°.

Free Stream Velocity (m/s)	Experiment 1: Single airfoil			Experiment 2: Two airfoils with separating distance of 1 chord length (13cm)			Experiment 3: Two airfoils with separating distance of 2 chord length (26cm)		
	C _L	C _D	Re	C _L	C _D	Re	C _L	C _D	Re
5	0.10	0.08	4.19E+04	0.15	0.08	4.19E+04	0.02	0.02	4.34E+04
10	0.21	0.07	8.46E+04	0.04	0.08	8.22E+04	0.09	0.03	8.40E+04
15	0.24	0.04	1.26E+05	0.05	0.06	1.26E+05	0.10	0.03	1.25E+05
20	0.25	0.05	1.69E+05	0.06	0.04	1.68E+05	0.12	0.03	1.68E+05
25	0.25	0.04	2.09E+05	0.07	0.04	2.10E+05	0.13	0.03	2.10E+05
30	0.25	0.04	2.52E+05	0.08	0.03	2.51E+05	0.15	0.03	2.52E+05

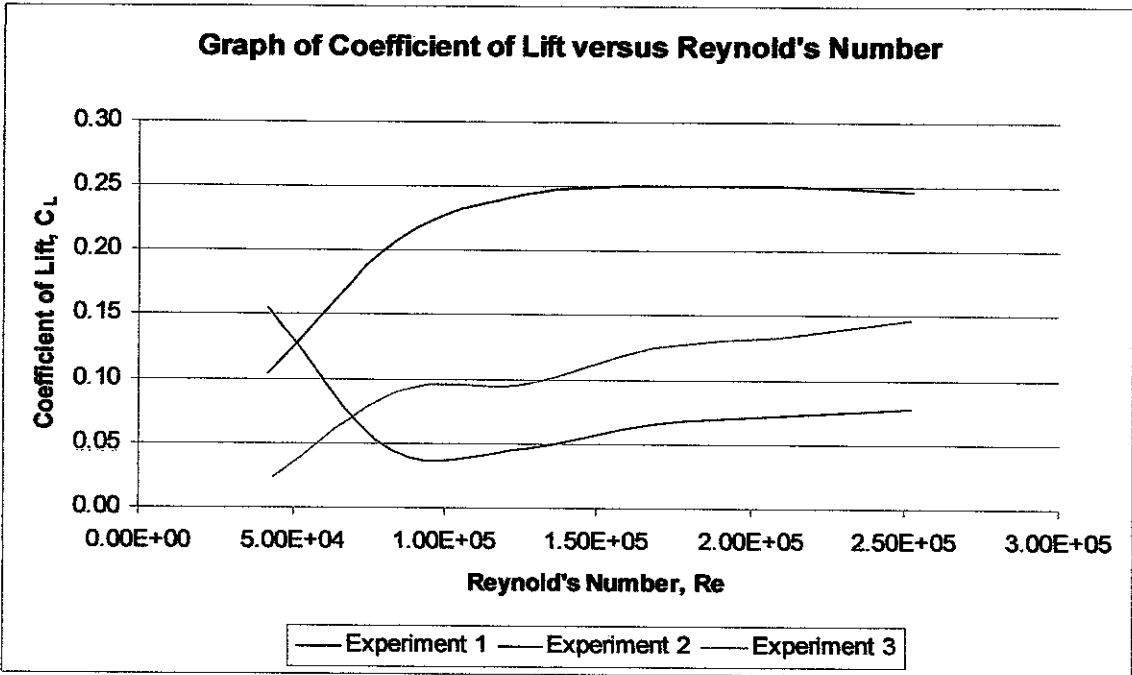


Figure 52: Graph of coefficient of lift versus Reynolds number at 0° .

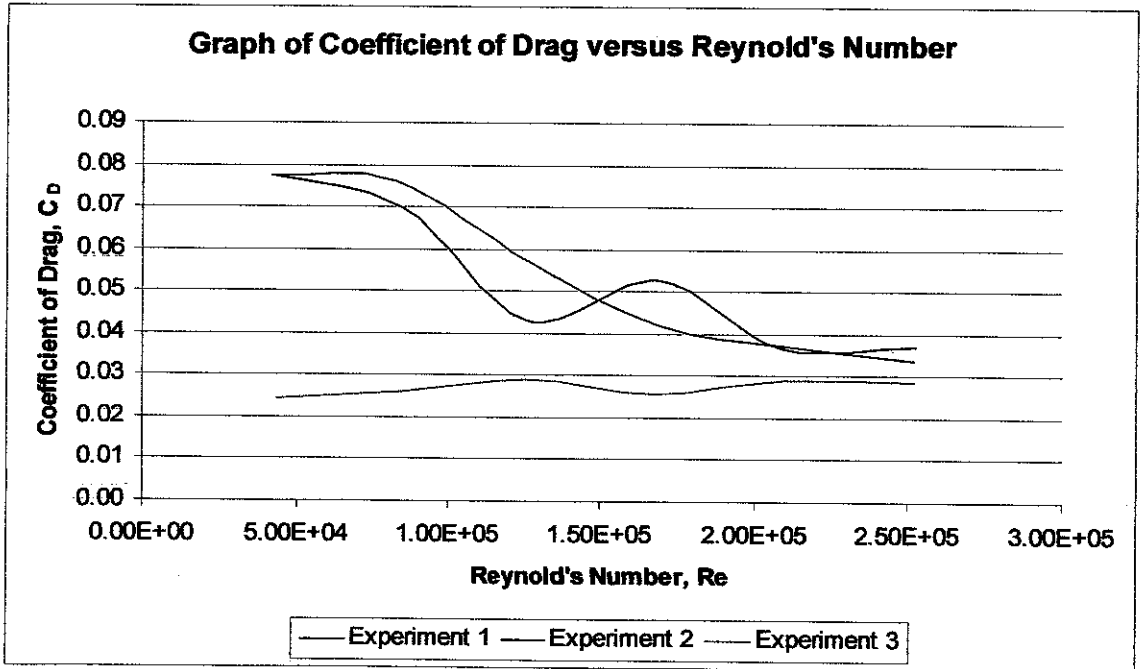


Figure 53: Graph of coefficient of drag versus Reynolds number at 0° .

Table 15: Experimental results for three experiments when angle of attack is 2°.

Free Stream Velocity (m/s)	Experiment 1: Single airfoil			Experiment 2: Two airfoils with separating distance of 1 chord length (13cm)			Experiment 3: Two airfoils with separating distance of 2 chord length (26cm)		
	C_L	C_D	Re	C_L	C_D	Re	C_L	C_D	Re
5	0.28	0.10	4.19E+04	0.18	0.08	4.19E+04	0.13	0.05	4.19E+04
10	0.32	0.05	8.40E+04	0.19	0.04	8.29E+04	0.19	0.03	8.40E+04
15	0.34	0.04	1.26E+05	0.18	0.04	1.26E+05	0.21	0.03	1.26E+05
20	0.33	0.04	1.69E+05	0.19	0.04	1.68E+05	0.22	0.03	1.68E+05
25	0.32	0.04	2.10E+05	0.19	0.03	2.10E+05	0.23	0.03	2.09E+05
30	0.34	0.04	2.52E+05	0.20	0.04	2.51E+05	0.23	0.03	2.52E+05

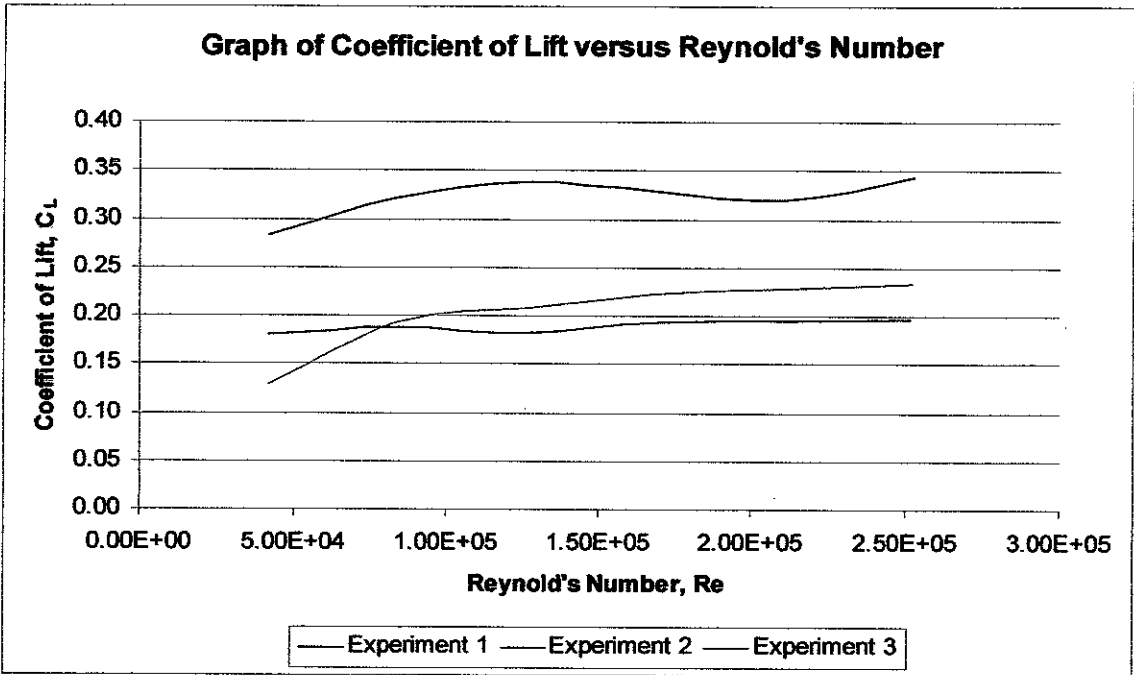


Figure 54: Graph of coefficient of lift versus Reynolds number at 2°.

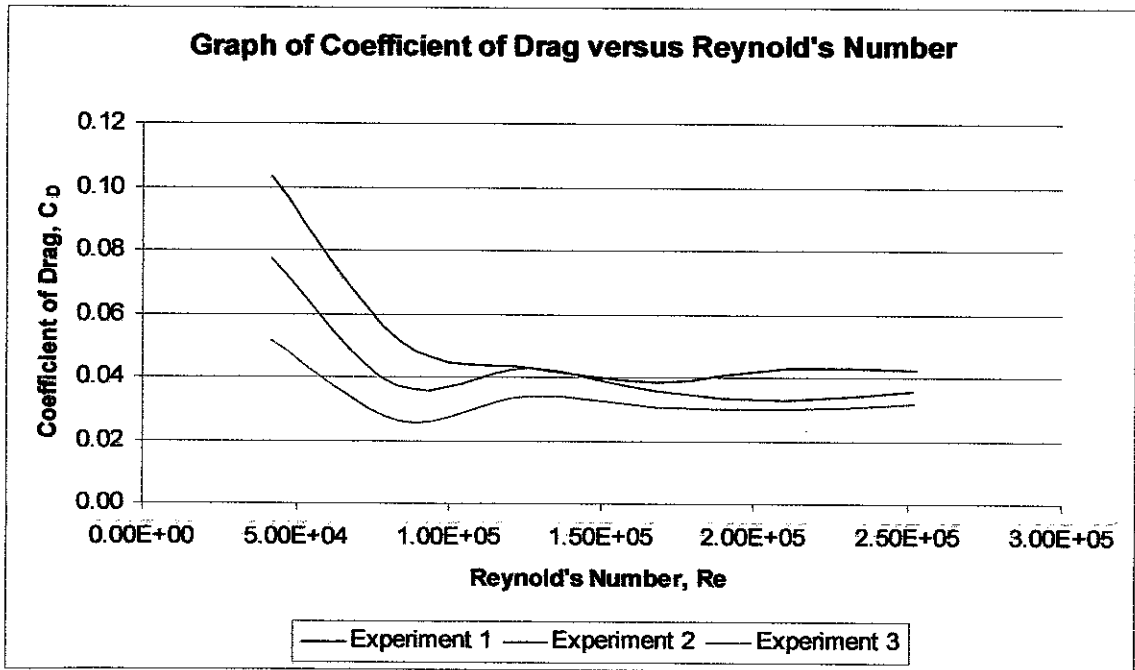


Figure 55: Graph of coefficient of drag versus Reynolds number at 2°.

Table 16: Experimental results for three experiments when angle of attack is 4°.

Velocity (m/s)	Experiment 1: Single airfoil			Experiment 2: Two airfoils with separating distance of 1 chord length (13cm)			Experiment 3: Two airfoils with separating distance of 2 chord length (26cm)		
	C_L	C_D	Re	C_L	C_D	Re	C_L	C_D	Re
5	0.33	0.08	4.19E+04	0.23	0.05	4.19E+04	0.33	0.05	4.19E+04
10	0.37	0.05	8.40E+04	0.27	0.04	8.22E+04	0.32	0.05	8.40E+04
15	0.41	0.05	1.26E+05	0.28	0.04	1.26E+05	0.33	0.05	1.25E+05
20	0.41	0.05	1.69E+05	0.30	0.05	1.68E+05	0.34	0.05	1.68E+05
25	0.42	0.05	2.10E+05	0.30	0.05	2.10E+05	0.36	0.05	2.10E+05
30	0.44	0.05	2.53E+05	0.31	0.05	2.51E+05	0.37	0.05	2.51E+05

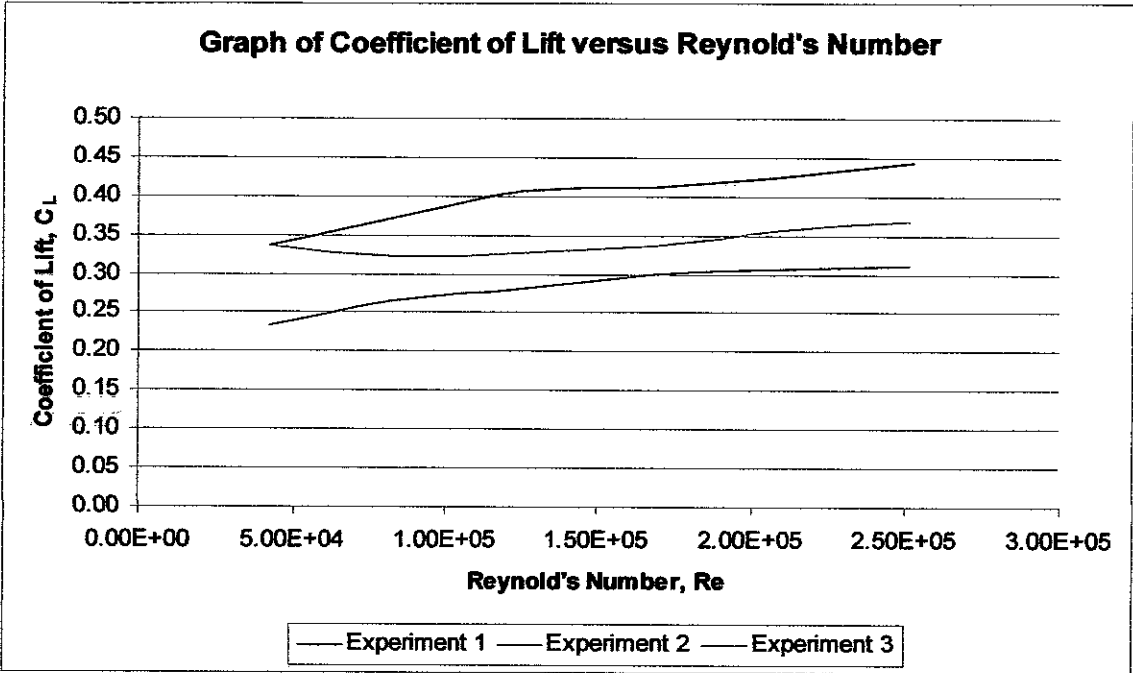


Figure 56: Graph of coefficient of lift versus Reynolds number at 4°.

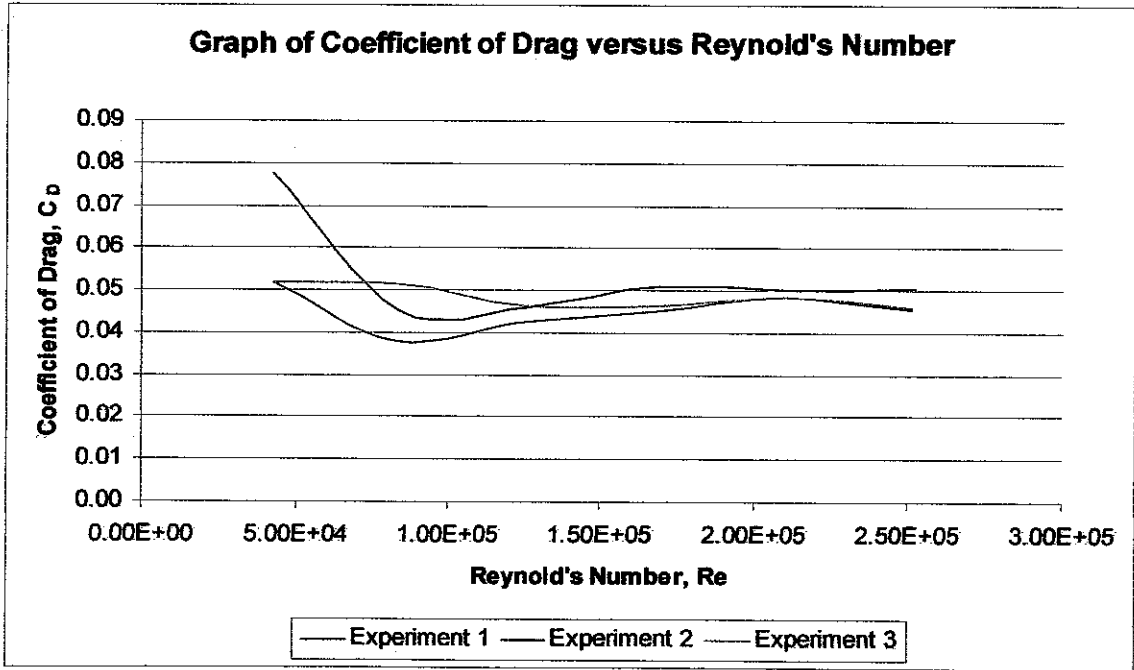


Figure 57: Graph of coefficient of drag versus Reynolds number at 4°.

Table 17: Experimental results for three experiments when angle of attack is 6°.

Velocity (m/s)	Experiment 1: Single airfoil			Experiment 2: Two airfoils with separating distance of 1 chord length (13cm)			Experiment 3: Two airfoils with separating distance of 2 chord length (26cm)		
	C_L	C_D	Re	C_L	C_D	Re	C_L	C_D	Re
5	0.51	0.12	4.34E+04	0.41	0.05	4.34E+04	0.39	0.05	4.19E+04
10	0.50	0.08	8.40E+04	0.41	0.06	8.16E+04	0.42	0.04	8.46E+04
15	0.51	0.07	1.26E+05	0.42	0.06	1.26E+05	0.44	0.05	1.25E+05
20	0.52	0.07	1.67E+05	0.43	0.07	1.68E+05	0.44	0.06	1.68E+05
25	0.53	0.07	2.10E+05	0.44	0.07	2.11E+05	0.46	0.06	2.09E+05
30	0.53	0.06	2.52E+05	0.45	0.06	2.51E+05	0.46	0.06	2.51E+05

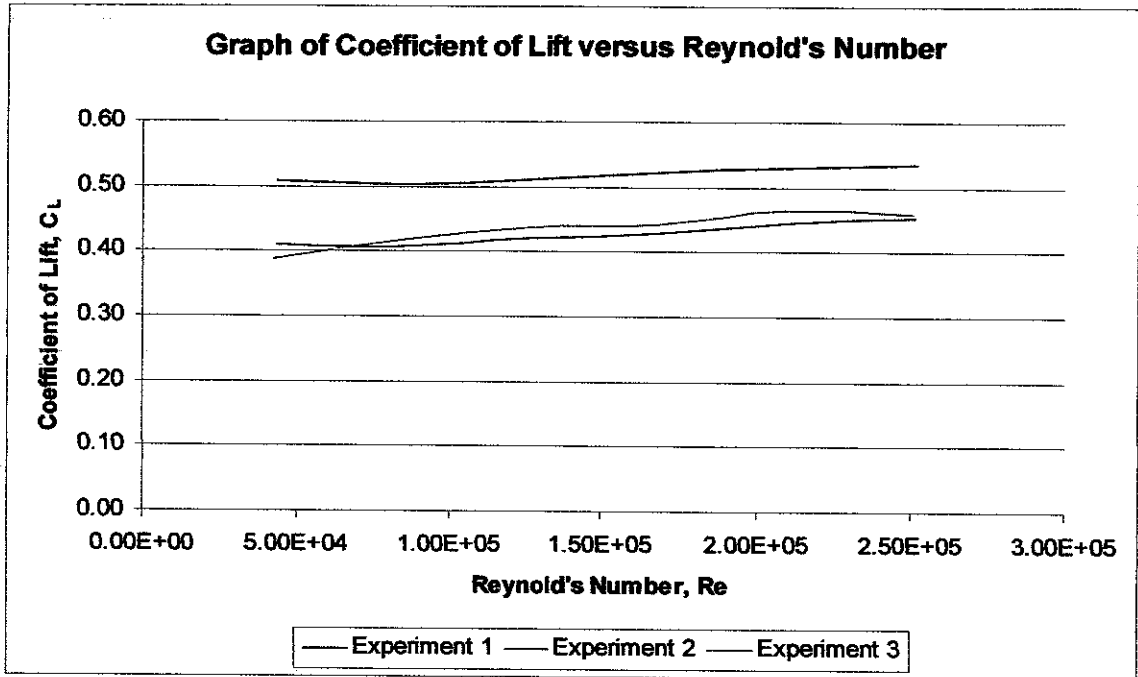


Figure 58: Graph of coefficient of lift versus Reynolds number at 6°.

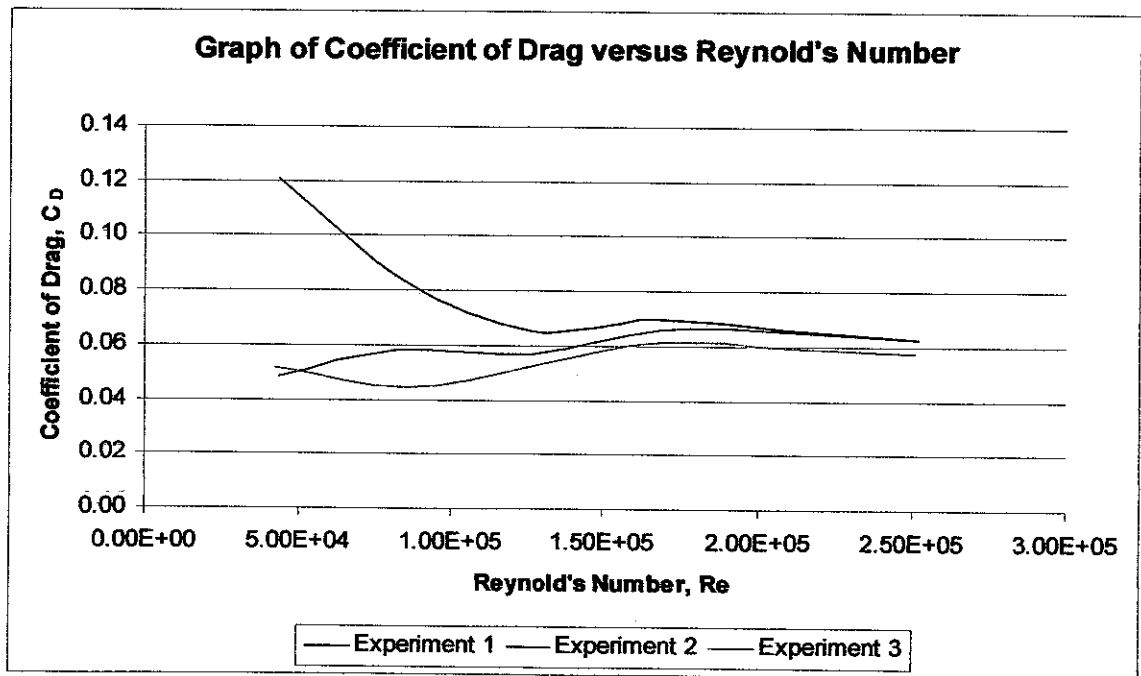


Figure 59: Graph of coefficient of drag versus Reynolds number at 6°.

Table 18: Experimental results for three experiments when angle of attack is 8°.

Velocity (m/s)	Experiment 1: Single airfoil			Experiment 2: Two airfoils with separating distance of 1 chord length (13cm)			Experiment 3: Two airfoils with separating distance of 2 chord length (26cm)		
	C_L	C_D	Re	C_L	C_D	Re	C_L	C_D	Re
5	0.52	0.15	4.19E+04	0.46	0.10	4.19E+04	0.41	0.10	4.19E+04
10	0.59	0.08	8.46E+04	0.50	0.08	8.22E+04	0.50	0.08	8.40E+04
15	0.58	0.07	1.26E+05	0.53	0.09	1.26E+05	0.53	0.07	1.26E+05
20	0.60	0.08	1.68E+05	0.56	0.09	1.68E+05	0.56	0.08	1.68E+05
25	0.62	0.08	2.09E+05	0.57	0.09	2.10E+05	0.58	0.08	2.09E+05
30	0.62	0.08	2.52E+05	0.57	0.08	2.52E+05	0.59	0.07	2.51E+05

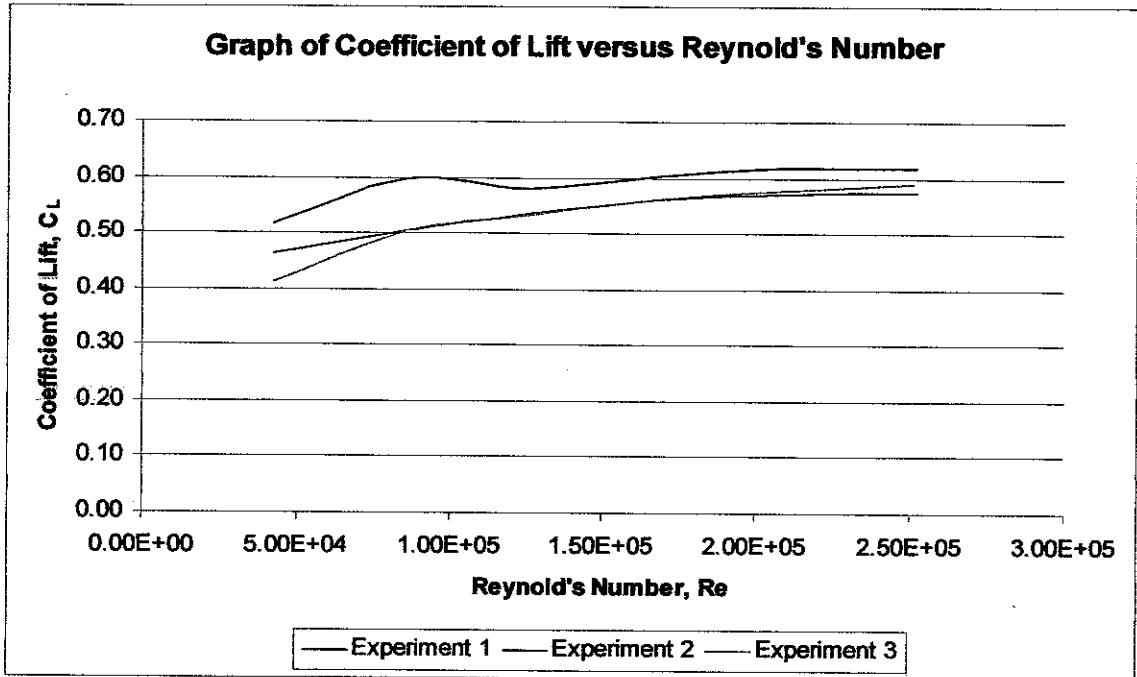


Figure 60: Graph of coefficient of lift versus Reynolds number at 8°.

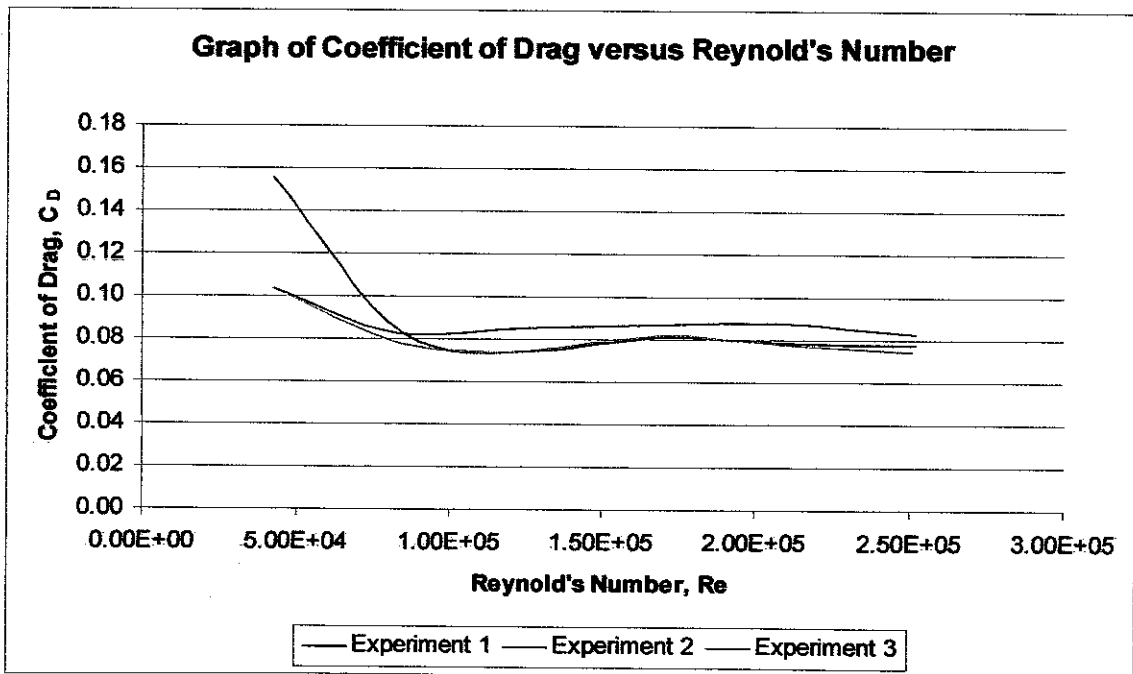


Figure 61: Graph of coefficient of drag versus Reynolds number at 8°.

Table 19: Experimental results for three experiments when angle of attack is 10°.

Velocity (m/s)	Experiment 1: Single airfoil			Experiment 2: Two airfoils with separating distance of 1 chord length (13cm)			Experiment 3: Two airfoils with separating distance of 2 chord length (26cm)		
	C _L	C _D	Re	C _L	C _D	Re	C _L	C _D	Re
5	0.59	0.15	4.19E+04	0.57	0.10	4.19E+04	0.54	0.15	4.19E+04
10	0.66	0.11	8.46E+04	0.61	0.11	8.22E+04	0.61	0.08	8.40E+04
15	0.69	0.10	1.26E+05	0.66	0.11	1.26E+05	0.65	0.11	1.26E+05
20	0.71	0.11	1.69E+05	0.66	0.11	1.68E+05	0.68	0.10	1.68E+05
25	0.73	0.10	2.10E+05	0.68	0.10	2.10E+05	0.71	0.10	2.10E+05
30	0.73	0.10	2.52E+05	0.68	0.10	2.51E+05	0.71	0.10	2.52E+05

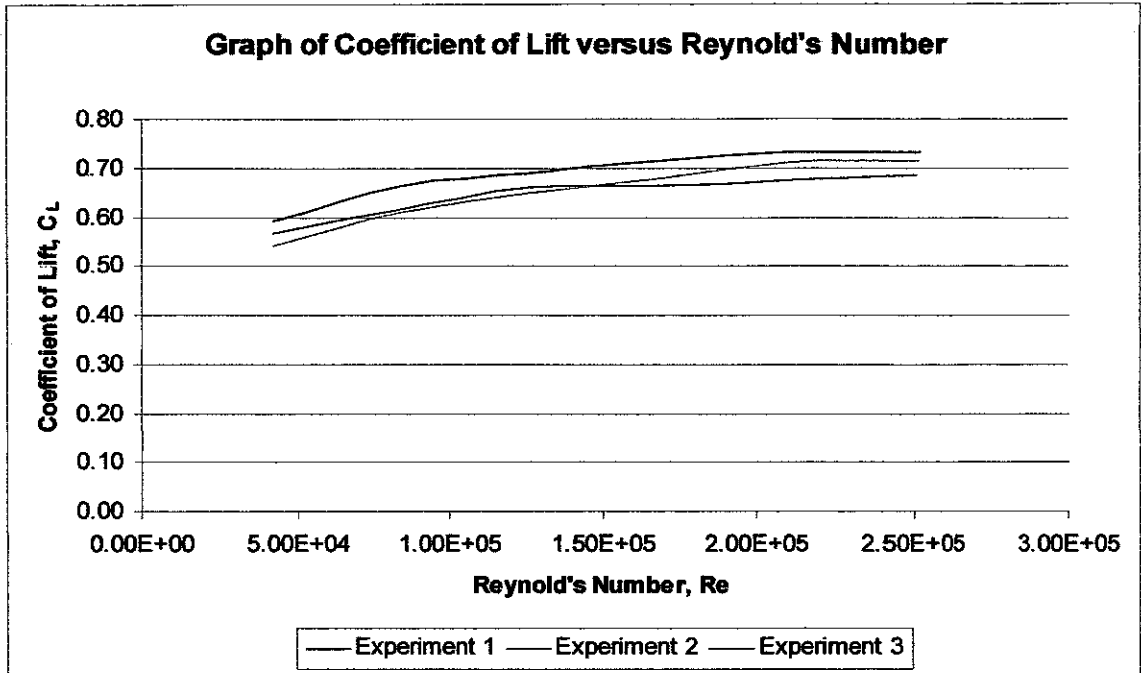


Figure 62: Graph of coefficient of lift versus Reynolds number at 10° .

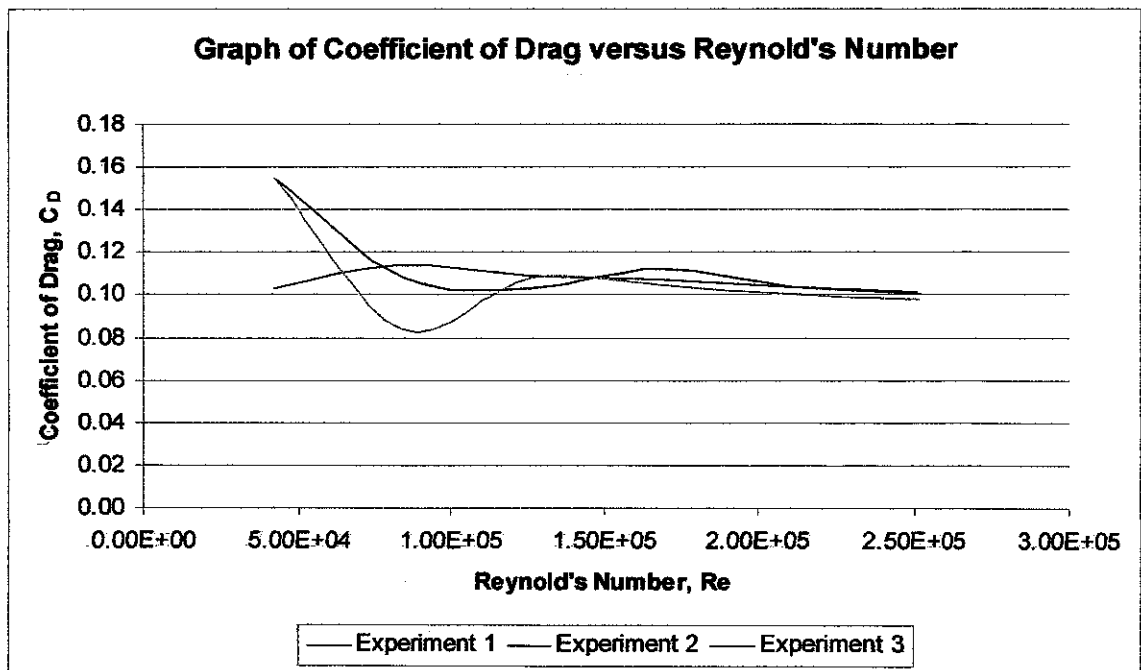


Figure 63: Graph of coefficient of drag versus Reynolds number at 10° .

Table 20: Experimental results for three experiments when angle of attack is 12°.

Velocity (m/s)	Experiment 1: Single airfoil			Experiment 2: Two airfoils with separating distance of 1 chord length (13cm)			Experiment 3: Two airfoils with separating distance of 2 chord length (26cm)		
	C_L	C_D	Re	C_L	C_D	Re	C_L	C_D	Re
5	0.72	0.14	4.34E+04	0.77	0.13	4.19E+04	0.67	0.15	4.19E+04
10	0.75	0.13	8.46E+04	0.73	0.14	8.22E+04	0.73	0.12	8.40E+04
15	0.79	0.13	1.26E+05	0.78	0.14	1.26E+05	0.79	0.14	1.26E+05
20	0.82	0.13	1.69E+05	0.79	0.14	1.68E+05	0.81	0.13	1.67E+05
25	0.82	0.12	2.10E+05	0.80	0.14	2.10E+05	0.85	0.13	2.10E+05
30	0.83	0.12	2.51E+05	0.80	0.13	2.51E+05	0.87	0.13	2.51E+05

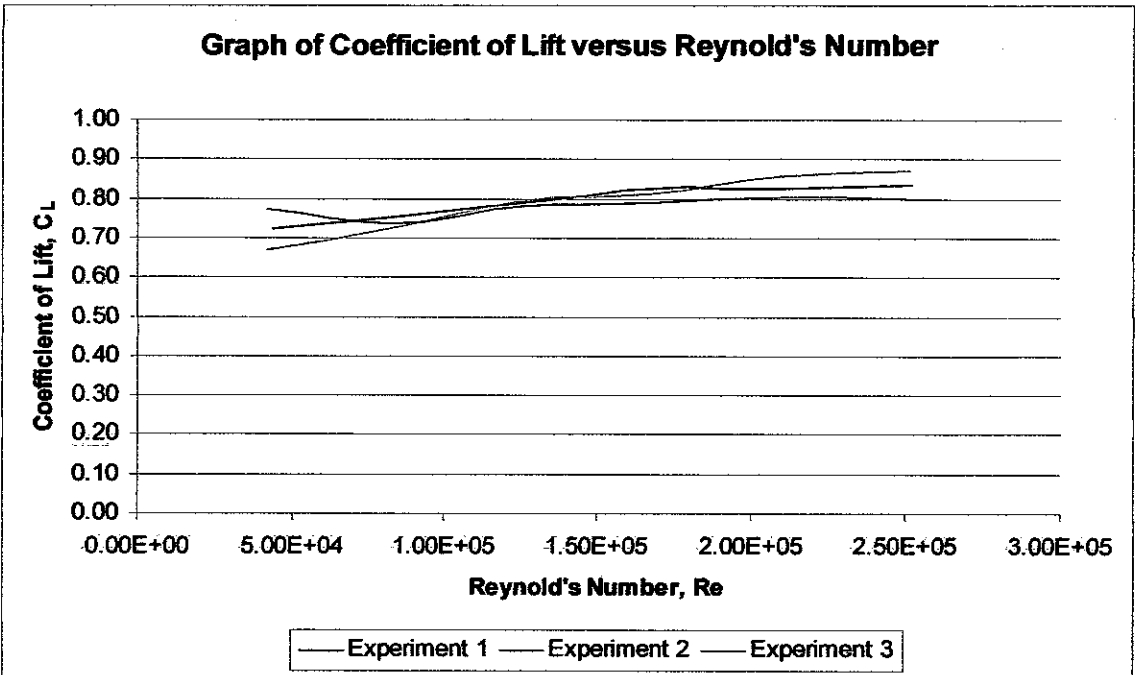


Figure 64: Graph of coefficient of lift versus Reynolds number at 12°.

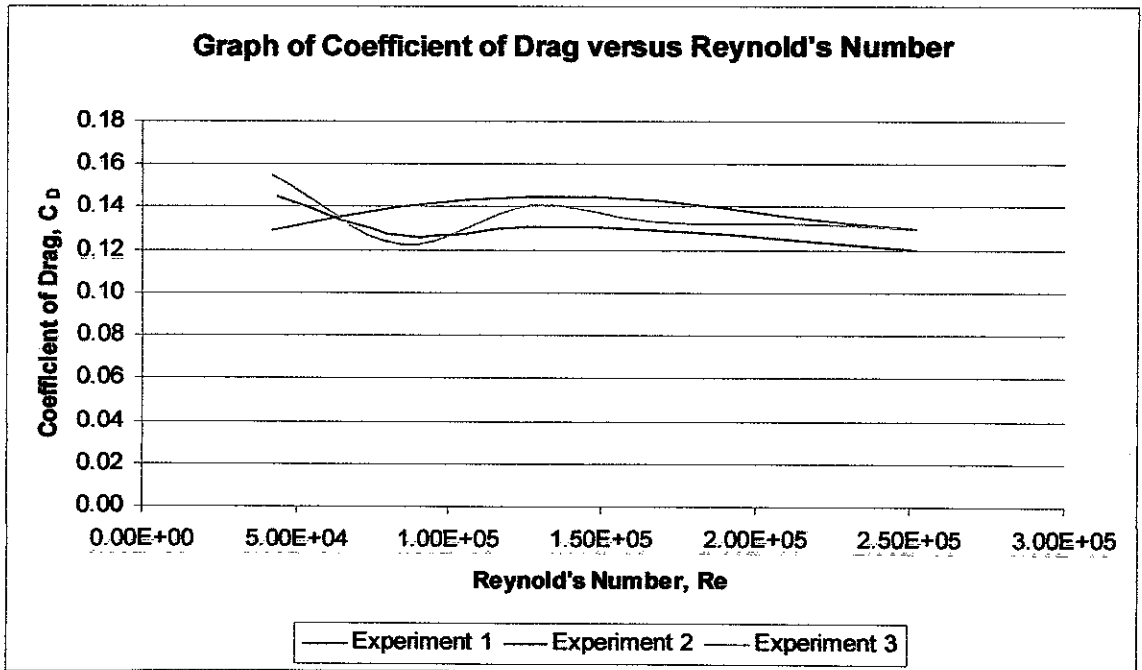


Figure 65: Graph of coefficient of drag versus Reynolds number at 12°.

Table 21: Experimental results for three experiments when angle of attack is 14°.

Velocity (m/s)	Experiment 1: Single airfoil			Experiment 2: Two airfoils with separating distance of 1 chord length (13cm)			Experiment 3: Two airfoils with separating distance of 2 chord length (26cm)		
	C_L	C_D	Re	C_L	C_D	Re	C_L	C_D	Re
5	0.82	0.19	4.34E+04	0.80	0.17	4.34E+04	0.77	0.21	4.19E+04
10	0.84	0.16	8.53E+04	0.86	0.16	8.22E+04	0.86	0.14	8.40E+04
15	0.88	0.17	1.27E+05	0.90	0.18	1.26E+05	0.89	0.16	1.26E+05
20	0.91	0.16	1.69E+05	0.91	0.18	1.68E+05	0.88	0.16	1.68E+05
25	0.92	0.15	2.11E+05	0.93	0.17	2.10E+05	0.96	0.16	2.09E+05
30	0.93	0.15	2.51E+05	0.94	0.16	2.50E+05	0.94	0.16	2.51E+05

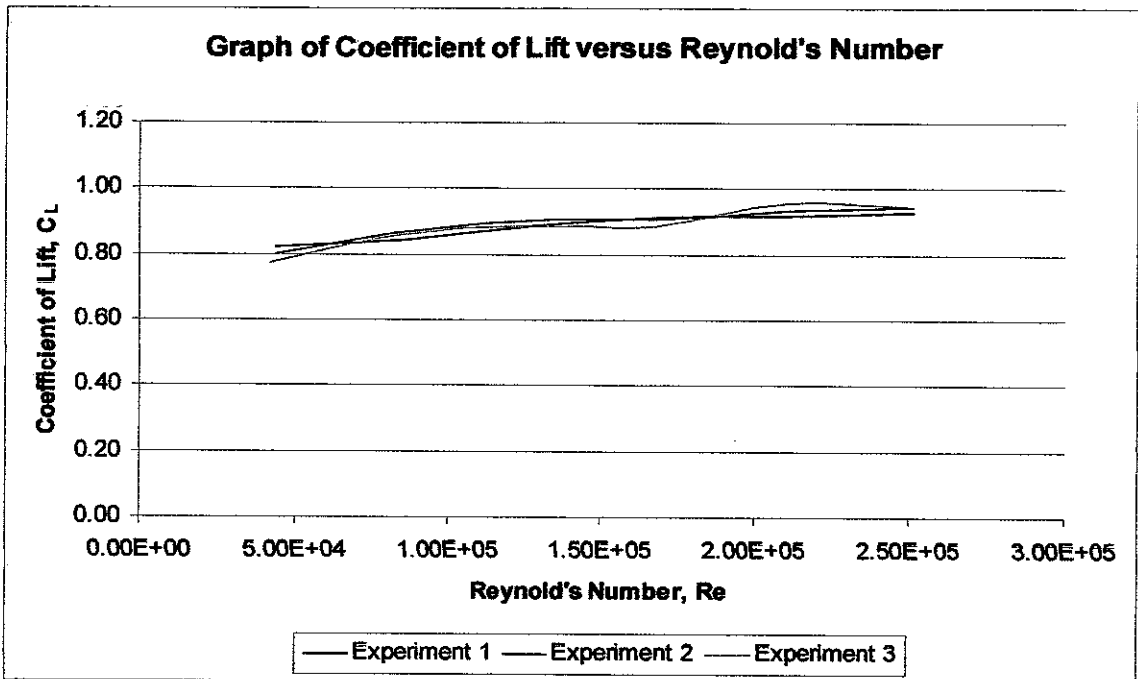


Figure 66: Graph of coefficient of lift versus Reynolds number at 14°.

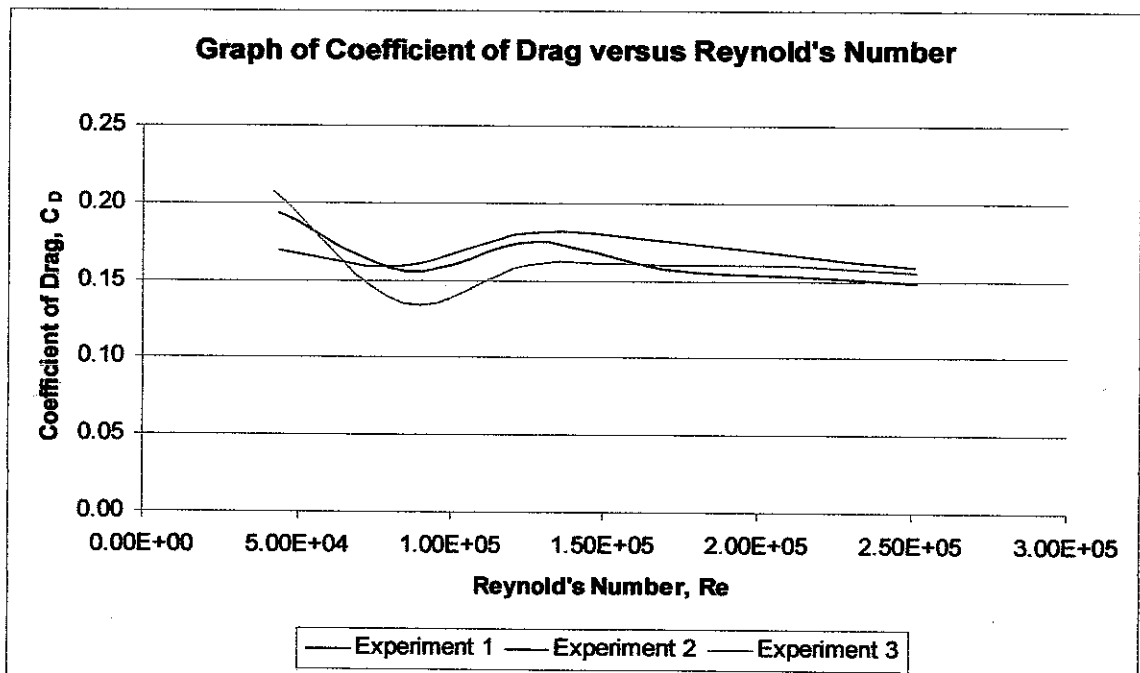


Figure 67: Graph of coefficient of drag versus Reynolds number at 14°.

Table 22: Experimental results for three experiments when angle of attack is 16°.

Velocity (m/s)	Experiment 1: Single airfoil			Experiment 2: Two airfoils with separating distance of 1 chord length (13cm)			Experiment 3: Two airfoils with separating distance of 2 chord length (26cm)		
	C_L	C_D	Re	C_L	C_D	Re	C_L	C_D	Re
5	0.84	0.29	4.34E+04	0.85	0.18	4.19E+04	0.90	0.21	4.19E+04
10	0.90	0.21	8.53E+04	0.93	0.19	8.16E+04	0.93	0.17	8.40E+04
15	0.94	0.18	1.26E+05	0.98	0.23	1.26E+05	1.01	0.21	1.25E+05
20	0.96	0.18	1.69E+05	1.03	0.22	1.67E+05	1.02	0.20	1.68E+05
25	0.98	0.18	2.11E+05	1.06	0.21	2.09E+05	1.07	0.19	2.09E+05
30	0.98	0.18	2.51E+05	1.08	0.20	2.52E+05	0.97	0.19	2.54E+05

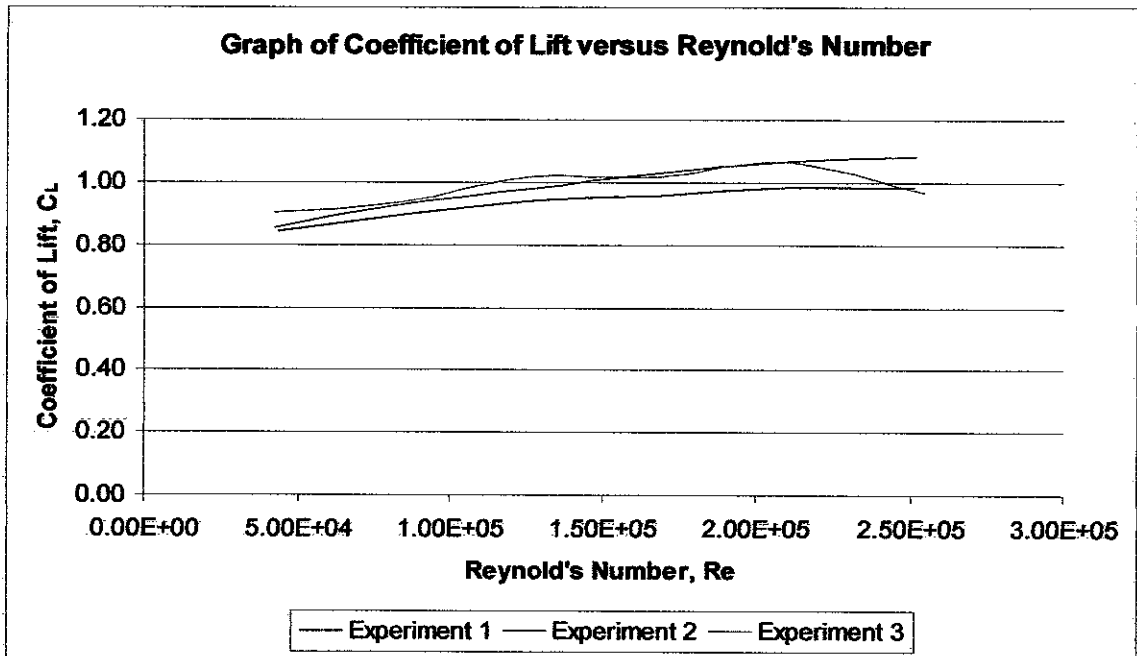


Figure 68: Graph of coefficient of lift versus Reynolds number at 16°.

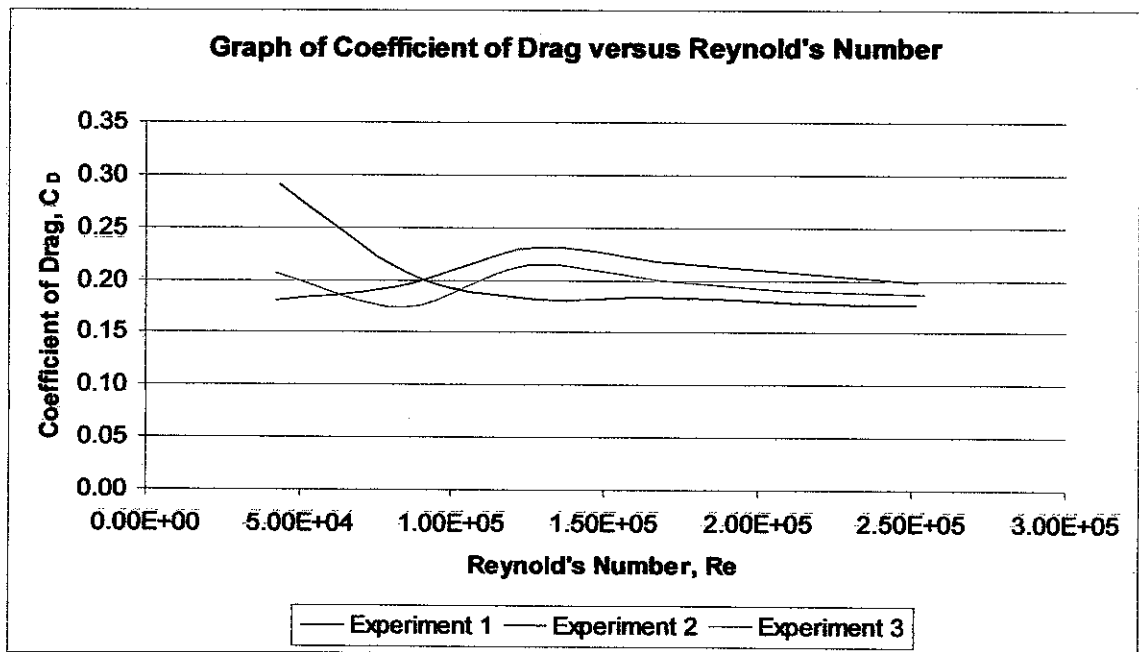


Figure 69: Graph of coefficient of drag versus Reynolds number at 16°.

Table 23: Experimental results for three experiments when angle of attack is 18°.

Velocity (m/s)	Experiment 1: Single airfoil			Experiment 2: Two airfoils with separating distance of 1 chord length (13cm)			Experiment 3: Two airfoils with separating distance of 2 chord length (26cm)		
	C_L	C_D	Re	C_L	C_D	Re	C_L	C_D	Re
5	0.79	0.30	4.28E+04	1.00	0.23	4.19E+04	0.80	0.23	4.19E+04
10	0.89	0.32	8.40E+04	1.04	0.23	8.22E+04	0.85	0.21	8.46E+04
15	0.95	0.32	1.26E+05	1.10	0.25	1.26E+05	0.99	0.23	1.26E+05
20	0.95	0.22	1.68E+05	1.08	0.23	1.68E+05	1.01	0.22	1.68E+05
25	0.99	0.21	2.10E+05	1.09	0.23	2.09E+05	1.06	0.21	2.09E+05
30	0.98	0.25	2.52E+05	1.11	0.22	2.52E+05	0.81	0.21	2.52E+05

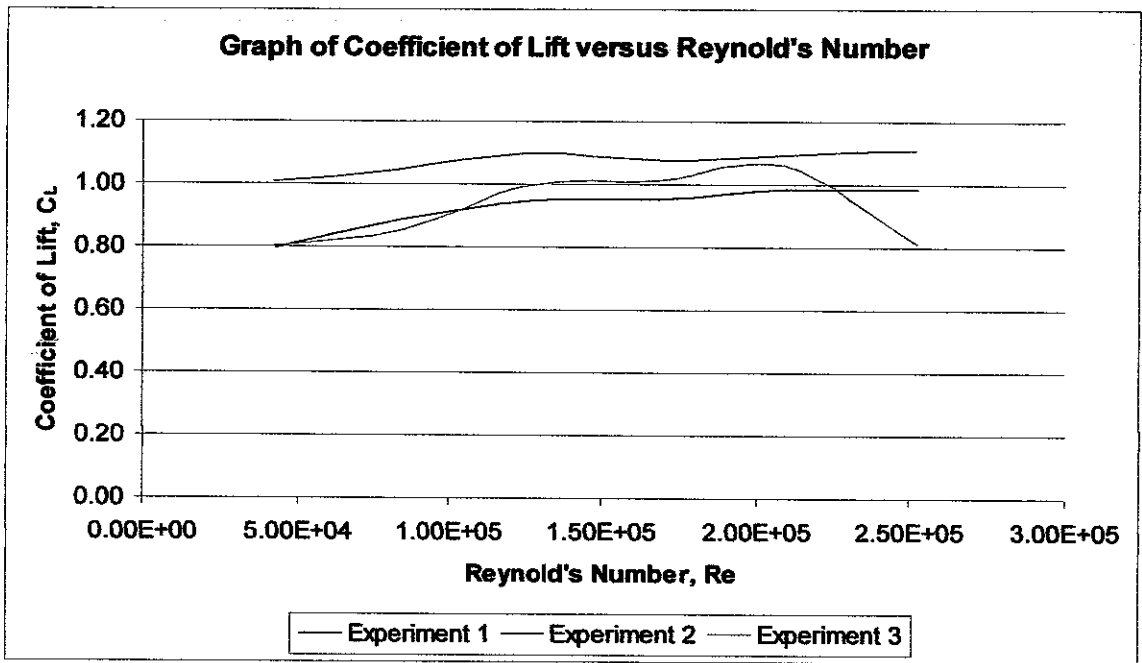


Figure 70: Graph of coefficient of lift versus Reynolds number at 18°.

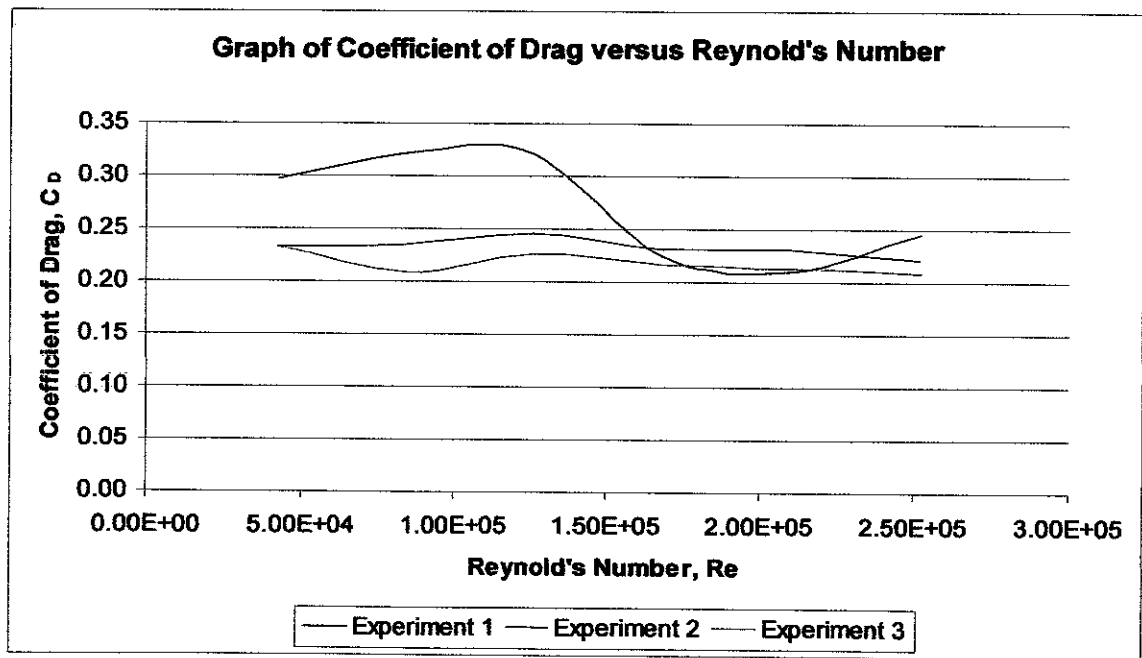


Figure 71: Graph of coefficient of drag versus Reynolds number at 18°.

Table 24: Experimental results for three experiments when angle of attack is 20°.

Velocity (m/s)	Experiment 1: Single airfoil			Experiment 2: Two airfoils with separating distance of 1 chord length (13cm)			Experiment 3: Two airfoils with separating distance of 2 chord length (26cm)		
	C_L	C_D	Re	C_L	C_D	Re	C_L	C_D	Re
5	0.77	0.46	4.19E+04	0.87	0.29	4.34E+04	0.95	0.31	4.19E+04
10	0.82	0.40	8.46E+04	1.02	0.27	8.29E+04	1.01	0.39	8.46E+04
15	0.87	0.40	1.25E+05	1.07	0.33	1.26E+05	1.04	0.36	1.26E+05
20	0.91	0.40	1.68E+05	0.95	0.37	1.68E+05	0.97	0.36	1.68E+05
25	0.97	0.36	2.10E+05	0.96	0.37	2.09E+05	1.04	0.35	2.09E+05
30	0.92	0.39	2.51E+05	0.96	0.36	2.51E+05	0.80	0.31	2.50E+05

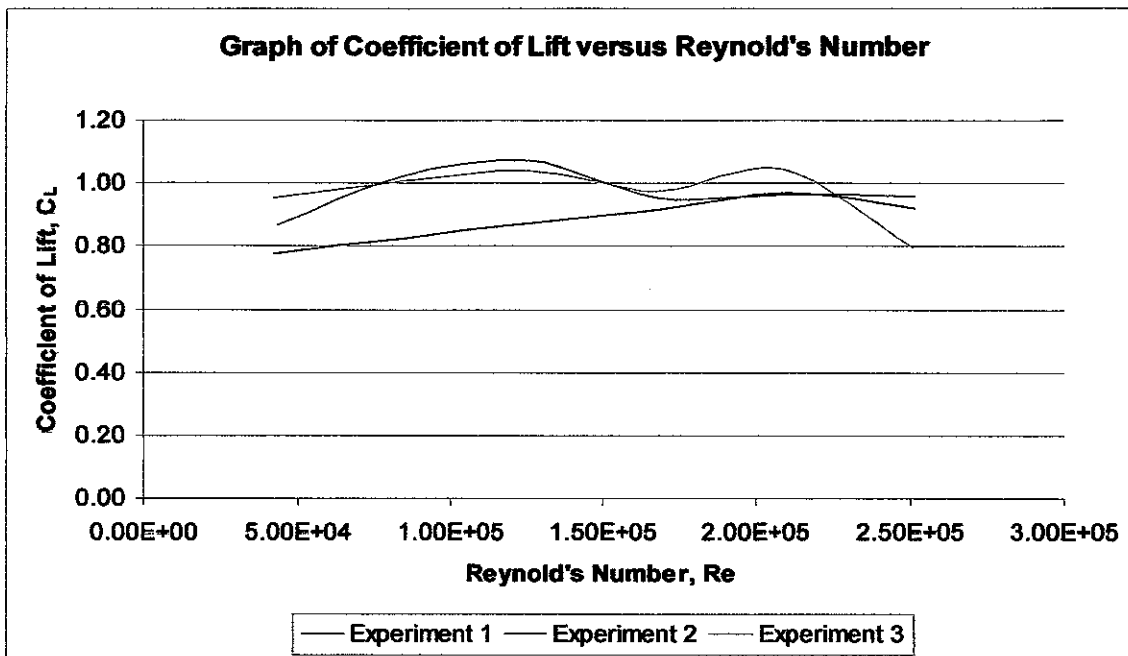


Figure 72: Graph of coefficient of lift versus Reynolds number at 20°.

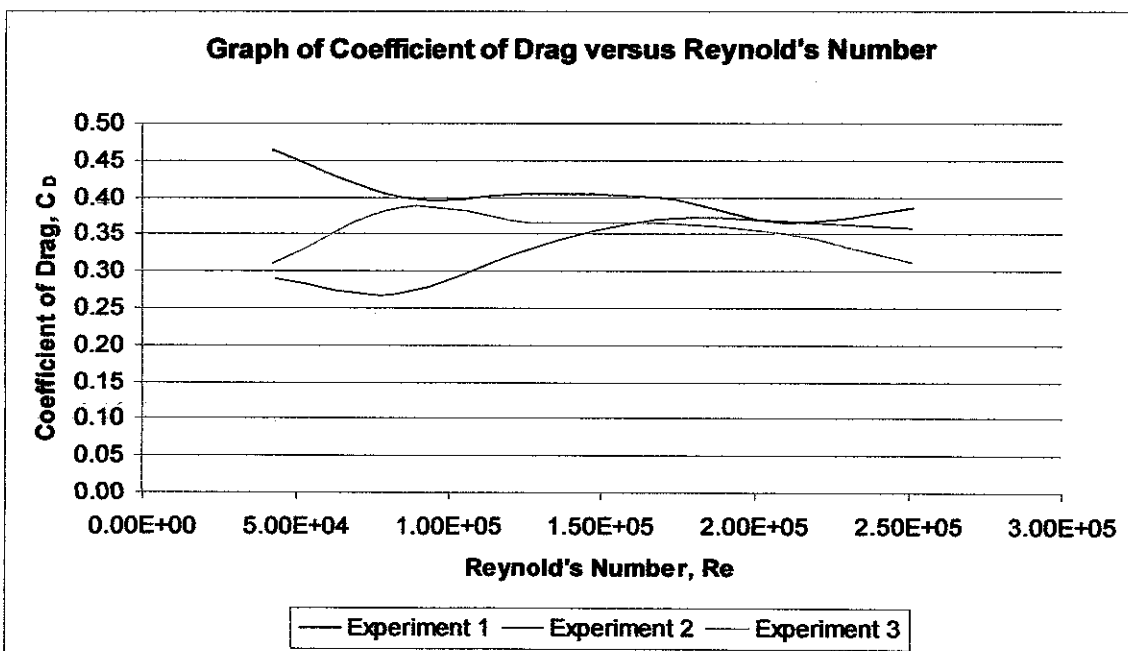


Figure 73: Graph of coefficient of drag versus Reynolds number at 20°.

4.6.6 Analysis of the coefficient of lift with Reynolds number.

Coefficient of lift for three experiments increases with Reynolds number for angle of attack from 0° to 18° . When the angle of attack is 0° , Figure 52 shows that the coefficient of lift for Experiment 1 is higher than the coefficient of lift for Experiment 2 and Experiment 3 from the Reynolds number of 80000 onwards. From the angle of attack of 2° to 6° , the trend of graph plotted shows that the coefficient of lift increases with Reynolds number for three experiments as shown in Figure 54, Figure 56 and Figure 58. The gap between the trend lines is getting closer which means the coefficient of lift is getting closer. From the angle of attack of 6° to 10° , Figure 58, Figure 60 and Figure 62 show that the gap between the trend lines is still getting closer and the coefficient of lift is getting closer. But, the coefficient of lift for Experiment 3 is higher than the coefficient of lift for Experiment 2 at some point of the Reynolds number. From the angle of attack of 10° to 14° , the coefficient of lift is recover and almost the same for three experiments as shown in Figure 62, Figure 64 and Figure 66.

At the angle of attack of 16° , the coefficient of lift for Experiment 2 and Experiment 3 are higher than the coefficient of lift for Experiment 1 as shown in Figure 68. Stall angle for Experiment 1 is in the range of 15° to 17.5° . At the angle of attack of 16° , the coefficient of lift for Experiment 1 is highest where further increase of angle of attack will decrease the coefficient of lift due to separation of flow over the airfoil model. At the angle of attack of 18° , the coefficient of lift for Experiment 2 is higher than the coefficient of lift for Experiment 3 and Experiment 1 as shown in Figure 70. Stall angle for Experiment 2 is in the range of 17.5° to 18.5° . At the angle of attack of 18° , the coefficient of lift for Experiment 2 is highest where further increase of angle of attack will decrease the coefficient of lift due to flow separation over the airfoil model. It may be due to wake produced from the front airfoil model to the trailing airfoil model and increases the stall angle from the range of 15° to 17.5° in Experiment 1 to the range of 17.5° to 18.5° in Experiment 2. Besides, the coefficient of lift for Experiment 3 is lower than coefficient of lift for Experiment 2 and almost similar to the coefficient of lift for Experiment 1. The results show that the stall angle for Experiment 3 is in the range of 16°

$^{\circ}$ to 16.5° is almost similar to the stall angle of Experiment 1 in the range of 15° to 17.5° . The reason behind this may be due to the wake produced from the front airfoil model to the trailing airfoil model is too weak and it has little effect to the velocity inlet of the trailing airfoil model.

At the angle of attack of 20° , the coefficient of lift for Experiment 1, Experiment 2 and Experiment 3 are decreasing with increasing Reynolds number. This is due to the flow separation over the airfoil where the coefficient of lift decreases after the stall angle.

4.6.7 Analysis of the coefficient of drag with Reynolds number.

Coefficient of drag for three experiments decreases with Reynolds number for angle of attack from 0° to 10° . When the angle of attack is from 0° to 2° , Figure 53 and Figure 55 show that the coefficients of drag for Experiment 1 and Experiment 2 are higher than the coefficient of drag for Experiment 3 with increasing Reynolds number. At the angle of attack of 4° , Figure 57 shows that the coefficient of drag for Experiment 1 higher than coefficient of drag for Experiment 2 and Experiment 3 at the Reynolds number of 125000 onwards. At the angle of attack of 6° , Figure 59 shows that the coefficient of drag for Experiment 1 higher than coefficient of drag for Experiment 2 and Experiment 3. At the angle of attack of 8° , the coefficient of drag for Experiment 2 is higher than coefficient of drag for Experiment 1 and Experiment 3 at the Reynolds number of 80000 onwards as shown in Figure 61. At the angle of attack of 10° , Figure 63 shows that the coefficient of drag for three experiments is almost the same at the Reynolds number of 125000 onwards. The gap between the trend lines is getting closer which means the coefficient of drag is getting closer. The coefficient of drag decrease with increasing Reynolds number most of the time. This reason may be due to the skin friction drag acting on the surface of the airfoil model decreases at high Reynolds number. Besides, coefficient of drag decreases at high free stream velocity.

From the angle of attack of 12° to 16° , Figure 65, Figure 67 and Figure 69 show that the trend of graphs plotted for experiments are almost same where the coefficient of drag decreases with increasing Reynolds number of 125000 onwards. At the angle of attack of 18° , Figure 71 shows that the coefficient of drag for Experiment 2 and Experiment 3 decrease with increasing Reynolds number of 125000 onwards. Meanwhile, the drag coefficient for Experiment 1 decreases from the Reynolds number of 125000 to 200000. At the angle of attack of 20° , Figure 73 shows that the coefficient of drag for Experiment 1 decreases from the Reynolds number of 41900 to 225000. The coefficient of drag for Experiment 3 decreases from the Reynolds number of 84000 to 250000. But, the coefficient of drag for Experiment 2 is not following the trend, it increase from the Reynolds number of 82900 to 251000. The results show that the coefficient of drag decrease with increasing Reynolds number most of the time because of the skin friction drag acting on the surface of the airfoil model decreases. When the free stream velocity is increased, the coefficient of drag decreases. The coefficient of drag for Experiment 2 is increasing with Reynolds number may be due to the blockage of the front airfoil model which affects the velocity at the inlet of the trailing airfoil model. Skin friction drag can be considered to appear over the surface of the airfoil model all the times. At the same time, pressure drag may be obvious during the separation flow and increases the coefficient of drag for Experiment 2.

CHAPTER 5

CONCLUSION

The experimental study of the effects of wake turbulence on aircraft wing model has shown good results and meets the objective of the project. In Experiment 1, a single airfoil model is tested in the wind tunnel. The experimental results show that the coefficient of lift increases with angle of attack and decreases after the stall angle. The stall angle for Experiment 1 is in the range of 15° to 17.5° and the coefficient of lift at the stall angle is in the range of 0.86 to 0.99. The experimental results from Experiment 1 are validated and within the range of the airfoil data for NACA 2412 wing section in Appendix I. The coefficient of drag shows steady behavior and increases with angle of attack. The coefficient of drag for Experiment 1 is in the range of 0.04 to 0.46. Besides, the coefficient of lift increase with Reynolds number before the stall angle and decreases with Reynolds number after the stall angle. It may be due to the separation of flow over the airfoil. Meanwhile, the coefficient of drag decreases when Reynolds number increases. This may be due to the skin friction drag acting on the surface of the airfoil and the pressure drag during the separation of flow.

The experimental results from Experiment 1 is functioning as a reference to figure out the effects and changes that will be experienced when another airfoil model is located in front of the trailing airfoil model at a certain distance. In Experiment 2, two airfoil models with a separating distance of 1 chord length (13cm) are tested in the wind tunnel. The coefficient of lift increases with angle of attack and decreases after the stall angle. The stall angle for Experiment 2 is increased and it is in the range of 17.5° to 18.5° . During the experiments, it can be noticed that the following airfoil model is vibrating and oscillating due to the wake produced by front airfoil model. The coefficient of drag shows steady behavior and increase with angle of attack. The coefficient of drag in Experiment 2 is in the range of 0.03 to 0.37 which is slightly lower than the coefficient

of drag in Experiment 1 due to the blockage of airflow of the front airfoil model to the trailing airfoil model. Besides, the coefficient of lift in Experiment 2 increase with Reynolds number before the stall angle and decreases with Reynolds number after the stall angle. The reason may be due to the separation of flow over the airfoil model. Meanwhile, the coefficient of drag decreases when Reynolds number increases because the skin friction drag acting on the surface of the airfoil model decreases. After the stall angle, the coefficient of drag for Experiment 2 increases with Reynolds number may be due to the pressure drag during the separation of flow over the trailing airfoil model.

In Experiment 3, two airfoil models with a separating distance of 2 chord length (26cm) are tested in the wind tunnel. The coefficient of lift increases with angle of attack and decreases after the stall angle. The stall angle for Experiment 3 is the range of 16° to 16.5° which is almost the same as the coefficient of lift in Experiment 1. During the experiments, it can be noticed that the following airfoil model is vibrating and oscillating slightly from the angle of attack of 12° onwards. This shows the wake produced by front airfoil model is very weak. The weak wake may have little effect to the flow at the inlet of the trailing airfoil model. The coefficient of drag shows steady behavior and increase with angle of attack. The coefficient of drag in Experiment 2 is in the range of 0.02 to 0.39 which is slightly lower than the coefficient of drag in Experiment 1 due to the blockage of air flow of the front airfoil model to the trailing airfoil model. Besides, the coefficient of lift in Experiment 3 increase with Reynolds number before the stall angle and decreases with Reynolds number after the stall angle. It may be due to the separation of flow over the airfoil. Meanwhile, the coefficient of drag decreases when Reynolds number increases. This is because of the skin friction drag acting on the surface of the airfoil model decreases and the high free stream velocity.

As a conclusion, the separating distance between the two airfoil models from Experiment 2 and Experiment 3 has shown that the coefficient of lift and coefficient of drag of the trailing airfoil model are affected due to the wake turbulence produced from the front airfoil model. At the same time, Reynolds number can be related to the change

of the coefficient of lift and coefficient of drag of the trailing airfoil model. Meanwhile, the results from this research project are very applicable in future especially to prevent or at least reduced the unnecessary aircraft accident due to wake turbulence.

CHAPTER 6

RECOMMENDATION

A few recommendations are suggested for the improvement of this project on study the effect of wake turbulence on the aircraft wing model. The experiments can be conducted in the high speed or supersonic wind tunnel so that the airfoil models can be tested at real condition. The airfoil models are recommended to be tested in a longer wind tunnel test section at variable distances such as 1 span, 2 spans and more in order to obtain the accurate and precise data. Besides, it is suggested that the airfoil model is fabricated by using 5-axis MAZAK CNC machining in order to get one piece of complete aircraft wing model and a better surface finish.

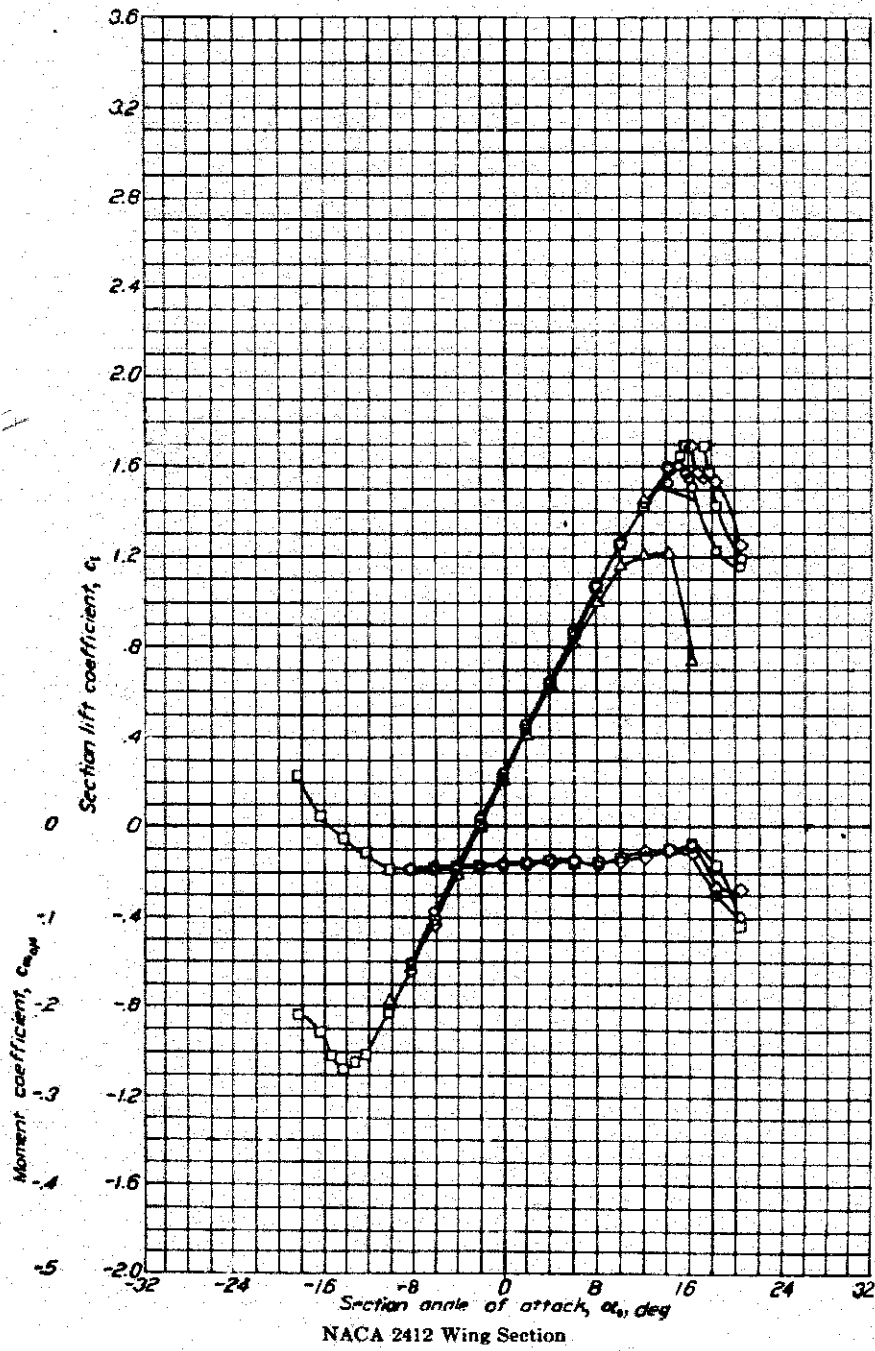
REFERENCES

- [1]. Capt. N.p. Puri & FLT.LT.Flt Lt Ramiah Saravanan, Wake Turbulence: Understand and Avoid the Danger, Airlines Magazines, e-zine edition, Issue 27
- [2]. "Wake turbulence and light aircraft",
www.ultraflight.com/thornburgh/wake_turbulece
- [3]. "Flight Safety", http://www.pilotfriend.com/safe/safety/wake_turb.htm
- [4]. R H Barnard and D R Philpott, Aircraft Flight, 3rd Edition, Pearson Prentice Hall, 2004, pg1,2
- [5]. R H Barnard and D R Philpott, Aircraft Flight, 3rd Edition, Pearson Prentice Hall, 2004, pg36,65
- [6]. A.C. Kermode, Mechanics of Flight, 11th Edition, Pearson Prentice Hall, 2006, pg70
- [7]. R H Barnard and D R Philpott, Aircraft Flight, 3rd Edition, Pearson Prentice Hall, 2004, pg19,22,23
- [8]. "Aircraft Wake Turbulence", <http://www.aviationwise.org/>
- [9]. Richard S. Shevell, Fundamentals of flight, 2nd Edition, Prentice Hall, 1989, pg 218
- [10]. Clayton T. Crowe, Donald F. Elger, John. A. Roberson, Engineering Fluid Mechanics 8th Edition, John Wiley & Sons, 2005, pg462
- [11]. A.C. Kermode, Mechanics of Flight, 11th Edition, Pearson Prentice Hall, 2006, pg80
- [12]. "Cessna 172 Aircraft", <http://flyadi.net/cessna172.aspx>
- [13]. "NACA 4 digits series",
<http://www.ppart.de/programming/java/profiles/NACA4.html>
- [14]. John D. Anderson, Jr. , Introduction to flight, 5th Edition, McGraw Hill, 2005, pg784

[15]. Z. Husain, M. Z. Abdullah and T. C. Yap, Two-dimensional analysis of tandem/staggered airfoils using computational fluid dynamics, *International Journal of Mechanical Engineering Education* 33/3.

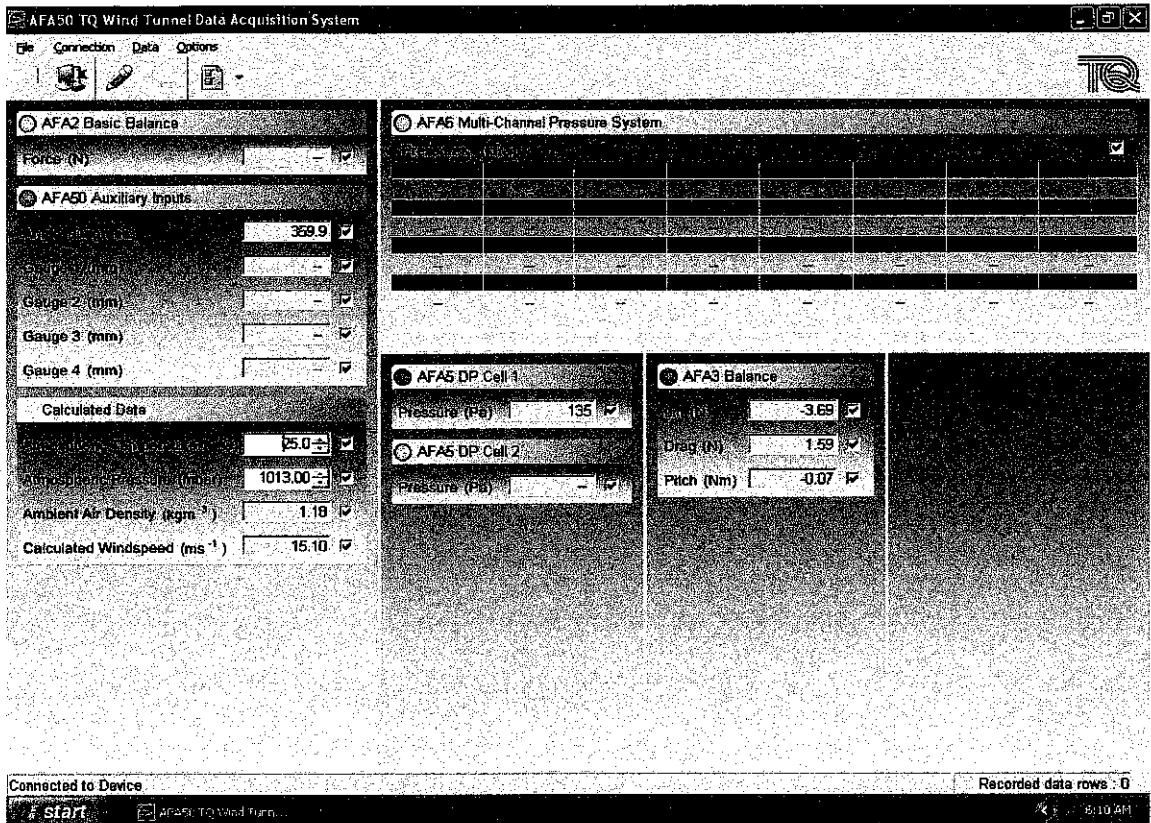
APPENDIX I

NACA 2412 Wing Section Airfoil Data



APPENDIX II

Lift and Drag Forces Measured by 3-Components Balance

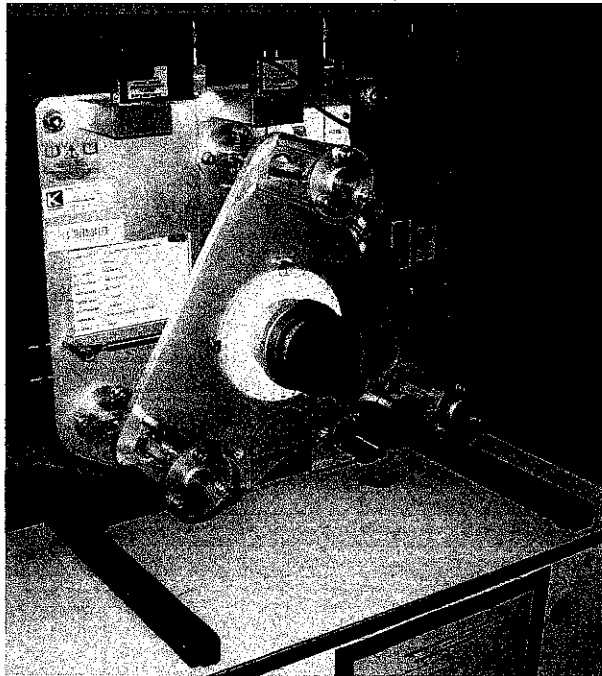


APPENDIX III

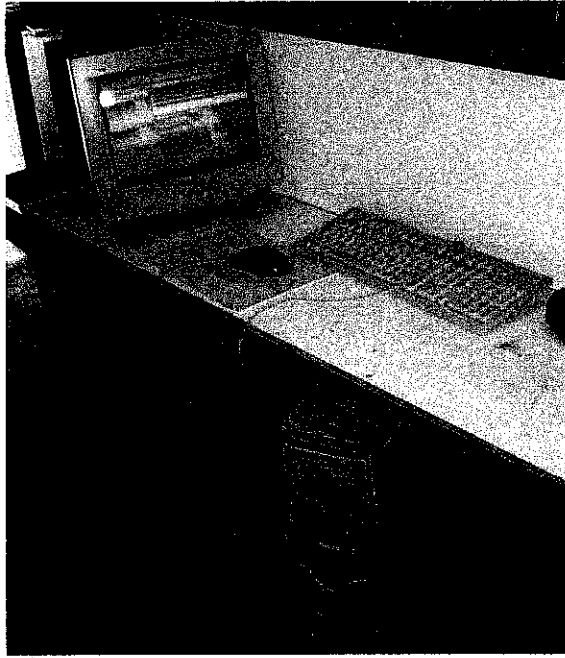
Components of the Wind Tunnel



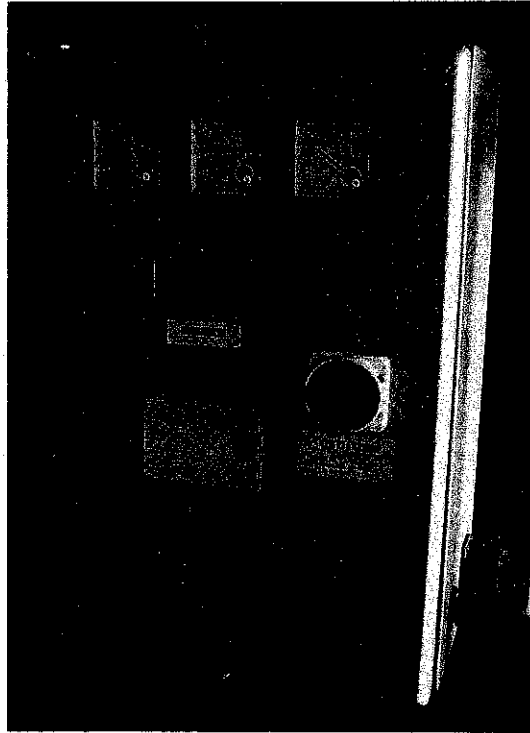
Test Section



3-Components Balance to Measure the Lift and Drag Forces



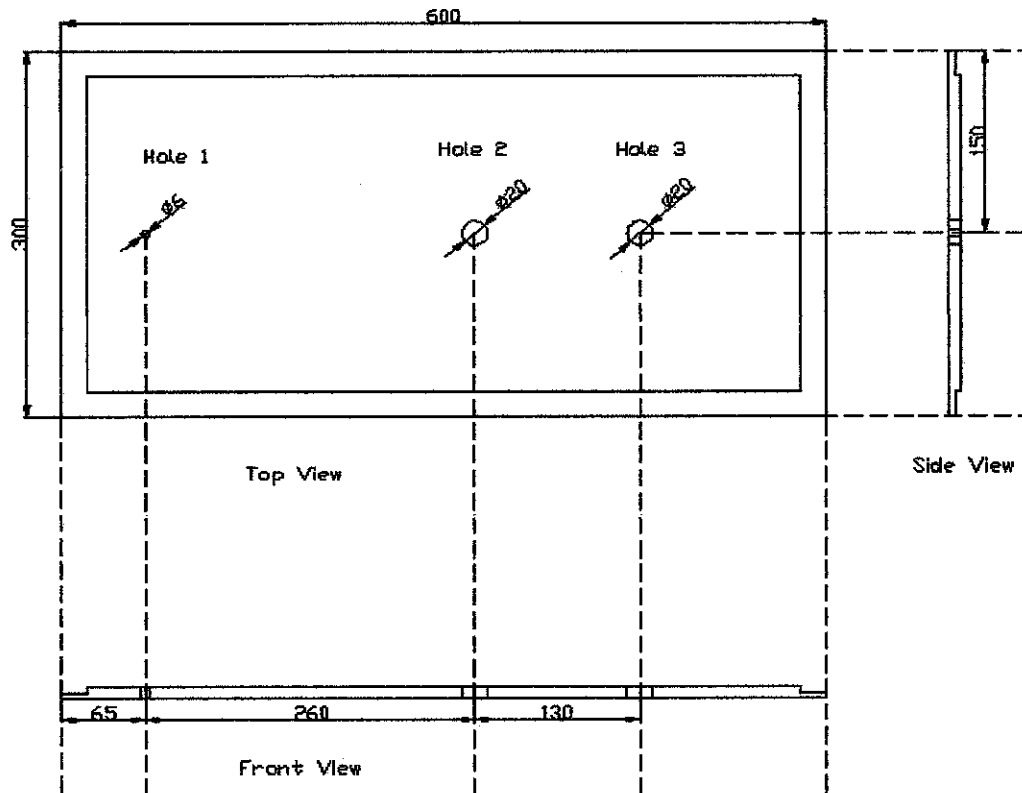
Automatic Data Acquisition System



Electrical Control Panel to Control the Wind Tunnel Velocity

APPENDIX IV

Details Drawing of the Perspex Wall of the Test Section



Remarks:

1. The size of the perspex wall of the test section is 300mm (W) x 600mm (L) x 10mm (H).
2. Airfoil wing model shown in Figure 35 is fixed at Hole 1 during Experiment 2 and Experiment 3.
3. Airfoil wing model shown in Figure 36 is connected to the 3-Components Balance shown in Appendix III through the Hole 2 during Experiment 1 and Experiment 2.
4. Airfoil wing model shown in Figure 36 is connected to the 3-Components Balance shown in Appendix III through the Hole 3 during Experiment 3.

APPENDIX V

Lift and Drag Forces Measured by the 3-Components Balance for Section 4.6.1

Experimental Results for three experiments at 5m/s.

Angle of Attack (Degree)	Experiment 1: Single airfoil		Experiment 2: Two airfoils with separating distance of 1 chord length (13cm)		Experiment 3: Two airfoils with separating distance of 2 chord length (26cm)	
	F _L (N)	F _D (N)	F _L (N)	F _D (N)	F _L (N)	F _D (N)
0	0.04	0.03	0.06	0.03	0.01	0.01
2	0.11	0.04	0.07	0.03	0.05	0.02
4	0.13	0.03	0.09	0.02	0.13	0.02
6	0.21	0.05	0.17	0.02	0.15	0.02
8	0.2	0.06	0.18	0.04	0.16	0.04
10	0.23	0.06	0.22	0.04	0.21	0.06
12	0.3	0.06	0.3	0.05	0.26	0.06
14	0.34	0.08	0.33	0.07	0.3	0.08
16	0.35	0.12	0.33	0.07	0.35	0.08
18	0.32	0.12	0.39	0.09	0.31	0.09
20	0.3	0.18	0.36	0.12	0.37	0.12

Experimental Results for three experiments at 10m/s.

Angle of Attack (Degree)	Experiment 1: Single airfoil		Experiment 2: Two airfoils with separating distance of 1 chord length (13cm)		Experiment 3: Two airfoils with separating distance of 2 chord length (26cm)	
	F _L (N)	F _D (N)	F _L (N)	F _D (N)	F _L (N)	F _D (N)
0	0.33	0.11	0.07	0.12	0.14	0.04
2	0.5	0.08	0.3	0.06	0.3	0.04
4	0.58	0.07	0.42	0.06	0.5	0.08
6	0.78	0.13	0.63	0.09	0.66	0.07
8	0.94	0.13	0.79	0.13	0.78	0.12
10	1.05	0.17	0.97	0.18	0.95	0.13
12	1.19	0.2	1.16	0.22	1.13	0.19
14	1.35	0.25	1.36	0.25	1.33	0.21
16	1.44	0.33	1.44	0.3	1.45	0.27
18	1.38	0.5	1.65	0.37	1.35	0.33
20	1.3	0.63	1.63	0.43	1.59	0.61

Experimental Results for three experiments at 15m/s.

Angle of Attack (Degree)	Experiment 1: Single airfoil		Experiment 2: Two airfoils with separating distance of 1 chord length (13cm)		Experiment 3: Two airfoils with separating distance of 2 chord length (26cm)	
	F _L (N)	F _D (N)	F _L (N)	F _D (N)	F _L (N)	F _D (N)
0	0.85	0.15	0.16	0.2	0.33	0.1
2	1.18	0.15	0.64	0.15	0.73	0.12
4	1.42	0.16	0.99	0.15	1.13	0.16
6	1.8	0.23	1.48	0.2	1.51	0.18
8	2.04	0.26	1.88	0.3	1.86	0.26
10	2.41	0.36	2.31	0.38	2.29	0.38
12	2.78	0.46	2.74	0.51	2.77	0.49
14	3.14	0.62	3.14	0.63	3.1	0.56
16	3.3	0.64	3.44	0.81	3.52	0.74
18	3.34	1.13	3.84	0.86	3.47	0.79
20	3.02	1.4	3.74	1.15	3.65	1.28

Experimental Results for three experiments at 20m/s.

Angle of Attack (Degree)	Experiment 1: Single airfoil		Experiment 2: Two airfoils with separating distance of 1 chord length (13cm)		Experiment 3: Two airfoils with separating distance of 2 chord length (26cm)	
	F _L (N)	F _D (N)	F _L (N)	F _D (N)	F _L (N)	F _D (N)
0	1.57	0.33	0.4	0.26	0.78	0.16
2	2.06	0.24	1.2	0.22	1.38	0.19
4	2.58	0.32	1.86	0.28	2.1	0.29
6	3.22	0.43	2.67	0.41	2.76	0.38
8	3.74	0.5	3.48	0.54	3.49	0.51
10	4.46	0.7	4.13	0.67	4.22	0.65
12	5.19	0.81	4.91	0.89	5.01	0.82
14	5.7	0.99	5.64	1.09	5.49	0.99
16	6.02	1.15	6.34	1.34	6.32	1.24
18	5.9	1.39	6.71	1.44	6.28	1.34
20	5.7	2.49	5.94	2.31	6.04	2.26

Experimental Results for three experiments at 25m/s.

Angle of Attack (Degree)	Experiment 1: Single airfoil		Experiment 2: Two airfoils with separating distance of 1 chord length (13cm)		Experiment 3: Two airfoils with separating distance of 2 chord length (26cm)	
	F _L (N)	F _D (N)	F _L (N)	F _D (N)	F _L (N)	F _D (N)
0	2.41	0.35	0.7	0.36	1.28	0.28
2	3.11	0.42	1.88	0.32	2.2	0.29
4	4.14	0.49	2.96	0.47	3.46	0.47
6	5.13	0.64	4.36	0.64	4.49	0.57
8	5.93	0.75	5.51	0.85	5.57	0.75
10	7.13	1.01	6.56	1.01	6.87	0.97
12	8.05	1.22	7.79	1.31	8.28	1.28
14	8.99	1.5	9.05	1.62	9.23	1.54
16	9.63	1.74	10.27	2.01	10.31	1.84
18	9.57	2.04	10.56	2.23	10.19	2.04
20	9.45	3.55	9.31	3.55	10.04	3.37

Experimental Results for three experiments at 30m/s.

Angle of Attack (Degree)	Experiment 1: Single airfoil		Experiment 2: Two airfoils with separating distance of 1 chord length (13cm)		Experiment 3: Two airfoils with separating distance of 2 chord length (26cm)	
	F _L (N)	F _D (N)	F _L (N)	F _D (N)	F _L (N)	F _D (N)
0	3.44	0.52	1.07	0.47	2.05	0.4
2	4.82	0.59	2.73	0.49	3.26	0.44
4	6.23	0.71	4.32	0.63	5.12	0.64
6	7.47	0.88	6.31	0.87	6.34	0.79
8	8.62	1.09	8.02	1.16	8.19	1.03
10	10.21	1.41	9.5	1.41	9.94	1.37
12	11.61	1.67	11.15	1.81	12.08	1.8
14	12.88	2.07	13.01	2.2	13.13	2.16
16	13.67	2.45	15.05	2.77	13.75	2.65
18	13.81	3.44	15.44	3.09	11.36	2.92
20	12.76	5.37	13.32	4.96	11.05	4.32

APPENDIX VI

Lift and Drag Forces Measured by the 3-Components Balance for Section 4.6.5

Experimental Results for three experiments when angle of attack is 0°.

Free Stream Velocity (m/s)	Experiment 1: Single airfoil		Experiment 2: Two airfoils with separating distance of 1 chord length (13cm)		Experiment 3: Two airfoils with separating distance of 2 chord length (26cm)	
	F _L (N)	F _D (N)	F _L (N)	F _D (N)	F _L (N)	F _D (N)
5	0.04	0.03	0.06	0.03	0.01	0.01
10	0.33	0.11	0.07	0.12	0.14	0.04
15	0.85	0.15	0.16	0.2	0.33	0.1
20	1.57	0.33	0.4	0.26	0.78	0.16
25	2.41	0.35	0.7	0.36	1.28	0.28
30	3.44	0.52	1.07	0.47	2.05	0.4

Experimental Results for three experiments when angle of attack is 2°.

Free Stream Velocity (m/s)	Experiment 1: Single airfoil		Experiment 2: Two airfoils with separating distance of 1 chord length (13cm)		Experiment 3: Two airfoils with separating distance of 2 chord length (26cm)	
	F _L (N)	F _D (N)	F _L (N)	F _D (N)	F _L (N)	F _D (N)
5	0.11	0.04	0.07	0.03	0.05	0.02
10	0.5	0.08	0.3	0.06	0.3	0.04
15	1.18	0.15	0.64	0.15	0.73	0.12
20	2.06	0.24	1.2	0.22	1.38	0.19
25	3.11	0.42	1.88	0.32	2.2	0.29
30	4.82	0.59	2.73	0.49	3.26	0.44

Experimental Results for three experiments when angle of attack is 4°.

Free Stream Velocity (m/s)	Experiment 1: Single airfoil		Experiment 2: Two airfoils with separating distance of 1 chord length (13cm)		Experiment 3: Two airfoils with separating distance of 2 chord length (26cm)	
	F _L (N)	F _D (N)	F _L (N)	F _D (N)	F _L (N)	F _D (N)
5	0.13	0.03	0.09	0.02	0.13	0.02
10	0.58	0.07	0.42	0.06	0.5	0.08
15	1.42	0.16	0.99	0.15	1.13	0.16
20	2.58	0.32	1.86	0.28	2.1	0.29
25	4.14	0.49	2.96	0.47	3.46	0.47
30	6.23	0.71	4.32	0.63	5.12	0.64

Experimental Results for three experiments when angle of attack is 6°.

Free Stream Velocity (m/s)	Experiment 1: Single airfoil		Experiment 2: Two airfoils with separating distance of 1 chord length (13cm)		Experiment 3: Two airfoils with separating distance of 2 chord length (26cm)	
	F _L (N)	F _D (N)	F _L (N)	F _D (N)	F _L (N)	F _D (N)
5	0.21	0.05	0.17	0.02	0.15	0.02
10	0.78	0.13	0.63	0.09	0.66	0.07
15	1.8	0.23	1.48	0.2	1.51	0.18
20	3.22	0.43	2.67	0.41	2.76	0.38
25	5.13	0.64	4.36	0.64	4.49	0.57
30	7.47	0.88	6.31	0.87	6.34	0.79

Experimental Results for three experiments when angle of attack is 8°.

Free Stream Velocity (m/s)	Experiment 1: Single airfoil		Experiment 2: Two airfoils with separating distance of 1 chord length (13cm)		Experiment 3: Two airfoils with separating distance of 2 chord length (26cm)	
	F _L (N)	F _D (N)	F _L (N)	F _D (N)	F _L (N)	F _D (N)
5	0.2	0.06	0.18	0.04	0.16	0.04
10	0.94	0.13	0.79	0.13	0.78	0.12
15	2.04	0.26	1.88	0.3	1.86	0.26
20	3.74	0.5	3.48	0.54	3.49	0.51
25	5.93	0.75	5.51	0.85	5.57	0.75
30	8.62	1.09	8.02	1.16	8.19	1.03

Experimental Results for three experiments when angle of attack is 10°.

Free Stream Velocity (m/s)	Experiment 1: Single airfoil		Experiment 2: Two airfoils with separating distance of 1 chord length (13cm)		Experiment 3: Two airfoils with separating distance of 2 chord length (26cm)	
	F _L (N)	F _D (N)	F _L (N)	F _D (N)	F _L (N)	F _D (N)
5	0.23	0.06	0.22	0.04	0.21	0.06
10	1.05	0.17	0.97	0.18	0.95	0.13
15	2.41	0.36	2.31	0.38	2.29	0.38
20	4.46	0.7	4.13	0.67	4.22	0.65
25	7.13	1.01	6.56	1.01	6.87	0.97
30	10.21	1.41	9.5	1.41	9.94	1.37

Experimental Results for three experiments when angle of attack is 12°.

Free Stream Velocity (m/s)	Experiment 1: Single airfoil		Experiment 2: Two airfoils with separating distance of 1 chord length (13cm)		Experiment 3: Two airfoils with separating distance of 2 chord length (26cm)	
	F _L (N)	F _D (N)	F _L (N)	F _D (N)	F _L (N)	F _D (N)
5	0.3	0.06	0.3	0.05	0.26	0.06
10	1.19	0.2	1.16	0.22	1.13	0.19
15	2.78	0.46	2.74	0.51	2.77	0.49
20	5.19	0.81	4.91	0.89	5.01	0.82
25	8.05	1.22	7.79	1.31	8.28	1.28
30	11.61	1.67	11.15	1.81	12.08	1.8

Experimental Results for three experiments when angle of attack is 14°.

Free Stream Velocity (m/s)	Experiment 1: Single airfoil		Experiment 2: Two airfoils with separating distance of 1 chord length (13cm)		Experiment 3: Two airfoils with separating distance of 2 chord length (26cm)	
	F _L (N)	F _D (N)	F _L (N)	F _D (N)	F _L (N)	F _D (N)
5	0.34	0.08	0.33	0.07	0.3	0.08
10	1.35	0.25	1.36	0.25	1.33	0.21
15	3.14	0.62	3.14	0.63	3.1	0.56
20	5.7	0.99	5.64	1.09	5.49	0.99
25	8.99	1.5	9.05	1.62	9.23	1.54
30	12.88	2.07	13.01	2.2	13.13	2.16

Experimental Results for three experiments when angle of attack is 16°.

Free Stream Velocity (m/s)	Experiment 1: Single airfoil		Experiment 2: Two airfoils with separating distance of 1 chord length (13cm)		Experiment 3: Two airfoils with separating distance of 2 chord length (26cm)	
	F _L (N)	F _D (N)	F _L (N)	F _D (N)	F _L (N)	F _D (N)
5	0.35	0.12	0.33	0.07	0.35	0.08
10	1.44	0.33	1.44	0.3	1.45	0.27
15	3.3	0.64	3.44	0.81	3.52	0.74
20	6.02	1.15	6.34	1.34	6.32	1.24
25	9.63	1.74	10.27	2.01	10.31	1.84
30	13.67	2.45	15.05	2.77	13.75	2.65

Experimental Results for three experiments when angle of attack is 18°.

Free Stream Velocity (m/s)	Experiment 1: Single airfoil		Experiment 2: Two airfoils with separating distance of 1 chord length (13cm)		Experiment 3: Two airfoils with separating distance of 2 chord length (26cm)	
	F _L (N)	F _D (N)	F _L (N)	F _D (N)	F _L (N)	F _D (N)
5	0.32	0.12	0.39	0.09	0.31	0.09
10	1.38	0.5	1.65	0.37	1.35	0.33
15	3.34	1.13	3.84	0.86	3.47	0.79
20	5.9	1.39	6.71	1.44	6.28	1.34
25	9.57	2.04	10.56	2.23	10.19	2.04
30	13.81	3.44	15.44	3.09	11.36	2.92

Experimental Results for three experiments when angle of attack is 20°.

Free Stream Velocity (m/s)	Experiment 1: Single airfoil		Experiment 2: Two airfoils with separating distance of 1 chord length (13cm)		Experiment 3: Two airfoils with separating distance of 2 chord length (26cm)	
	F _L (N)	F _D (N)	F _L (N)	F _D (N)	F _L (N)	F _D (N)
5	0.3	0.18	0.36	0.12	0.37	0.12
10	1.3	0.63	1.63	0.43	1.59	0.61
15	3.02	1.4	3.74	1.15	3.65	1.28
20	5.7	2.49	5.94	2.31	6.04	2.26
25	9.45	3.55	9.31	3.55	10.04	3.37
30	12.76	5.37	13.32	4.96	11.05	4.32

APPENDIX VII

Formulas Used to Calculate Coefficient of Lift, Coefficient of Drag and Reynolds Number

1. Lift Force, $F_L = \frac{1}{2} \rho V^2 A C_L$

- Density of air, $\rho = 1.18 \text{ kg} / \text{m}^3$
- Free stream velocity, V
- Lift area, $A = 0.026 \text{ m}^2$
- Coefficient of lift, C_L

2. Drag Force, $F_D = \frac{1}{2} \rho V^2 A C_D$

- Density of air, $\rho = 1.18 \text{ kg} / \text{m}^3$
- Free stream velocity, V
- Drag Area, $A = 0.026 \text{ m}^2$
- Coefficient of drag, C_D

3. Reynolds number, $Re = \frac{\rho V L}{\mu}$

- Density of air, $\rho = 1.18 \text{ kg} / \text{m}^3$
- Free stream velocity, V
- Length of model = Chord Length, $L = 0.13 \text{ m}$
- Viscosity of air, $\mu = 1.8395 \times 10^{-5} \text{ kg} / \text{m.s}$ at atmospheric temperature, $T = 25^\circ \text{C}$